

Deletion of *dhc1* to investigate mating-dependent nuclear migration in the basidiomycete *Schizophyllum commune*

Dissertation

zur Erlangung des akademischen Grades

doctor rerum naturalium (Dr. rer. nat.)

vorgelegt dem Rat der Biologisch-Pharmazeutischen Fakultät

der Friedrich-Schiller-Universität Jena



vorgelegt von

Melanie Brunsch, Mag. Sc.

geb. am 14.10.1982 in Apolda

Jena, 09.10.2012

Gutachter:

1. Prof. Dr. Erika Kothe, Institut für Mikrobiologie, FSU Jena
2. Prof. Dr. Axel A. Brakhage, Institut für Mikrobiologie, FSU Jena
3. Dr. Kirk Bartholomew, Biology Department, Sacred Heart University, Fairfield, CT, USA

Tag der öffentlichen Disputation: 13.12.2012

Index

1.) Introduction	1
1.1. The fungal kingdom	1
1.2. <i>Schizophyllum commune</i> as a model organism	2
1.3. The cytoskeleton of filamentous fungi	5
1.4. The motor protein dynein	7
1.4.1. Molecular composition and functions of dynein molecules	7
1.4.2. The dynein heavy chain	8
1.5. Aim of this study	10
2.) Material and methods	11
2.1. Chemicals	11
2.2. Organisms, oligonucleotides, plasmids and antibodies	11
2.3. Media and solutions	13
2.3.1. Growth media for <i>S. commune</i>	13
2.3.2. Solutions for immunofluorescence	13
2.3.3. Solutions for DNA-Isolation	14
2.3.4. Solutions for plasmidpreparation	14
2.3.5. Solutions for transformation of <i>S. commune</i>	14
2.3.6. Solutions for protein isolation	14
2.3.7. Solutions for 2-D gelelectrophoresis	15
2.3.8. Solutions for tryptic digestion	15
2.4. Growth conditions	16
2.5. Microscopical investigations	16
2.5.1. General microscopy	16
2.5.2. Immunofluorescence	16
2.5.3. Scanning electron microscopy	17
2.6. Phylogenetic studies	17
2.7. Construction of the deletion-cassette of <i>dhc1</i>	17
2.7.1. DNA-Isolation	17
2.7.2. Polymerase chain reaction (PCR)	18
2.7.3. Cloning of PCR fragments	18
2.7.4. Plasmidpreparation	19
2.8. Transformation of <i>S. commune</i> strain after Specht <i>et al.</i> , 1988	20
2.8.1. Protoplast preparation	20
2.8.2. Transfection of protoplasts	20
2.8.3. Inoculation of protoplasts	21
2.8.4. Verification of successful transformation	21
2.9. Transcriptome-Analysis	21
2.9.1. Sample preparation	21

2.9.2.	Next generation sequencing via Illumina HiSeq 2000	21
2.9.3.	Analysis of raw data	21
2.10.	Proteome analysis <i>via</i> 2-dimensional gelelectrophoresis	22
2.10.1.	Sample preparation of cytoplasmatic protein	22
2.10.2.	Sample loading	22
2.10.3.	First dimension of 2-D gelelectrophoresis	23
2.10.4.	Second dimension of 2-D gelelectrophoresis	23
2.11.	Protein analysis	24
2.11.1.	Tryptic digestion	24
2.11.2.	Protein analysis	24
3.)	Results	25
3.1.	Organization of dynein heavy chain encoding genes in <i>S. commune</i>	25
3.2.	Localization of Dhc1 and Dhc2 in hyphae	28
3.3.	Deletion of <i>dhc1</i>	31
3.4.	Characterization of Δ dhc1 knock-out strains	34
3.4.1.	Cell length is reduced in Δ dhc1 strains	35
3.4.2.	Nuclear position changes in deletion mutants lacking <i>dhc1</i>	37
3.4.3.	Additional anomalies in the Δ dhc1 strains	38
3.4.4.	Mating and sexual development	41
3.4.5.	Comparison of Δ dhc1 strains with Δ dhc2	43
3.5.	Transcriptome analysis	43
3.5.1.	Detailed investigation of Δ dhc2	46
3.5.2.	Transcriptome differences between the wildtypes 12-43 and E6	48
3.6.	The proteome of <i>S. commune</i>	49
4.)	Discussion	55
4.1.	Phylogeny of the dynein heavy chain	55
4.2.	The deletion of either <i>dhc1</i> or <i>dhc2</i> is viable	57
4.2.1.	Δ dhc1 strains show a different phenotype	57
4.2.2.	Phenotypes in Δ dhc1 strains are dependent on the parental background	58
4.2.3.	Kinesin-5 and Kinesin-14 can substitute for the function of <i>dhc2</i>	59
4.2.4.	The transcriptome of Δ dhc2 shows differences in 250 genes	60
4.3.	Transcriptome differences can be found in all three investigated strains	61
4.3.1.	High genomic diversity between different strains of <i>S. commune</i> wildtypes	61
4.3.2.	Between all three strains, 22 genes show differential regulation	63
4.3.3.	Correlation between the transkriptome und proteome in monokaryons	64
4.4.	A protein map of <i>S. commune</i> will allow future analyses	65
4.5.	Differences associated with the dikaryotic proteome	65
4.6.	Outlook	66

5.) Summary	68
6.) Zusammenfassung	69
7.) References	70
8.) Appendix	
9.) Acknowledgement	
Selbständigkeitserklärung	

Figures

Figure 1: Fungal tree of life	1
Figure 2: Fruiting bodies of <i>S. commune</i>	2
Figure 3: Sexual development in <i>S. commune</i>	3
Figure 4: Life cycle of <i>S. commune</i>	4
Figure 5: Tetrapolar mating-system in <i>S. commune</i>	5
Figure 6: Organization of cytoskeleton in tips of filamentous fungi	6
Figure 7: Structure of the dynein complex	7
Figure 8: Functionality of dynein	9
Figure 9: Organization of <i>dhc1</i> and <i>dhc2</i>	25
Figure 10: Gene distribution of <i>dhc1</i> and <i>dhc2</i> in elected Agaricomycetes	27
Figure 11: Phylogeny of the dynein heavy chain	29
Figure 12: Threedimensional image of a dikaryotic hyphae	30
Figure 13: Localization of Dhc1 and Dhc2 in the cytoplasm	31
Figure 14: Deletion plasmid p Δ <i>dhc1</i>	32
Figure 15: PCR strategy to prove the integration of the deletion cassette	32
Figure 16: Gel picture of PCR results	33
Figure 17: PCR strategy to show the replacement of the wildtype gene	33
Figure 18: Colony morphology of transformants obtained from Δ ku80	34
Figure 19: Colony morphology of transformants obtained from 12-43	35
Figure 20: Diagram showing the cell length of tip cells in strains obtained from Δ ku80	35
Figure 21: Diagram showing the cell length of hyphal cells in strains obtained from Δ ku80	36
Figure 22: Diagram showing the cell length of tip cells in strain obtained from 12-43	36
Figure 23: Diagram showing the cell length of hyphal cells in strain obtained from 12-43	37
Figure 24: Diagram showing the nuclear position in strains obtained from Δ ku80	37
Figure 25: Diagram showing the nuclear position in strain obtained from 12-43	38
Figure 26: Protuberances at hyphae of Δ <i>dhc1</i> strains	39
Figure 27: Coil formation in Δ <i>dhc1</i> strains	39
Figure 28: Hyper branching effects in Δ <i>dhc1</i> strains	40
Figure 29: Bi- and Multinuclear cells in Δ <i>dhc1</i> strains	40
Figure 30: Fruiting body formation of the compatible mating interaction between wildtype T41 and Δ <i>dhc1</i> _2	41
Figure 31: Mating experiment between a compatible wildtype and Δ <i>dhc1</i> _59	42
Figure 32: Venn diagram of RNA-Sequencing	44
Figure 33: Distribution of 250 differentially regulated genes in Δ <i>dhc2</i>	47
Figure 34: Distribution of 110 annotated, differentially regulated genes in Δ <i>dhc2</i>	47
Figure 35: Distribution of 93 differentially regulated genes in 12-43 compared to E6	48
Figure 36: Gene regulation in 12-43 compared to E6	48
Figure 37: Distribution of analyzed proteins of the mastergel from 12-43	49

Figure 38: Mastergel of 12-43	50
Figure 39: Comparison of 2d-gels from 12-43 vs 4-39	51
Figure 40: Diagram showing the different abundance of proteins in strain 4-39 compared to 12-43	52
Figure 41: Comparison of 2d-gels from 12-43 vs dikaryon	53
Figure 42: Diagram showing the different abundance of proteins in the dikaryon compared to 12-43	54
Figure A1: Proof of the successful deletion of <i>dhc1</i> via nested PCR	

Tables

Table 1: Organisms used in this study	11
Table 2: Oligonucleotides used in this study	11
Table 3: Plasmids used in this study	12
Table 4: Antibodies used in this study	12
Table 5: Program for isoelectric focussing of IPG-strips	23
Table 6: Amino acid sequence of the first four AAA-modules of the dynein heavy chain in different species	26
Table 7: Sequence of aa and the split point of Dhc1 and Dhc2	28
Table 8: Similarities and differences in dynein heavy chain deletion mutants	43
Table 9: Amount of genes identified with the four statistical tests in every comparison of RNA-Seq	44
Table 10: 22 differentially regulated genes in all three strains	45
Table A1: Dataset of phylogenetic tree	
Table A2: Differentially expressed genes in 3 investigated strains	
Table A3: 250 genes differentially expressed in $\Delta dhc2$	
Table A4: 93 differentially expressed genes in wildtype strains	
Table A5: List of proteins identified on the mastergel	
Table A6: Spots with a low mascot score	
Table A7: Different abundance of proteins in strain 4-39	
Table A8: Different abundance of proteins in dikaryon	

Abbreviations

aa	=	amino acid
AAA	=	ATPase associated diverse cellular activities
APS	=	ammonium persulfate
bp	=	base pairs
CTAB	=	cetyl trimethylammonium bromide
DAPI	=	4',6-diamidino-2-phenylindole
DMSO	=	Dimethyl sulfoxide
DNA	=	desoxyribonucleic acid
dNTP	=	desoxynucleoside triphosphate
DTT	=	dithiothreitol
EDTA	=	Ethylenediaminetetraacetic acid
GFP	=	green fluorescent protein
HCCA	=	alpha-cyano-4-hydroxy-cinnamic acid
IPG	=	immobilized pH gradient
Kb	=	kilo base pairs
kDa	=	kilodalton
KOG	=	EuKaryotic Orthologous Groups
MAPK	=	Mitogen-Activated protein kinase
MT	=	microtubule/s
MTOC	=	microtubule organized centers
Ncbi	=	National Center for Biotechnology Information
NLS	=	Nuclear localization sequence
PCR	=	polymerase chain reaction
PEG	=	polyethylene glycol
RFP	=	red fluorescent protein
RNA	=	ribonucleic acid
RPKM	=	reads per kilobase of exon model per million mapped reads
rpm	=	rounds per minute
RT	=	room temperature
SDS	=	sodium dodecyl sulfate
TCA	=	trichloroacetic acid
TEMED	=	tetramethylethylenediamine
TFA	=	trifluoroacetic acid
UV	=	ultraviolet
V	=	volumes
Vhr	=	volt hours
vs.	=	<i>versus</i>
wt	=	wild type

1.) Introduction

1.1. The fungal kingdom

Fungi are described as eukaryotic organisms with filamentous growth forms, as hyphae or mycelium as well as yeast forms. Fungi are ubiquitous saprobes or degraders of dead organic material, symbiotic partners for other organisms and pathogens in all kingdoms (Redecker, 2002).

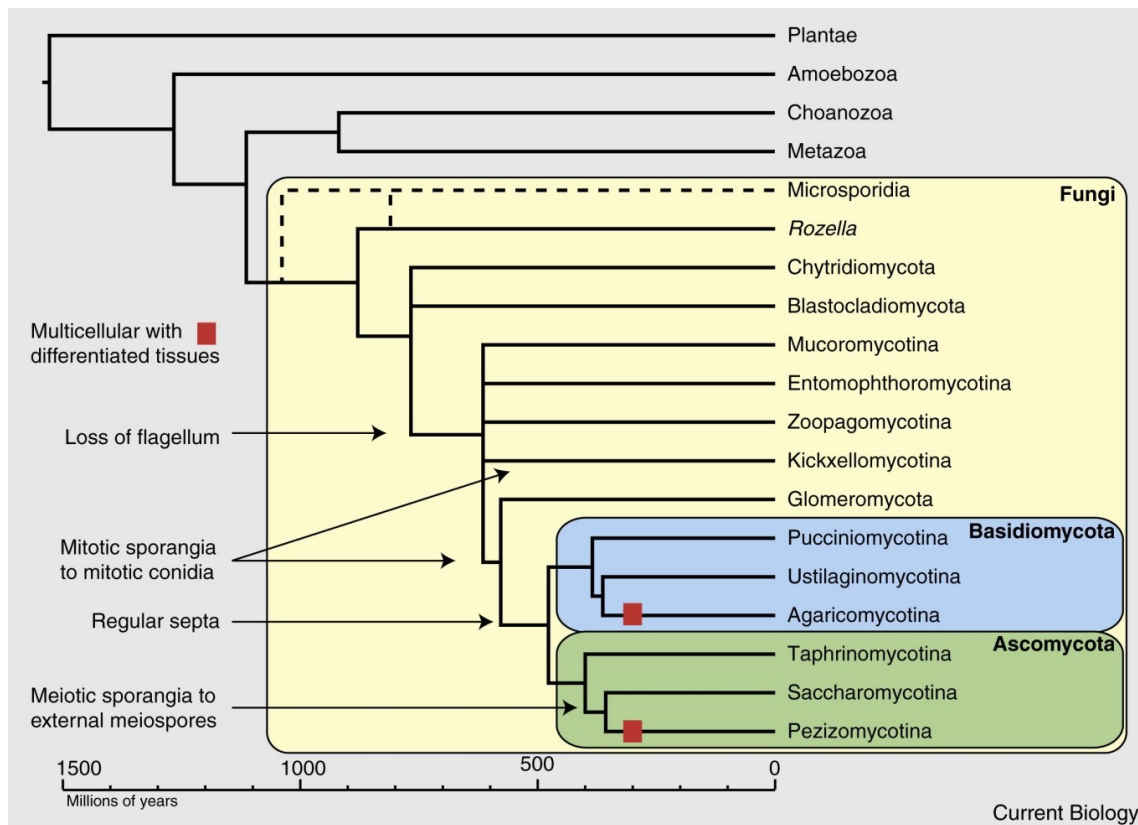


Figure 1: Fungal tree of life (Stajich *et al.*, 2009)

True fungi are summarized in three groups (Fig 1). The evolutionary oldest group contains the simple, very basal fungi, like Chytridiomycota. Also Mucoromycotina (former Zygomycetes) belong to this domain. The higher developed Ascomycetes form the second large domain. Basidiomycota, containing mushrooms, jelly fungi and basidiomycetous yeasts form the third group which encompasses Pucciniomycotina, Ustilaginomycotina and Agaricomycotina. Molecular biology studies have shown that the Agaricomycotina are divided into Tremellomycetes, Dacrymycetes and Agaricomycetes (Hibbett, 2006; Stajich *et al.*, 2009).

1.2. *Schizophyllum commune* as a model organism

The split gill fungus *Schizophyllum commune*, a mushroom forming agaricomycete, is a cosmopolitan wood decaying fungus causing white rot on hard wood. It is characterized by conspicuous shell-shaped, 2-3 cm large fruiting bodies (Fig. 2). The fungus is used as a model organism in basic molecular biology research to understand the regulation of sexual development, hyphal growth or the lignolytical capability. It completes its entire life cycle within approximately 14 days under laboratory conditions and a well established transformation and gene deletion protocol can be applied for genetical manipulation. Additionally, the published genome of *S. commune* allows investigation on of the transcriptome or proteome at molecular levels (Cooke, 1961; Kothe, 1996; Palmer and Horton, 2006; Ohm *et al.*, 2010).

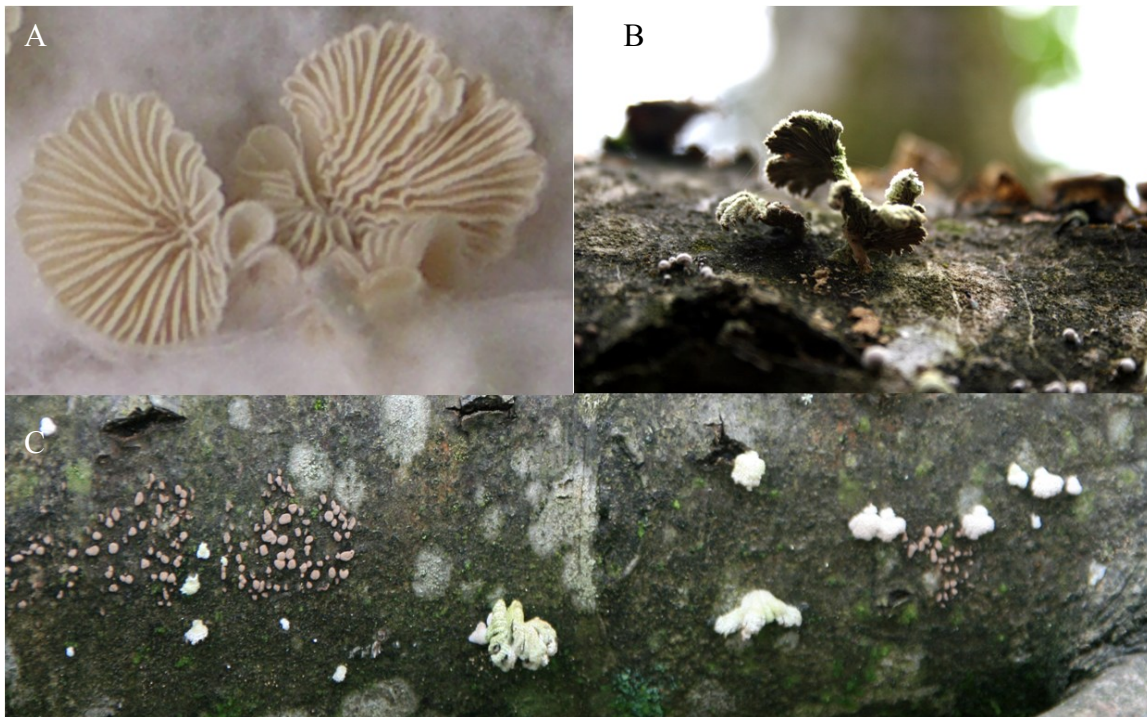


Figure 2: Fruiting bodies of *S. commune*: A) on well defined media under laboratory conditions 10 days past inoculation; B/C) under natural conditions on beech (biosphere reserve Berchtesgadener Land, Königssee, peninsula St. Bartholomä, Germany)

The German botanist Hans Kniep characterized the mating system of basidiomycetes, especially of *S. commune*, already in the early 1920s. He detected two independent mating type loci, called *A* and *B*. In the 1950s, Papazian completed the knowledge of the mating type genes and found out that there are two linked multiallelic subloci, α and β , in every mating type locus. For $A\alpha$, $B\alpha$ and $B\beta$, each with 9 allelic specificities, and 32 allelic specificities in $A\beta$, a total of more than 23,000 mating types can be found in nature. To form a fertile mating,

both partners have to be mating type compatible. In detail, that means that both need a different genetic background, or specificity, in their mating type genes. Only if both partners differ in either or both α and β specificities in both A and B genes, a compatible mating reaction can take place. After the fusion of the hyphae, the nuclei migrate to build a pair – one nucleus from each mating partner – per tip cell. Then, both nuclei divide synchronously. The tip cell forms a so called hook cell, where one nucleus of the first pair migrates to the hook cell. Then, septa are laid down at the places of both mitotic spindles separating the daughter nuclei. Thus, one nucleus is trapped in the hook cell until the hook fuses with the subterminal cell and the trapped nucleus migrates to join its partner in the subterminal cell. This assures that each cell of the growing mycelium has two different nuclei, one of each mating partner. The fused hook cell – then called clamp cell – is the typical structure in dikaryons of basidiomycetes, although not all basidiomycetes show such nice and constant clamp formation as is observed with *S. commune* (Fig. 3). Under promoting environmental conditions, the mycelium of the dikaryon starts to aggregate and form primordia. These structures are pre-stages of fruiting bodies. The fertile fruiting bodies release haploid basidiospores which are able to germinate again to form haploid, monokaryotic strains (Fig 4.; Niederpruem and Wessels, 1969; Raudaskoski and Koltin, 1973; Palmer and Horton, 2006; Schubert *et al.*, 2006).

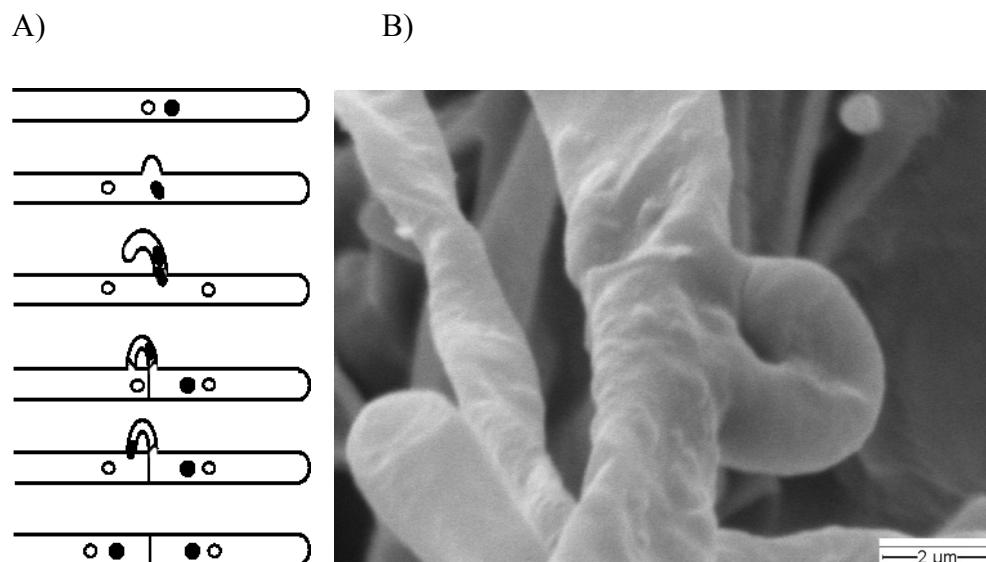


Figure 3: Sexual development in *S. commune*. A) Process of dikaryon formation B) SEM-image of a clamp cell of *S. commune*.

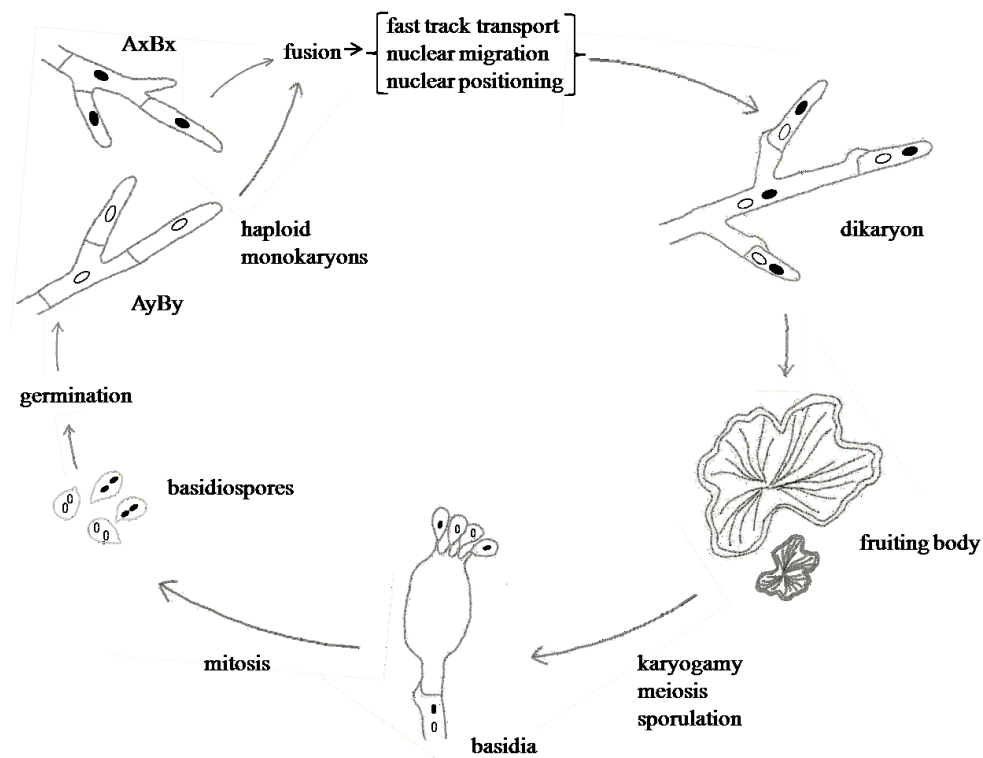


Figure 4: Life cycle of *S. commune* (see text for details) (modified after Stankis *et al.*, 1990)

If both mating partners share a common *A* factor, nuclear migration can take place. The nuclei do not undergo the pairing and the conjugated nuclear division, and also the hook cell cannot be formed. The phenotype of this mating reaction is called “flat”. This phenotype is characterized by less aerial mycelium and hyperbranched hyphae with highly variable numbers of nuclei in every cell, as well as a decrease of septation. A second semi-compatible reaction occurs when both mating partner share a common *B* factor. The nuclei do not migrate after cell fusion; instead they form pairs and one nucleus migrates to the formed hook cell. The hook cell is not able to fuse with the cell behind the tip and the nucleus stays trapped in the hook. This cell is called “pseudoclamp”. The phenotype of this reaction is called “Barrage”, because it is characterized by a separation zone of mycelium that is formed between the two mating partners. If both mating loci are of the same specificity, mating fails to appear (Fig. 5; Raper and Miles, 1958; Koltin *et al.*, 1979; Kothe, 1999; Raudaskoski and Kothe, 2010). Because of these four possible mating interactions, the mating system has been termed tetrapolar (Kniep, 1920, 1922).

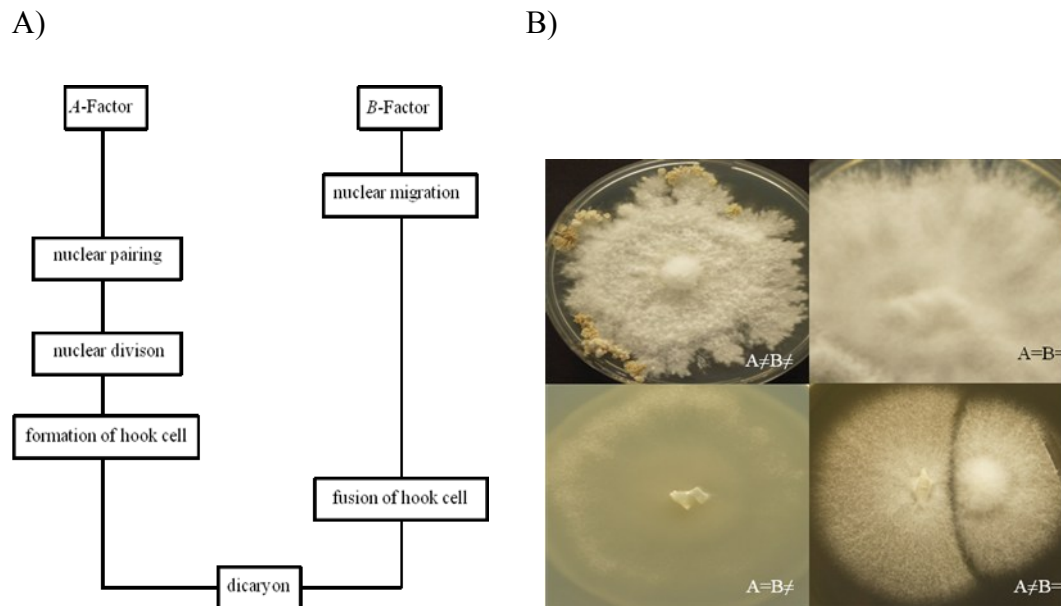


Figure 5: A) Cycle of sexual development influenced by mating-type loci *A* and *B*; B) tetrapolar mating-reactions in *S. commune* (pictures modified after E.-M. Jung)

1.3. The cytoskeleton of filamentous fungi

In filamentous fungi, the cytoskeleton is responsible for polarized growth and hyphae formation. Two main structures play an essential role – microtubules and actin. Microtubules appear as tracks in hyphae; they are organized from MTOCs (microtubule organizing centers) which contain γ -tubulin at the minus-end of microtubules. Growth of microtubules starts at MTOCs by extension of α/β -tubulin dimers starting from γ -tubulin. Depolymerization of tubulin dimers at the plus-end leads to shortening of microtubules (Xiang and Fischer, 2004; Steinberg, 2007a).

Microtubules (MTs) are necessary for formation and stabilization of the mitotic spindle during the cell cycle in filamentous fungi. Additionally, MTs are involved in vesicle transport from the central parts of the cell to the tip. Vesicles containing cell wall material, which is needed at the hyphal tip to synthesize the growing cell wall, are transported this way. The Spitzenkörper or vesicle supply center is located at the hyphal tip, where the vesicles are accumulated (Girbhardt, 1957; Wessels, 1986; Bartnicki-Garcia *et al.*, 2000; Steinberg, 2007b; Fischer *et al.*, 2008).

Actin is a globular protein (G-actin), which can polymerize to filaments (F-actin). Actin is responsible for flexibility of hyphae, morphological changes, cell division and intracellular trafficking (Hennessey *et al.*, 1993). It exists in different forms in hyphae – as patches located at the growing tip, as cables at the cell periphery and as ring-like structures at septa.

Therefore, it is assumed that actin is required for cell wall assembly at the growing tip (Xiang and Plamann, 2003).

Actin and microtubules are tracks, on which motor proteins can move cargo to different locations in the cell. Three types of molecular motors are known: kinesins and dynein, which ride along microtubules, and myosin, which transports cargo along actin. They translate chemical to mechanical energy. In this pathway, ATP is hydrolyzed at the globular head domain of motor proteins. This results in a conformation change of the molecule and makes movement along microtubules or actin possible (Schliwa and Woehlke, 2003).

Myosin consists of one to two heavy chains each with one or several light chains (Korn, 2000). The heavy chains form the head domain that interacts with actin, the neck region links the heavy chain to light chains. The tail region is formed by light chains that carry the particular cargo (Foth *et al.*, 2006). Myosins are necessary for contractions at the cell surface, for vesicle transport and intracellular streaming (Hoyt *et al.*, 1997).

Fungal cells contain 10 to 11 different kinesins. They are plus-end directed, microtubule-dependent motor proteins formed by two identical heavy chains and two identical light chains (Lakämper *et al.*, 2003). Kinesins are involved in all plus-end directed transport at microtubules, including spindle formation and spindle function. They are essential for long distance transport of cell organelles and vesicles (Xiang, 2003; Fig 6).

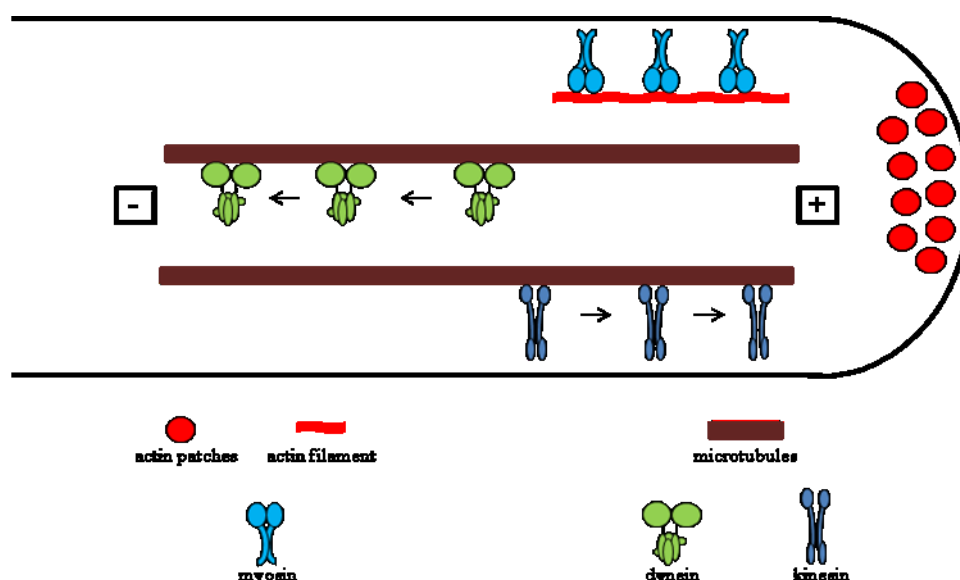


Figure 6: Organization of the cytoskeleton in tip cells of filamentous fungi. Dynein and Kinesin move their cargo along microtubules in opposite directions, myosin is connected to actin filaments.

1.4. The motor protein dynein

1.4.1. Molecular composition and functions of dynein molecules

Dynein is required for vesicle transport, perinuclear localization of the Golgi apparatus, nuclear and spindle positioning, as well as spindle assembly during mitosis and meiosis. In fungi, dynein is also required for nuclear migration (Karki and Holzbaaur, 1999; Yamamoto and Hiraoka, 2003). Dynein accumulates at the hyphal tip, where – in addition to MTOCs at the nuclear envelope - the minus-end of MTs is located. This ensures that vesicles reach the hyphal tip and polarized growth of hyphae can take place (Schuster *et al.*, 2011).

Dynein is a macromolecular complex composed of different protein subunits that interact with microtubules. This complex consists of two heavy chains (~500 kDa), several intermediate (~70 kDa) and light intermediate chains (53 – 59 kDa) and light chains (8 – 23 kDa). The dynein heavy chain forms the globular head of the molecule which associates with microtubules. A neck region links the heavy chain to light and intermediate chains which bind the cargo for fast track transportation from the plus- to the minus-end of microtubules (Fig. 7; Holzbaaur and Vallee, 1994; Plamann *et al.*, 1994; Hirakawa *et al.*, 2000; Pfister *et al.*, 2006).

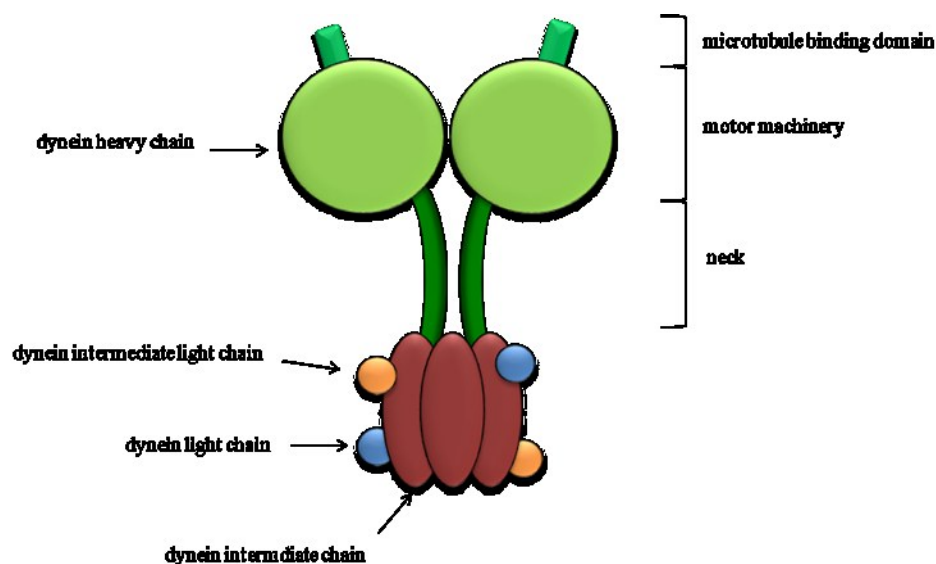


Figure 7: Structure of the dynein complex. Shown are the different subunit chains of the dynein complex. The heavy chain consists of 3 domains which are described in the text.

To exploit their entire functionality, dynein molecules need several interacting proteins. Dynactin is a protein complex consisting of two important structures: an actin-like filament composed of the actin-related protein Arp1, and a side chain. This structure is formed by the dimer p150^{Glued} which contains binding sites for microtubules, dynein intermediate chains and Arp1. Dynactin acts as a regulator for dynein motility and connects dynein molecules to other cell components (Yamamoto and Hiraoka, 2003; King *et al.*, 2003).

Further proteins interacting with dynein are Lis1 and Clip-170. Lis1 was first identified as the protein causing lissencephaly in humans (Markus *et al.*, 2011). The C-terminus of Lis1 binds at dynein molecules and is therefore required for nuclear and spindle positioning in fungi (Xiang, 2003; Torisawa *et al.*, 2011). Clip-170, in contrast, is necessary for accumulation of dynactin at the plus-end of microtubules and for nuclear migration in fungi (Yamamoto and Hiraoka 2003).

1.4.2. The dynein heavy chain

The dynein heavy chain is a 4600 aa large protein subunit of the dynein complex. It consists of a 1300 aa large N-terminal region which contains the dimerization domain of the protein, needed to dimerize with the second heavy chain of the molecule. The 3300 aa large C-terminal region contains the motor machinery, where chemical energy is converted into mechanical energy. The motor domain is formed by six AAA-modules (ATPase associated diverse cellular activities). AAA1 to AAA4 each contain a Walker A (P-loop) and a Walker B motif. Walker A motifs are known to function as nucleotide binding site. AAA1 and AAA3 have a strong binding activity, whereas AAA2 and AAA4 have a decreased activity which leads to the assumption of a regulatory role of these modules. AAA5 and AAA6 have lost nucleotide binding sites. Between AAA4 and AAA5, the microtubule binding site (or B-link, a 10-12 nm long stalk) is located (Carter *et al.* 2011).

ATP can bind directly to the first AAA modules. This results in a re-orientation of the dynein heavy chain. In this process, the modules move closer to each other and the microtubule binding site moves towards the microtubule. Hydrolysis of ATP at AAA1 leads to movement of the neck domain, which is linked to AAA1. The microtubule binding site is lifted upwards and connects to the microtubule. The hydrolyzed products at AAA1 to AAA4 are discharged from the AAA modules and the neck domain swings to the left, while the dynein molecule moves to the right (Fig. 8; Asai and Koonce, 2001).

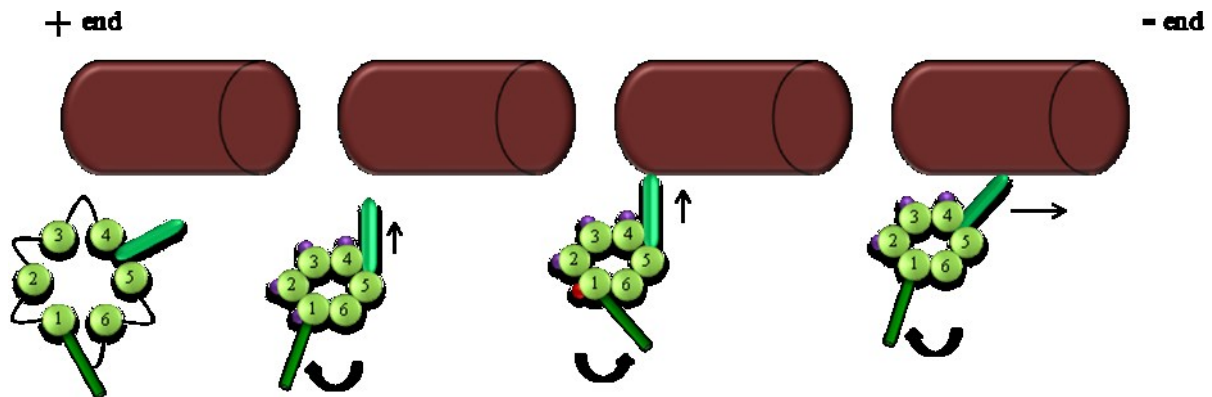


Figure 8: Functionality of dynein. Detailed description is to be found in the text. (brown = microtubule, light green ring = AAA modules, bright green = microtubule binding site, dark green = neck, violet = bound nucleotides, purple = hydrolysed nucleotides). (modified after Asai and Koonce, 2001)

In contrast to other eukaryotes, the dynein heavy chain of the rust fungus *Ustilago maydis* (Ustilaginomycotina) is encoded by two separate proteins. Both proteins cover the entire length of approximately 4600 aa together. The dynein heavy chain is split in *U. maydis* between the fourth AAA module and the microtubule binding domain. The deletion of either *dyn1* or *dyn2* in *U. maydis* is lethal, which proves the essential functionality of the dynein heavy chain in eukaryotes (Straube *et al.*, 2001).

In *S. commune*, also two separate genes encoding the dynein heavy chain, were found (D. Schubert, personal communication).

1.5. Aim of this study

The dynein heavy chain of *S. commune* is encoded by two genes – *dhc1* and *dhc2*. A detailed phylogenetic investigation of the dynein heavy chain has to be performed to provide information on the split event during basidiomycete evolution and the organization of the dynein heavy chain encoding gene(s) in other fungi.

Via immunofluorescence microscopy, the localization of both gene products in the cell has to be demonstrated. Also cellular localization of other cytoskeleton components should be investigated through antibody staining methods to complete the knowledge about their organization in the cell. It is expected, that a co-localization of both gene products can be detected. As dynein is involved in the cell cycle of *S. commune*, *dhc1* and *dhc2* could form a complex to fulfill its function in mitosis.

The deletion of *dhc2* is not lethal in *S. commune*. As this gene contains the important motor machinery, which is essential for the functionality of the dynein complex, other genes or complexes must provide the transport of cargo to the minus-end of microtubules. Transcriptome analysis of the $\Delta dhc2$ strain and its parental strains should be performed to identify cytoskeletal components or motor proteins which can fulfill the function of dynein. With the current RNA sequencing method, differences in the transcriptome of all strains can be demonstrated.

To complete the knowledge of the function of the dynein heavy chain genes in *S. commune*, a knock-out of *dhc1* needs to be accomplished. As the knock-out of *dhc2* is viable, it is assumed that also $\Delta dhc1$ strains are able to survive. To compare these strains to the already existing $\Delta dhc2$ strains, detailed microscopic investigations according to cell morphology, nuclear migration and mating behavior should be performed.

To simplify proteomic studies, a protein map of cytosolic proteins of *S. commune* should be developed. *Via* 2-dimensional gelelectrophoresis the reference gel of a monokaryotic strain of *S. commune* shall be produced. Exclusive protein spots on the reference gel should be identified with mass spectrometry. Possible posttranslational modifications could be shown. A second monokaryotic strain shall be adducted to demonstrate strain specific differences in *S. commune*. Additionally, a dikaryotic proteome shall be created *via* 2-dimensional gelelectrophoresis to identify dikaryon specific proteins.

2.) Material and methods

2.1. Chemicals

Chemicals, used in this study, were purchased from Merck KGaA (Darmstadt, Germany), Carl Roth (Karlsruhe, Germany), Sigma-Aldrich Laborchemikalien GmbH (Seelze, Germany) and Serva Electrophoresis GmbH (Heidelberg, Germany). Special chemicals are mentioned separately. Endonucleases were purchased from New England Biolabs GmbH (Frankfurt am Main, Germany) and Jena Bioscience GmbH (Jena, Germany).

2.2. Organisms, oligonucleotides, plasmids and antibodies

Organisms, oligonucleotides and plasmids used in this study are listed in table 1, 2 and 3.

Table 1: Organisms used in this study. * Strains were obtained from the JMRC (Jena Microbial Resource Collection)

Strain description	Species	genotyp	source
12-43	<i>S. commune</i>	$A_{3,5} B_{2,2}$	*
$\Delta ku80$	<i>S. commune</i>	$A_{4,3} B_{4,1}$	L. Lugones, Utrecht, Netherlands; modified by S. Madhavan, Microbial Communication, FSU Jena, Germany
E6	<i>S. commune</i>	$A_{4,6} B_{2,1}$	*
4-39	<i>S. commune</i>	$A_{1,1} B_{3,2}$	*
W22	<i>S. commune</i>	$A_{4,6} B_{3,2}$	*
T41	<i>S. commune</i>	$A_{4,7} B_{8,4}$	*
$\Delta dhc1$	<i>S. commune</i>	$A_{4,3} B_{4,1}$	this study
$\Delta dhc2_5$	<i>S. commune</i>	$A_{3,5} B_{2,2}$	Strain collection FSU Jena, Microbial Communication, Germany
K12 DH5 α	<i>Escherichia coli</i>	/	Gibco Life Technologies, Karlsruhe, Germany

Table 2: Oligonucleotides used in this study

Primer	5'	3'
dhc1AaXbaI	AGT CTC TAG AGC CAC ACC GAA TCG CCA GCA AGT C	
dhc1AbXbaI	CCA TTC TAG AGG GGG AAG CAG CGC GAG CAG GTA	
dhc1Ba	ACG CGC ATA GGG GCA CCG ACA A	
dhc1Bb	GCA AGC GCC ATC CCC AGC AGT	
Dhc1for	TCG AGC TAT CGC TGC TGC AT	

Dhc1rev	AGC TTT TGG CCC TCG GCG TA
dhc1up	CGGTGGACAAGTATGGGAGGC
dhc1down	GAAACAACAATAGGAAGGAGAAAGCA
ura-forward	AGGGAGAATCGCGACTTCGT
B-test	GATCGAACTCCGAGCACCAT

Table 3: Plasmids used in this study

Name	Characterization	Source
pDrive	TA cloning vector, Amp ^R	Qiagen GmbH, Hilden, Germany
pChi	pBlueskript, Amp ^R <i>ura1</i> -marker gene of <i>S. commune</i>	K. Lengeler, former Microbial Communication, FSU Jena (now Heinrich-Heine-Universität, Düsseldorf, Germany)
pBluescript II SK	cloning vector	Stratagene GmbH, Heidelberg, Germany
p Δ <i>dhc1</i>	pBlueskript, Amp ^R deletion cassette for <i>dhc1</i>	this study

First antibodies ScDhc1 and ScDhc2 were produced by BioGenes GmbH (Berlin, Germany). All second antibodies were purchased from Sigma-Aldrich Chemie GmbH, Schnellendorf, Germany. Antibodies are listed in table 4.

Table 4: Antibodies used in this study

Antibody	Specificity	Label	Sequence	Concentration
ScDHC1	Anti-Dhc1 (from rabbit)	/	C-ALPPLRDITNKRRD	1:50
ScDHC2	Anti-Dhc2 (from rat)	/	C-GILKRERMQQARED	1:50
T6778	Anti-rabbit (IgG)	TRITC		1:100
T4280	Anti-rat (IgG)	TRITC		1:100
F6258	Anti-rat (IgG)	FITC		1:100
T9026	Anti-tubulin (from mouse)	/		1:500
F4018	Anti-mouse (IgG)	FITC		1:1000

2.3. Media and solutions

2.3.1. Growth media for *S. commune*

Media were sterilized at 120 °C for 30 minutes in an autoclave.

<u>C</u> omplex <u>y</u> east <u>m</u> edium (CYM):	2 g peptone 2 g yeast extract 20 g glucose 0.5 g MgSO ₄ 0.5 g KH ₂ PO ₄ 1 g K ₂ HPO ₄ 18 g Agar-Agar for solid media
CYM-T	CYM + 4mM tryptohane
<u>M</u> inimal <u>M</u> edia (MM)	20 g glucose 2 g aspartic acid 0.5 g MgSO ₄ 0.5 g KH ₂ PO ₄ 1 g K ₂ HPO ₄ 120 µg Thiaminiumdichloride pH 6.3 15 g Agar-Agar for solid media

2.3.2. Solutions for immunofluorescence

Fixation solution	50 mM PIPES, pH 6.7 25 mM EGTA, pH 8 5 mM MgSO ₄ 3.7% formaldehyde
PME	50 mM PIPES, pH 6.7 25 mM EGTA, pH 8 5 mM MgSO ₄
PBS	137 mM NaCl 2.68 mM KCl 8.45 mM Na ₂ HPO ₄ 1.47 mM KH ₂ PO ₄
Extraction solution	100 mM PIPES, pH 6.7 25 mM EGTA, pH 8 0.1 % Igepal
Embedding media	0.1 M Tris/HCl, pH 8 50% glycerin 1 mg/ml phenyldiamine 0.1 – 1 µg/ml DAPI

2.3.3. Solutions for DNA-Isolation

DNA-Extractionbuffer	100 mM Tris/HCl, pH 8.0 50 mM EDTA, pH 8.0 2 % SDS
CTAB/NaCl	0.7 M NaCl 10 % CTAB
1xTE	10 mM Tris/HCl 1 mM EDTA, pH 8.0

2.3.4. Solutions for plasmidpreparation

SolA	25 mM Tris, pH 8.5 10 mM EDTA, pH 8.0 50 mM glucose
SolB	200 mM NaOH 1 % SDS
SolC	2,55 M potassium acetate, pH 5.8

2.3.5. Solutions for transformation of *S. commune*

0.5M MgSO ₄	0.5 M MgSO ₄ 20 mM MES, pH 6.3
1M MgSO ₄	1 M MgSO ₄ 20 mM MES, pH 6.3
1M Sorbitol	1 M Sorbitol 20 mM MES, pH 6.3
PEG	50 % PEG 4000 10 mM MES, pH 6.3
Rescue-media	MM 0.5 M Sucrose
Top-agar	MM 0.8 % Agar
Bottom-agar	MM 1.5 % Agar

2.3.6. Solutions for protein isolation

Solution A	80 mM Tris-HCl, pH 7.4 1.2 M NaCl
Solution B	40 mM Tris-HCl, pH 7.4 600 mM NaCl 4 % Triton X-114
Precipitation buffer	20 % TCA 50 % acetone
Rehydration buffer	8 M urea 2 M thiourea 4 % CHAPS

2 % IPG buffer
12 µl/ml DeStreak reagent

2.3.7. Solutions for 2-D gelelectrophoresis

Solution 1	6 M urea 2 % SDS 30 % glycerin 75 mM Tris-HCl pH 8.8 1 % DTT
Solution 2	6 M urea 2% SDS 30 % glycerin 75 mM Tris-HCl pH 8.8 4 % iodacetamide
Polyacrylamid gel (for 6 gels)	189 ml polyacrylamid 1.5 M Tris-HCl pH 8.8 101 ml <i>Aqua dest.</i> 38 ml Rhinohide 4.5 ml 10 % SDS 62 µl TEMED 4.5 ml 10 % APS
Fixing solution	40 % methanol 7 % acetic acid
Staining solution	20 % methanol 2 % o-phosphoric acid (85 %) 10 % ammonium sulfate 0.1 % Coomassie Brilliant Blue G-250
Neutralization solution	12 g Tris-base pH 6.5 (with o-phosphoric acid (85 %))
Destaining solution	25 % methanol

2.3.8. Solutions for tryptic digestion

Enzyme solution	20 µg/µl trypsin (Promega, Mannheim, Germany) 25 mM NH ₄ HCO ₃
Extraction buffer	0.1 % TFA/acetonitrile, 1:1

2.4. Growth conditions

S. commune was grown on CYM/CYM-T at 30 °C for five days on solid media.

For DNA- and protein isolation, liquid media was used. *S. commune* was macerated in 50 ml of the adequate media with blender and incubated on a shaker at 30 °C and 150 rpm for two days. The pre-culture was mazerated again, filled up with media to 200 ml and incubated for two days at 30 °C and 150 rpm on a shaker. The well grown mycelium was filtered through a nylon membrane, washed with *Aqua dest.* and, if necessary, stored at -20 °C.

For immunofluorescence microscopy, solid media was covered with sterile cover slides. *S. commune* was inoculated in the gaps between two glass slides and was grown at 30 °C for three to four days.

For RNA-isolation *S. commune* was grown on solid media which was covered with sterile cellophane (Wilhelm Isermann KG, Walsrode, Germany). After seven days of incubation at 30 °C, mycelium was harvested and stored at -20 °C.

E. coli was grown on Standard I media (Carl Roth, Germany) at 37 °C. If necessary, antibiotics (100 µg/ml Ampicillin) were added. For cultivation on solid media, 1.8 g agar-agar was attached to the medium. For blue/white screening of cultures, transformed with a plasmid containing the *lacZ* gene, the indicator 5-bromo-4-chloro-indolyl-β-D-galactopyranoside (40 mg/ml solved in DMSO) was added to solid media.

2.5. Microscopical investigations

2.5.1. General microscopy

Microscopic samples were investigated with Axioplan 2 (Carl Zeiss AG, Jena). Images were analyzed with Spot Advanced (Version 4.6, Diagnostic Instruments, Sterling Heights).

2.5.2. Immunofluorescence

The immunofluorescence protocol was modified from Raju and Dahl (1982) and Fischer and Timberlake (1995). Overgrown cover slides were fixed with fixation solution for 90 minutes. After that, hyphae were washed with PME three times. Cell wall degradation was performed with 30 mg/ml lysing enzyme (*Trichoderma harzianum*, Glucanex, Sigma Aldrich, Munich, Germany), lysed in 500 µl egg white + 500 µl PME for 20 minutes. For permeabilization of the cells, extraction solution was added for five minutes. After five minutes of blocking with milk powder, the first antibody (Tab.4) was added and incubated over night at 4 °C. The first

antibody was removed by washing the hyphae with PBS. After the incubation with the second antibody for 1 h at 37 °C and washing with PBS, the cover slide was incorporated in embedding medium containing DAPI fluorescence dye (1 µg/ml).

Microscopic samples were investigated with LSM 5 Axio Observer (Carl Zeiss AG, Jena). Images were analyzed with Zen2009 (Carl Zeiss AG, Jena).

2.5.3. Scanning electron microscopy

Mycelium of *S. commune* colonies was air dried for one week on a sterile glass slide and additionally incubated in an exsiccator for three days. Samples were fixed on a sample holder sputtered with a thin layer of gold to receive a conductive surface of the sample (EMI Tech K500) Samples were analysed with SEM, Philips XL 30 ESEM. Images were recorded with Scandium software (version 5.0 analySIS Image Processing Soft Imaging System GmbH, Münster).

2.6. Phylogenetic studies

Amino acid sequences were downloaded from databases mentioned in Appendix 1.

Amino acid sequences were aligned with MAFFT v6 using the BLOSSUM80 matrix and the E-INS-i option. For alignment quality control and adjustment, BIOEDIT v 7.0.9.0 was used (Hall, 1999; Katoh and Toh, 2008).

Phylogenetic reconstruction was conducted using MrBayes v. 3.1.2. For validation of data, RAxML Blackbox v. 7.2.6 was used. Phylogenetic trees were evaluated with FigTree v 1.2.3 (<http://tree.bio.ed.ac.uk/software/figtree/>) and modified with CorelDraw9 (Version 9.337, Corel Corporation) (Huelsenbeck and Ronquist, 2001; Stamatakis *et al.*, 2008).

2.7. Construction of the deletion-cassette for *dhc1*

2.7.1. DNA-Isolation

Mycelium of a 200 ml liquid culture of *S. commune* 12-43 was harvested and ground in liquid nitrogen. 3 g of ground mycelium was mixed with 10 ml DNA-Extractionbuffer and incubated at 65 °C for one hour. Adjacent the sample was centrifuged at 11,000 rpm and 4 °C for ten minutes; the supernatant was transferred into a new reaction tube. Afterwards 1.4 ml 5

M NaCl and 0.1 V CTAB/NaCl was added and the sample was incubated at 65 °C for 20 minutes and adjacent cooled down on ice. The sample was mixed with 1 V chloroform and centrifuged at 11,000 rpm and 4 °C for ten minutes; the upper phase of the sample was transferred into a new reaction tube. This step was repeated three times. Afterwards 0.7 V isopropanol was added and the sample was centrifuged at 11,000 rpm and 4 °C for 30 minutes. The supernatant was removed, the DNA-pellet was cleaned with 70 % ethanol and dried in a vacuum centrifuge. The pellet was resuspended in 750 µl TE and incubated at 65 °C for five minutes. The sample was centrifuged at 11,000 rpm and 4 °C for ten minutes and the supernatant was collected in a new reaction tube. This step was repeated three times. DNA was precipitated with 2 V 98 % ethanol for 20 minutes. Adjacent, the sample was centrifuged at 11,000 rpm and 4 °C for 30 minutes. The supernatant was removed, the DNA-pellet was cleaned with 70 % ethanol and dried in a vacuum centrifuge. Pellet was resuspended in 1 ml 1 x TE and stored at -20°C.

2.7.2. Polymerase chain reaction (PCR) and agarose gel electrophoresis

A routinely used 20 µl PCR-reaction consists of 9.4 µl *Aqua dest.*, 4 µl polymerase buffer, 2 µl of each primer, 0.5 µl dNTPs, 2 µl DNA, 0.1 µl Taq-polymerase (GoTaq, Promega GmbH, Mannheim, Germany). PCR-run started with a denaturation of DNA for three minutes at 94 °C. This step was followed by 30 cycles of denaturation (30 seconds at 94 °C), annealing of primers (45 seconds at annealing temperature) and an elongation step at 72 °C for 1 min/kb. Cycles are followed by a final elongation step at 72 °C for one hour.

PCR-samples were loaded on a 1 % agarose gel. After the run, the gel was incubated in ethidiumbromide (1 µl/ 10 ml) and visualized under UV light.

If necessary, DNA bands with the expected size were extracted from the gel with Jetsorb (Genomed, Bad Oyenhausen, Germany) according to the protocol provided with the kit.

2.7.3. Cloning of PCR fragments

Amplificated fragments were cloned in the cloning vector pDrive (Qiagen, Hilden, Germany). Therefore, 2 µl amplified DNA, 2.5 µl ligation mix and 0.5 µl pDrive were incubated at 16 °C over night. Afterwards ligation reaction was stopped at 70 °C for ten minutes.

2 µl ligated sample were mixed to 100 µl electrocompetent cells of *E. coli* DH5α and added to an electroporation cuvette (Peqlab, Erlangen, Germany). In a gene pulser (E_C Apparatus

Corporation, Holbrook, USA) a voltage of 2.8 kV at 25 μ F and 220 Ω was applied to the cuvette. Adjacent the cells were resuspended in 900 μ l Standard I media and incubated at 37 °C for 30 minutes for cell reconstitution. At the end, 200 μ l of the sample were plate on Standard I plates containing Ampicillin and X-Gal. Plates were incubated at 37 °C over night.

2.7.4. Plasmidpreparation

White colonies of transformed *E.coli* cells were picked and transferred into 2 ml Standard I media containing Ampicillin. Samples were incubated at 37 °C over night. Adjacent cells were pelleted in a centrifuge for one minute at high speed. Pellet was resuspended in 200 μ l SolA. Afterwards 400 μ l SolB were added and sample was incubated at room temperature for three minutes. 300 μ l cold SolC were pipette to the mix and the sample was incubated on ice for 5 minutes. At 13,000 rpm, the sample was centrifuged for 20 minutes and the DNA containing supernatant was transferred into a new reaction tube. Subsequently, 0.7 V isopropanol was mixed to the sample to precipitate the plasmid DNA and centrifuged for 30 minutes at 13,000 rpm. Supernatant was removed and pellet was cleaned with 70 % ethanol and afterwards dried in a vacuum centrifuge. Pellet was resuspended in 40 μ l *Aqua. dest.* and stored at 4 °C.

To investigate the isolated plasmids a digestion with an appropriate restriction endonuclease followed (12,6 μ l *Aqua. dest.*, 2 μ l enzyme buffer, 0.2 μ l RNase, 0.2 μ l restriction enzyme, 5 μ l DNA) over night at 37 °C. Samples were loaded on a 1 % agarose gel. For DNA sequencing, or if especially purified DNA was needed, plasmid preparation was done with Fermentas mini (Fermentas, St. Leon-Rot, Germany) kit according to instruction manual. Sequencing was done at GATC Biotech (Konstanz, Germany) and for sequence analysis Vector NTI Advance 11.0 (Invitrogen Cooperation) was used.

Plasmid-DNA was digested with *Xba*I (12,8 μ l *Aqua. dest.*, 2 μ l B2 buffer, 0.2 μ l *Xba*I, 5 μ l DNA) for flank A and *Eco*RI (12,8 μ l *Aqua. dest.*, 2 μ l *Eco*RI buffer, 0.2 μ l *Eco*RI, 5 μ l DNA) for flank B in an over-night restriction at 37 °C. Both flanks were cloned successively in the restriction sites *Xba*I and *Eco*RI of plasmid pChi, respectively pBluescript II SK.

2.8. Transformation of *S. commune* strain after Specht *et al.*, 1988

2.8.1. Protoplast preparation

A 400 ml liquid culture of *S. commune* was allocated into sterile 50 ml reaction tubes and pelleted for five minutes at 4,000 rpm. The supernatant was removed, the mycelium was resuspended in 40 ml 0.5 M MgSO₄ and centrifuged for ten minutes at 4,000 rpm. The supernatant was removed, the pellet resuspended in 1 M MgSO₄ and again centrifuged as mentioned before. The supernatant was removed and the approximately 10 ml mycelium was solved in 10 ml 1 M MgSO₄. 100 mg/ml Caylase C3 (Cayla, France) from *Tolypocladium geodes* (0.1 g solved in 1 ml 1 M MgSO₄) was added to the solution. For transformation of strain 12-43, 100 mg/ml Novozyme 234 (InterSpex Products Inc, Foster City, USA) was used instead of Caylase C3. Mycelium was incubated at 30 °C for four hours and mixed every 30 minutes. After the digestion of the cell wall, 1 V cold *Aqua dest.* was added to mycelium to release an osmolaric shock to release protoplasts. The solution was centrifuged at 4 °C and 1,800 rpm for five minutes and the supernatant with protoplasts was collected in a new reaction tube. The mycelium was mixed with 20 ml 0.5 M MgSO₄ and again centrifuged for ten minutes at 1,800 rpm and 4 °C. Supernatant was collected again. This step was repeated three times. The protoplast solution was divided into new reaction tubes (20 ml per tube) and filled up with 1 V 1 M Sorbitol. Protoplasts were centrifuged for ten minutes at 1,100 rpm and 4 °C. The supernatant was removed and approximately 5 ml solution was left in the tube. Protoplasts were affiliated in one tube and centrifuged as mentioned above. The supernatant was removed and the protoplasts were mixed with 1 ml 0.5 M Sorbitol + 50 mM CaCl₂. Protoplasts were stored on ice at 4 °C over night.

2.8.2. Transfection of protoplasts

For transfection of protoplasts, 120 µl DNA-solution (6 µl 1M CaCl₂ and 5 µg DNA filled up with 1xTE to 120 µl) was prepared on ice. To each DNA-solution 200 µl protoplasts were pipetted. The mix was incubated on ice for 30 minutes. Afterwards 320 µl 50 % PEG-solution was added to the protoplasts and the samples were incubated on ice for one minute. Adjacent the sample was carefully mixed with the pipette and transferred into 5 ml rescue-media. Protoplasts were incubated at RT over night.

2.8.3. Inoculation of protoplasts

After melting and cooling down 5ml top-agar per protoplast sample, top agar and protoplasts were mixed and plated on MM. After an incubation of 5 to 8 days, transformants were transferred to new plates. Adjacent growing transformants were inoculated on full media plates containing bottom-agar.

2.8.4. Verification of successful transformation

Transformants were analyzed *via* PCR on the existence of the deletion cassette, respectively of the wild type gene, with the oligonucleotides *dhc1for* and *dhc1rev*. PCR-run started with a denaturation of DNA for two minutes at 95 °C. This step is followed by 30 cycles of denaturation (30 seconds at 95 °C), annealing of primers (45 seconds at 55 °C) and an elongation step (3 minutes at 72 °C). Cycles are followed by a final elongation step at 72 °C for five minutes.

2.9. Transcriptome Analysis

2.9.1. Sample preparation

Mycelium of *S. commune* was harvested and ground in liquid nitrogen. RNA was isolated according to the protocol delivered with the kit (RNeasy Plant Mini Kit, Qiagen, Hilden, Germany). RNA was stored at -80 °C.

2.9.2. Next generation sequencing via Illumina HiSeq 2000

RNA-sequencing was performed by LGC Genomics, Berlin (Germany). Therefore, a mRNA-based cDNA-library was created. Sequencing adaptors were ligated to cDNA fragments to result in 50 bp single reads of the expressed genes. After the run, adaptors were cut from the resulted reads.

2.9.3. Analysis of Raw Data

Raw data of RNA sequences were mapped against the genome of *S. commune* using the splice junction mapper TopHat (release 1.4.1). The number of reads mapped within each gene was defined with Htseq. Expression values (RPKM) for every gene was calculated using the statistical software R. For expression differences, fold changes of mean value (condition A) : mean-value (condition B) were determined. For different statistical tests, DeSeq, EdgeR,

BaySeq, and Noiseq were used to verify expression differences (Kvam *et al.*, 2012; Tarazona *et al.*, 2011). A gene was defined to be differentially expressed if each method reported differential expression (false discovery rate adjusted p-value cutoff 0.01).

2.10. Proteome analysis via 2-dimensional gelelectrophoresis

2.10.1. Sample preparation of cytoplasmatic protein

Mycelium of *S. commune* was harvested and ground in liquid nitrogen. Performance of protein isolation was modified after Bordier, 1981. 3 – 5 g mycelium was transferred into a 50 ml reaction tube, filled up to 25 ml with solution A and mixed with 10 ml solution B. The sample was incubated on ice for one hour and afterwards centrifuged at 11,000 rpm and 4 °C for 15 minutes. Supernatant was transferred into a new reaction tube. The sample was incubated at 30 °C for three minutes and adjacent centrifuged at 1,600 rpm and RT for ten minutes. The aqueous phase was transferred into a new reaction tube and filled up with 1 V precipitation buffer. The sample was incubated at 4 °C over night.

After incubation sample was centrifuged at 11,000 rpm and 4 °C for ten minutes. Pellet was separated in 1.5 ml reaction tubes and washed with acetone for four times. Afterwards pellet was dried in a vacuum centrifuge and adjacent resuspended in rehydration buffer. Sample was centrifuged for ten minutes at 13,000 rpm and 4 °C. Supernatant was transferred into new reaction tube and stored at -20 °C.

Amount of protein in the sample was defined *via* Bradford assay (1976).

2.10.2. Sample loading

To apply proteins onto an IPG-strip (Immobiline DryStrip pH 3 - 7 NL; pH 3 - 11 NL, 24 cm, GE Healthcare, Uppsala, Sweden), 250 µg protein were filled up with rehydration buffer up to a volume of 450 µl. To visualize proteins, 3 µl Coomassie Brilliant Blue was added to the mix. Protein sample was transferred into an IPG Box (GE, Healthcare, Uppsala, Sweden) and the IPG-strip was applied with gel downwards in the sample. Rehydration took place over night at RT.

2.10.3. First dimension of 2-D gelelectrophoresis

During isoelectric focusing, proteins were separated according to their isoelectric point on the IPG-strip. Therefore, strips were transferred into an Ettan™ IGPhor II™ focusing apparatus (GE Healthcare, Uppsala, Sweden). Program for isoelectric focusing was elected according to its pH-range (Tab. 5).

Table 5: Program for isoelectric focussing of IPG-strips

Step	Immobiline DryStrip pH 3 - 11 NL, 24 cm, GE Healthcare
1	4 h 300 V (gradient)
2	4 h 600 V (gradient)
3	4 h 1000 V (gradient)
4	4 h 8000 V (gradient)
5	24000 Vhr 8000 V (step)

2.10.4. Second dimension of 2-D gelelectrophoresis

The focused stripes were equilibrated for 20 minutes with solution 1 and adjacent 20 minutes with solution 2. Stripes were loaded on 10 % polyacrylamide gels. The gels were running in an Ettan™ DALTwelve chamber (GE Healthcare, Uppsala, Sweden) filled with 1x running buffer in the lower part and 2x running buffer in the upper part of the chamber. Gels were running at 1 W per gel for one hour and afterwards at 15 W per gel for four hours.

Gels were fixed for 30 minutes and stained with staining solution over night. Afterwards, gels were neutralized with Tris-base pH 6.5 for 10 minutes and destained with 25 % methanol.

Gels were scanned with an Epson Bio Step ViewPix scanner (Tokyo, Japan) and analyzed with Delta2D software v. 4.3 (Decodon, Greifswald, Germany).

2.11. Protein analysis

2.11.1. Tryptic digestion

Preparation of proteins was performed after method of Shevchenko, 1996. After washing the gels with *Aqua dest.* two times for 20 minutes, spots were picked and incubated in 200 µl 50 mM NH₄HCO₃/acetonitril 1:1 for 15 minutes. After repeating this step, protein spots were shrunk and rehydrated for four times. The spots were air dried and adjacent digested with 10 µl enzyme solution for 35 minutes on ice. After removal of the enzyme, 3 µl 25 mM NH₄HCO₃ was added and spots were incubated at 37 °C over night. Closing, the spots were resuspended in 10 µl extraction buffer.

2.11.2. Protein analysis

For analysis of proteins, 1 µl matrix was transferred to an Anchor Chip Target and mixed with 1 µl protein sample. After crystallization of the samples, proteins were analyzed on a ultrafleXtreme™ MALDI-TOF/TOF (Bruker Daltonics, Germany).

Measurement of samples was set up with flexControl software followed by analysis with flexAnalysis (both Bruker Compass 1.3). Protein peaks were assigned to software ProteinScape 2.1, which was connected to a *Schizophyllum commune*-database based on the genome sequence of *S. commune*.

fourth and the fifth AAA-module, the microtubule binding site is located at 6339 – 6714 bp. The fifth AAA-module (7137 – 7824 bp) and the sixth AAA-module (8478 – 9120 bp) do not show any Walker A structure (Fig. 9). Both genes are located on chromosome I with a distance of approximately 413 kb.

Table 6: Amino acid sequence of the first four AAA-modules of the dynein heavy chain in different species

species	p-loop in AAA1	p-loop in AAA2	p-loop in AAA3	p-loop in AAA4
<i>S. commune</i>	GPAGTGKT	GPSGSGKT	GPPGSGKT	GVSGSGKT
<i>A. nidulans</i>	GPAGTGKT	GKSGSGKS	GPPGSGKT	GVSGSGKT
<i>S. cerevisiae</i>	GPAGTGKT	GKAGCGKT	GPPGSGKT	GASRTGKT
<i>H. sapiens</i>	GPAGTGKT	GPSGSGKS	GPPGSGKT	GVSGAGKT

According to the phylogenetic tree (Fig. 11), the dynein heavy chain is highly conserved in all eukaryotic domains. Merely, the dynein heavy chain of Ascomycete yeasts is affected by a higher mutation rate, which can be deduced from long branches in the phylogenetic tree.

A split dynein heavy chain is a unique phenomenon in higher Basidiomycota. Within this group, three split events took place during evolution. The first split occurred in the group of Ustilaginomycotina, which contain usually dimorphic plant pathogens. The split point within this group is conserved between the fourth and fifth AAA module in all three species in the phylogenetic tree, where all three are smut fungi. A different split point can be seen in Wallemiomycetes, where the split is located between the first and the second AAA module. Wallemiomycetes contain only few species which are basidiomycetous molds. In Agaricomycetes and Dacrymycetes, the motor machinery is separated completely from the N-terminal region. This organization is highly conserved within this group. Both belong to the subdivision Agaricomycotina. This subdivision contains mycorrhizal fungi, wood rotting fungi and parasites which are well known because of their eye-catching fruiting bodies. In the very basal Basidiomycota shown in the phylogenetic tree, the dynein heavy chain is unsplit. Species in the phylogenetic tree belong either to rustfungi (Pucciniomycotina), which are parasites for plants, animals or fungi. The other basal group is Tremellomycetes containing the yeastlike basidiomycetes belonging to the genus *Cryptococcus*.

The organization of the distribution of *dhc1* and *dhc2* varies within the group of Agaricomycetes. Location of both genes on one scaffold indicates the location of both on one

chromosome as it is proven for *S. commune*. For some species a location on two different scaffolds occurs (Fig. 10).

In table 7, the composition of amino acids at the split point of the dynein heavy chain is shown. The last 10 aa of Dhc1 are highly conserved within Agaricomycetes, but are missing in all other investigated species in the phylogenetic tree. The first 22 aa of Dhc2 are also shown in the table. A conserved motif consisting of polar and nonpolar amino acids can be found. This motif can be found in Ustilaginomycotina, too, but at a different location within the sequence of the dynein heavy chain proteins. Additionally, other fungal domains, like filamentous ascomycetes, feature this motif less conserved in their dynein heavy chain sequence.

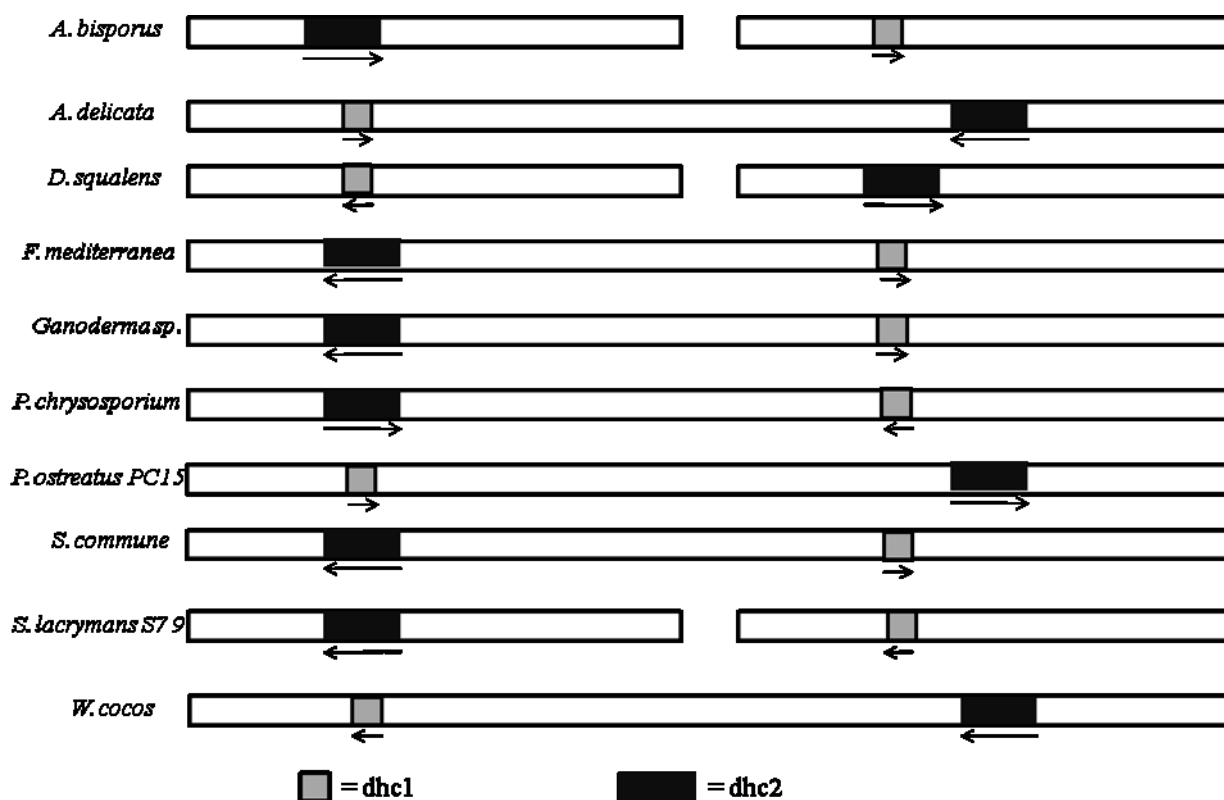


Figure 10: Gene distribution of *dhc1* and *dhc2* in elected Agaricomycetes. Arrows indicate the reading direction of the genes. Location on different scaffolds is illustrated by a split scaffold.

Table 7: Sequence of aa and the split point of Dhc1 and Dhc2. Identical aa are bold, differences in red.

Species	Dhc1	Dhc2
<i>A. bisporus</i>	EGLVGAPRRF	MEIFTP SNSSSTAAAVTFITFVQ
<i>A. delicata</i>	EGLVGAPRRF	MELIAP SNSSSTAAAVTFITFVQ
<i>D. squalens</i>	EGLVG PPRRF	MELLAP SNSSSTAAAVTFITFVQ
<i>F. mediterranea</i>	EGLQ GAPRRF	MEVRLEVA FASPNSSTAAAVTFITFVQ
<i>Ganoderma spec.</i>	EGLVGAPRRF	MELLAP SNSSSTAAAVTFITFVQ
<i>P. chrysosporium</i>	EGLVGAPRRF	MSMEVLAP SNSSSTAAAV Q FITFVQ
<i>P. ostreatus</i>	EGLVG G VRRF	MEAFAS SNSSSTAAAV Q FITFVQ
<i>S. commune</i>	EGLVGAPRRF	MPQATAS PNSSSTAAAVTFITFVQ
<i>S. lacrymans</i>	EGL LGG TRRF	MEAFSP STSSSTAAAVTFITFVQ
<i>W. cocos</i>	EGLVGAPRRF	MELLTSS SNSSSTAAAVTFITFVQ
<i>U. maydis</i>		RVELE QHSIEGS STA Q AVTFITFVQ
<i>W. sebi</i>		RYELE TQSIEGS ST VQ AVSFITFVQ
<i>S. roseus</i>		RHDLE QHSIETS STA AT VTFITFVQ
<i>N. crassa</i>		RKDLE GQAMTAN ST AEAVR FITIVQ
<i>A. fumigatus</i>		RHDLE GKSLDAS STA HAVS FITIVQ

3.2. Localization of Dhc1 and Dhc2 in hyphae

The proteins Dhc1 and Dhc2 are cytoplasmatic proteins. With specific antibodies for Dhc1 and Dhc2, both proteins were visualized in the cell. A higher abundance of Dhc1 compared to Dhc2 can be observed. Co-localization of both proteins appears at some places in the cell and in association to nuclei (Fig. 12, 13). Co-localization is an important hint, that both proteins could form a complex to migrate into the the nucleus to fulfill their function during the cell cycle.

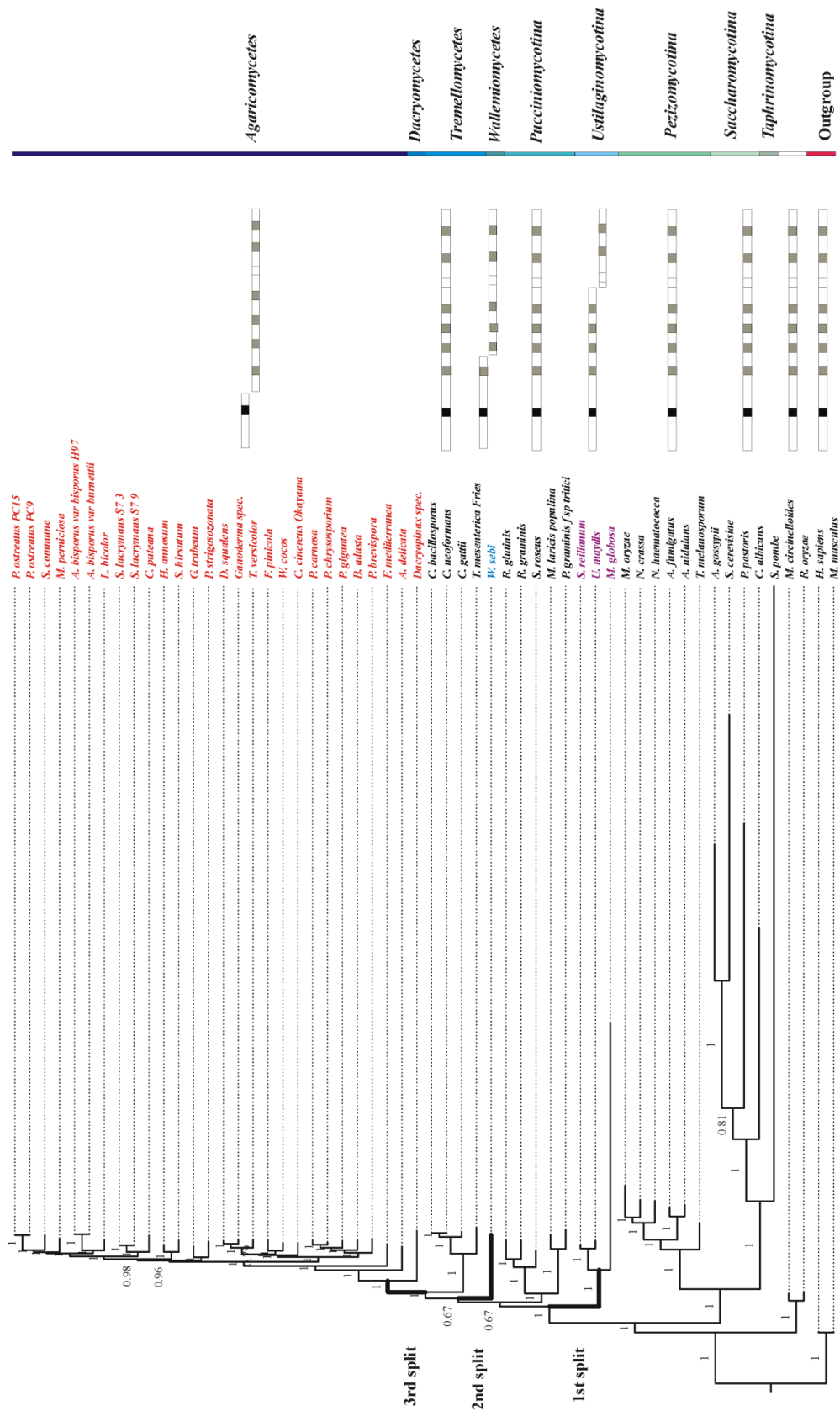


Figure 11: Phylogeny of the dynein heavy chain. Amino acid sequence of the dynein heavy chain of all organisms present in the phylogenetic tree, were aligned and used for calculation of their phylogeny.

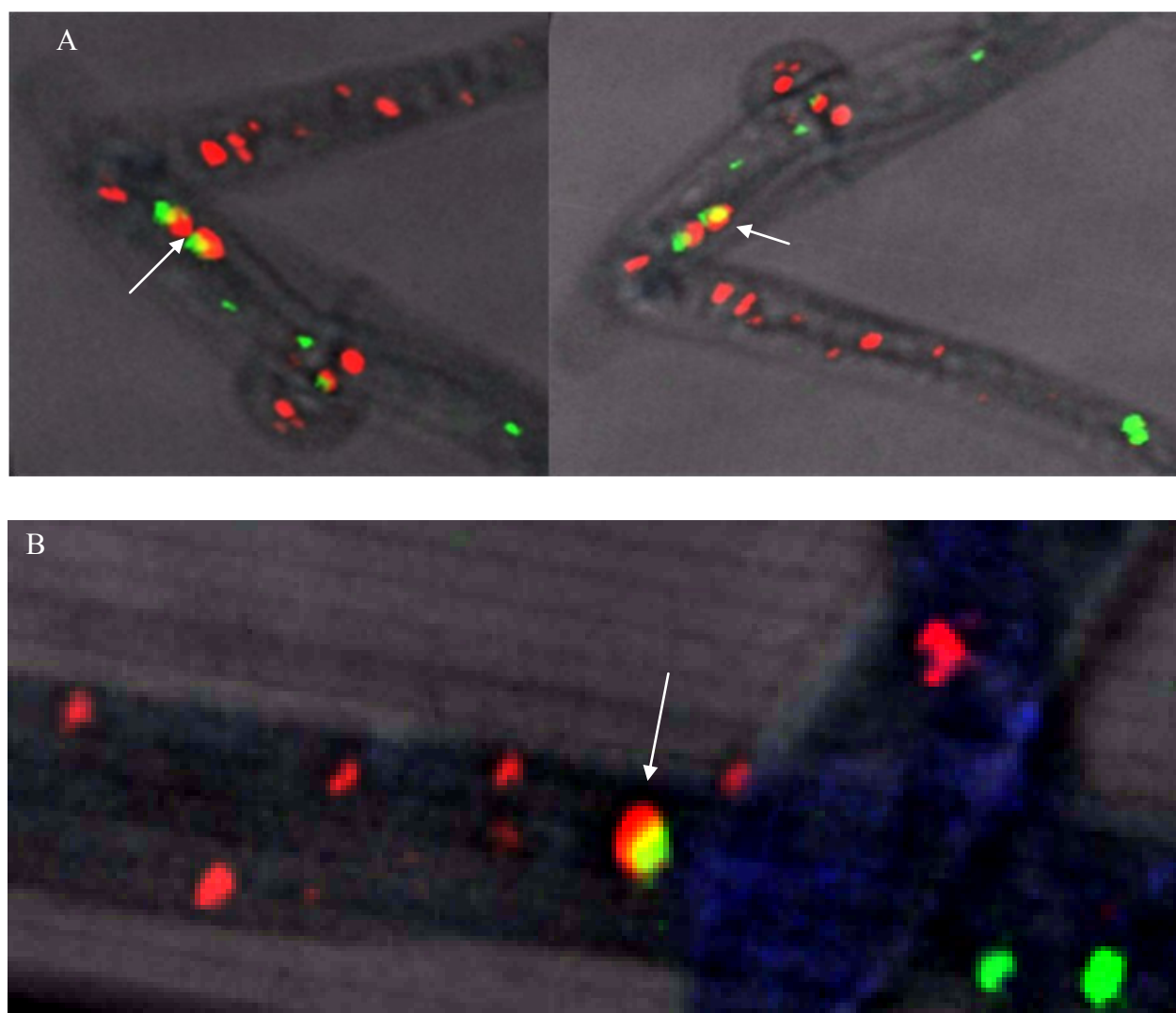


Figure 12: Threedimensional image of a hyphae of *S. commune*. Dhc1 TRITC-labeled (Filter BP 560-615; Laser 543 nm 22.0 %), Dhc2 FITC-labeled (Filter BP 505-530; Laser 488 nm 7.0 %). A) dikaryotic hyphae with a co-localization of Dhc1 and Dhc2 (arrows). B) detailed view on a co-localized Dhc1-Dhc2-“complex” in a hypha of *S. commune* (arrow).

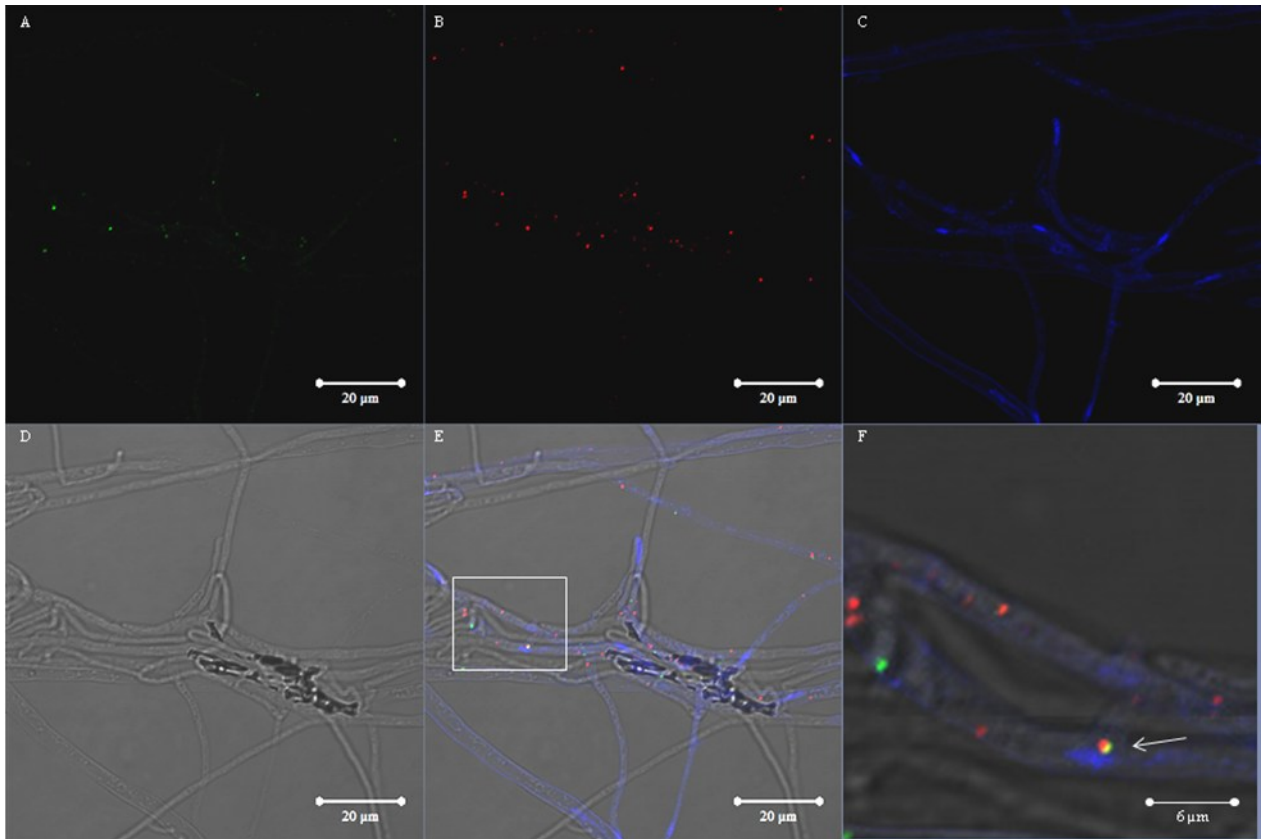


Figure 13: Localization of Dhc1 and Dhc2 in the cytoplasm of hyphae of *S. commune* 12-43. **A)** Dhc2 FITC-labeled (Filter BP 505-530; Laser 488 nm 7.0 %), **B)** Dhc1 TRITC-labeled (Filter BP 560-615; Laser 543 nm 22.0 %), **C)** DAPI staining (Filter BP 420-480; Laser 405 nm 5.0 %), **D)** brightfield image, **E)** merge of images A to D, **F)** detail of co-localization of Dhc1 and Dhc2 close to nucleus.

3.3. Deletion of *dhc1*

To create a dynein heavy chain 1 knock-out strain, a deletion cassette was constructed to replace the *dhc1* gene by the autotrophy marker gene *ura1* of *S. commune*. Flanks upstream and downstream of *dhc1* were amplified via PCR. The 1585 bp large Flank A contains 585 bp of *dhc1* and was amplified with primers dhc1AaXbaI and dhc1AbXbaI. The product was restricted with *XbaI* and cloned into the *XbaI* restriction site of vector pChi, which already contained the *ura1* marker gene of *S. commune*. Construct FlankA-ura1 was subsequently cloned into *BamHI* and *NotI* restriction sites of vector pBluescript II SK. Flank B (1.699 kb), which contained 699 bp of *dhc1* was amplified with primers dhc1Ba and dhc1Bb. It was cloned into the *EcoRI* restriction site of pBluescript II SK. The final deletion plasmid p Δ *dhc1* was used for transformation of *S. commune* strain 12-43 and Δ ku80 (Fig. 14).

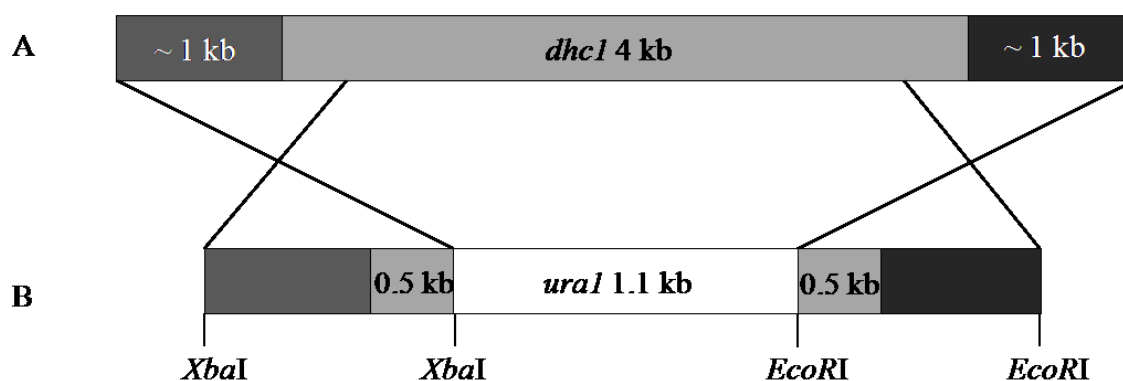


Figure 14: Deletion plasmid $p\Delta dhc1$. A) Wildtype gene *dhc1* with flanking regions upstream and downstream; B) deletion cassette in $p\Delta dhc1$.

Through protoplast transformation of strains $\Delta ku80$ and 12-43, 8 possible knock-out mutant strains could be generated. Transformant 1-7 were derived from strain $\Delta ku80$ and transformant 8 from 12-43. With the first PCR using primers *dhc1for* and *dhc1rev*, the amplification of either the wildtype gene (2.9 kb) or the integrated deletion cassette (1.5 kb) was proven (Fig. 15). An ectopic integration of the deletion cassette results in 2 bands in the agarose gel, whereas only one band at 1.5 kb indicates a knock-out event (Fig. 16).

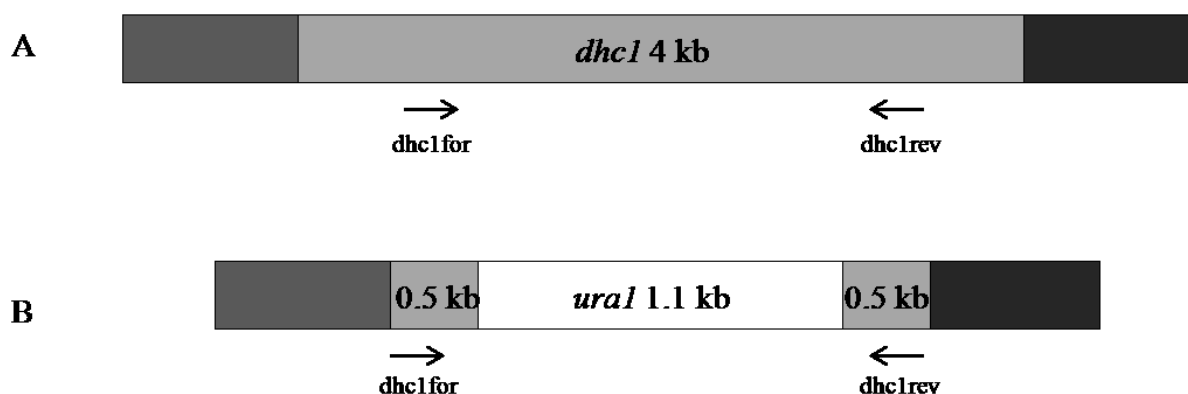


Figure 15: PCR strategy to prove the integration of the deletion cassette in the genome of *S. commune*

The second strategy was composed of testing the replacement of *dhc1* by *ura1* based on a nested PCR. First, a 6 kb and a 7 kb fragment, containing either the wildtype gene or the deletion cassette for *dhc1*, were amplified with primers *dhc1up* and *dhc1down*. This fragment was used as a template for the downstream PCR. For this second PCR, oligonucleotides *urafor* and B-test amplifying a 905 bp large fragment of the deletion cassette were used (Fig.17).

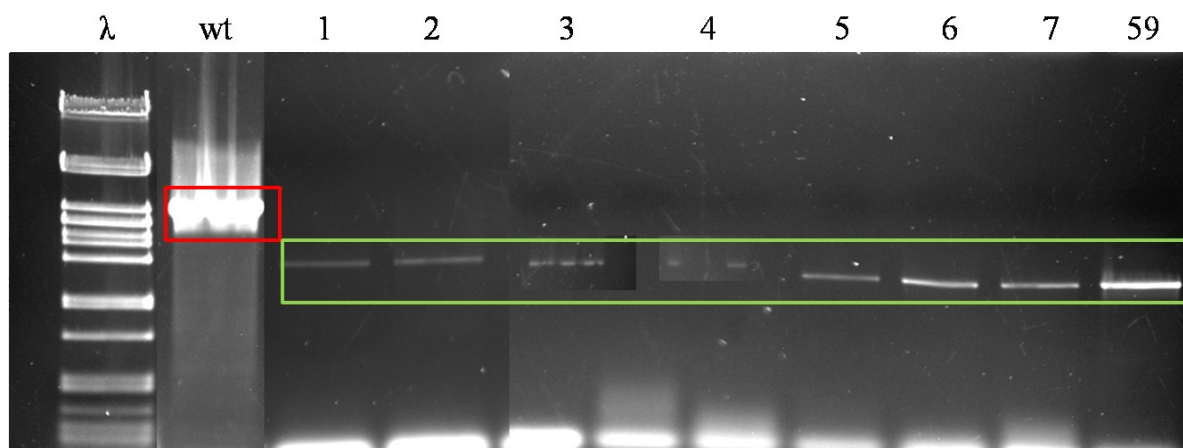


Figure 16: Illustration of PCR results to amplify the deletion cassette fragment. In the wildtype, the 2.9 kb band was amplified (red). In the transformants, the 1.5 kb fragment of the deletion cassette was amplified (green). PCR results were obtained from several runs.

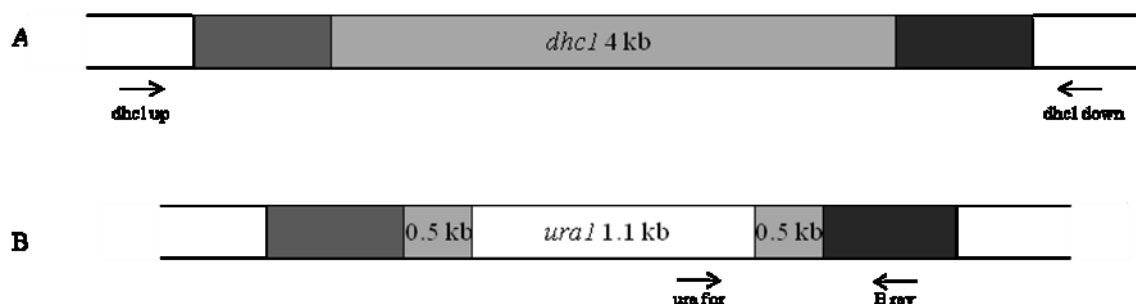


Figure 17: PCR strategy to show the replacement of the wildtype gene with the marker gene *ura1* A) first PCR sample to amplify the first target for the nested PCR; B) second PCR sample to amplify a fragment of the deletion cassette within the target DNA

The first PCR gave a result at the expected size for every tested strain. In the second PCR, a fragment with the expected size was amplified in all tested mutant strains. These mutant strains contain the deletion cassette at the correct position in their genome and are therefore *dhc1* knock-out strains. In the two wildtype strains, no DNA-fragment was amplified, which shows that *dhc1* is still intact (Fig. A1).

Via two independent PCR experiments with different strategies and in Southern hybridization (data shown in Mai, 2012), it could be shown that the deletion cassette was integrated in the genome of *S. commune* after transformation and replaced the gene *dhc1*.

3.4. Characterization of $\Delta dhc1$ knock-out strains

In total, 8 $\Delta dhc1$ strains were obtained, 7 from the transformation of the strain $\Delta ku80$ and one from the transformation of wildtype strain 12-43. Transformants, which have $\Delta ku80$ as parental strain, are named $\Delta dhc1_1$, $\Delta dhc1_2$, $\Delta dhc1_3$, $\Delta dhc1_4$, $\Delta dhc1_5$, $\Delta dhc1_6$, $\Delta dhc1_7$. The transformant which resulted from the transformation of strain 12-43 is named $\Delta dhc1_{59}$.

By comparing the colony shape of the mutant strains with the parental strain, no differences can be seen, except a slightly reduced formation of aerial mycelium in strains $\Delta dhc1_4$ and $\Delta dhc1_5$, a feature often associated with transformation or protoplasting and regeneration. Additionally, hyphal growth is not differing in mutants and the parental strain. The growth rate, as well, is similar to the progenitor (Fig. 18). A production of an indole-dye as a circle at the colony edge was observed in all mutants after long-term storage. This phenomenon did not occur in the wildtypes.

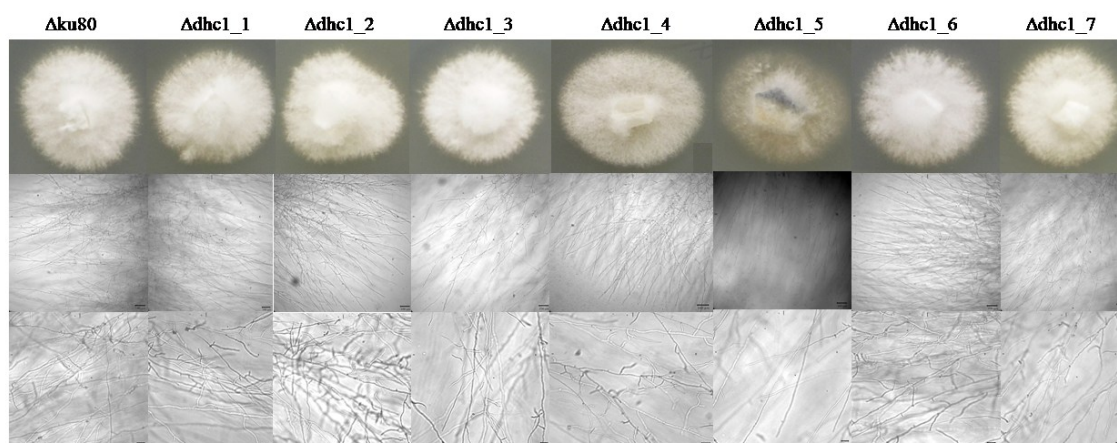


Figure 18: Colony morphology of transformants obtained from $\Delta ku80$. In the second and third row, hyphae of the investigated strains are shown, with a higher magnification in the third row.

Strain 12-43 has a fluffy colony structure and hyphae grow straight on the medium-surface. In contrast, $\Delta dhc1_{59}$ produces a high amount of aerial mycelium before it starts growing on the circumfluent medium (Fig. 19). After five days of incubation at 30 °C, the wildtype colony had covered an area of $9.5 \pm 0.6 \text{ cm}^2$, while knock-out mutants only reached $3.27 \pm 0.29 \text{ cm}^2$. Thus, growth was reduced 2.91-fold.

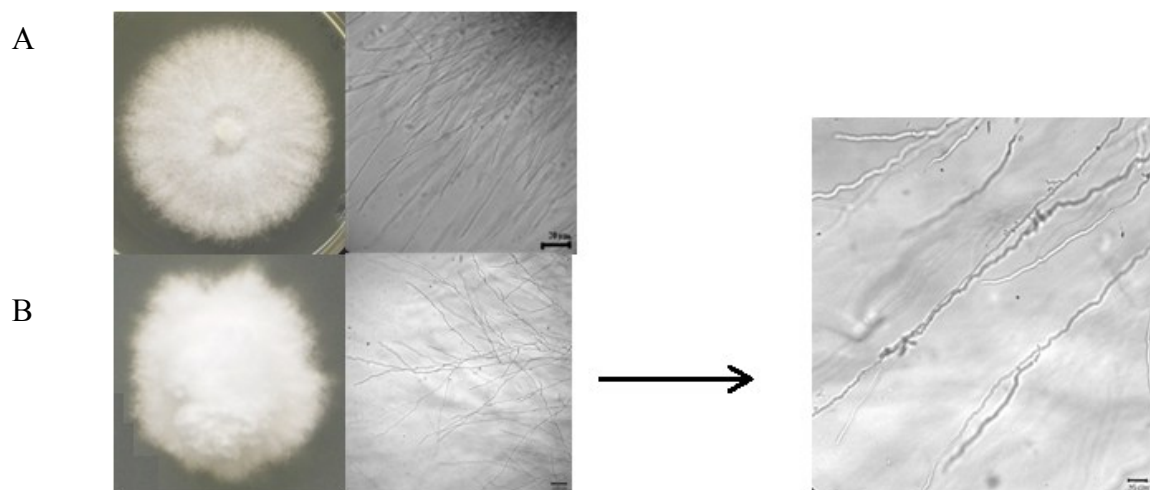


Figure 19: Colony morphology of transformant obtained from 12-43. In row A the wildtype colony and hyphal structure is shown. In row B strain $\Delta dhc1_{59}$ colony and hyphal structure can be seen. In picture C a detailed view on hypha of $\Delta dhc1_{59}$ show their curled growth, which is not present in strain 12-43.

3.4.1. Cell length is reduced in $\Delta dhc1$ strains

For analysis of cell sizes, 100 tip cells and 100 hyphal cells were measured for length. Three different strains were chosen according to their macroscopic shape: strain $\Delta dhc1_1$ and $\Delta dhc1_2$ show a similar shape, while $\Delta dhc1_5$ differs slightly from the other obtained mutants. In all mutant strains, a reduction of cell length was observed. While in the mutants, the cell length hardly reaches more than 200 μm , tip cells in the wildtype $\Delta ku80$ can reach a length up to 450 μm and more (Fig. 20).

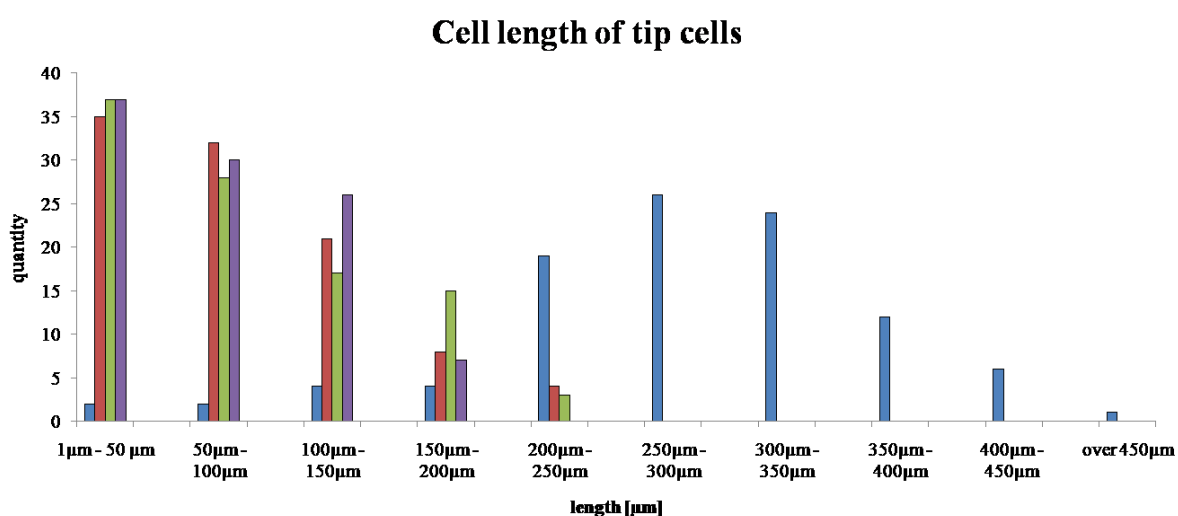


Figure 20: Diagram showing the cell length of tip cells (wildtype = blue, $\Delta dhc1_1$ = red, $\Delta dhc1_2$ = green, $\Delta dhc1_5$ = violet)

This effect can be seen also in hyphal cells. In the mutant strains, cells are not larger than 150 μm . In the wildtype, a few cells larger than 150 μm were documented (Fig. 21).

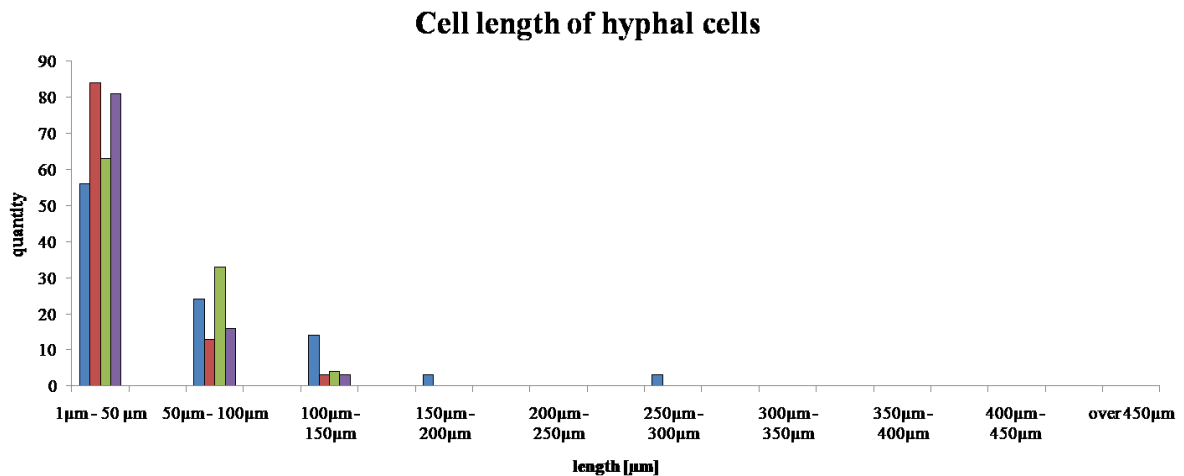


Figure 21: Diagram showing the cell length of hyphal cells (wildtype = blue, $\Delta dhc1_1$ = red, $\Delta dhc1_2$ = green, $\Delta dhc1_5$ = violet)

In the $\Delta dhc1_{59}$ a reduction of cell length was observed. Most cells are between 1 and 150 μm large. Cell length hardly reaches more than 300 μm . Tip cells in the wildtype 12-43 can reach a length up to 450 μm and more (Fig. 22).

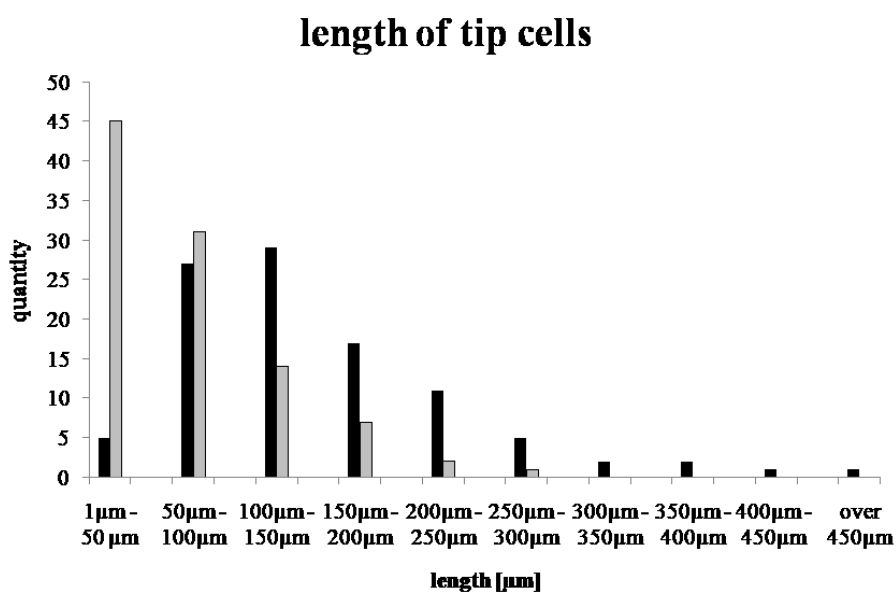


Figure 22: Diagram showing the cell length of tip cells (wildtype = black, $\Delta dhc1_{59}$ = grey).

This effect can be seen also in hyphal cells. In the mutant strains, cells are not larger than 150 μm , which was seen only for a small amount of cells. Most cells are short – only between 1 and 100 μm . In the wildtype strain cells can reach a length up to 350 μm with the highest amount of cells between 50 and 200 μm in length (Fig. 23).

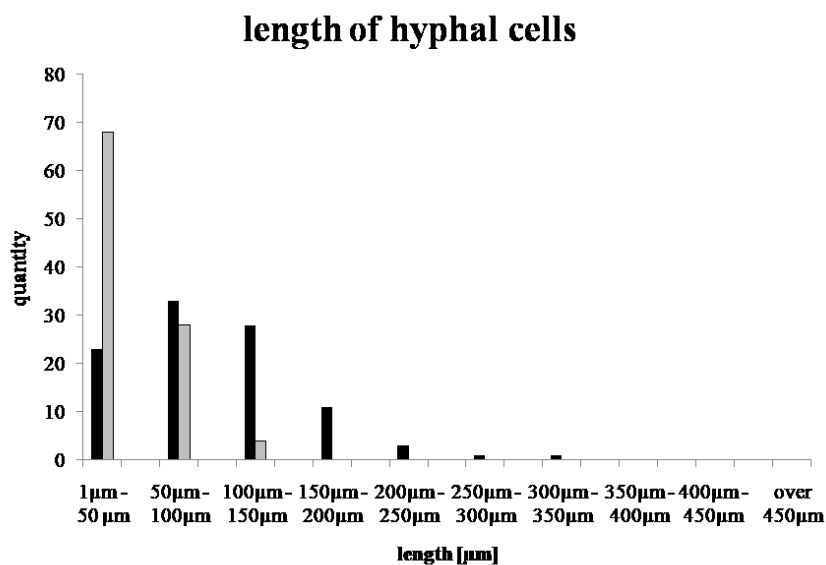


Figure 23: Diagram showing the cell length of hyphal cells (wildtype = black, $\Delta dhc1_{59}$ = grey).

3.4.2. Nuclear position changes in deletion mutants lacking *dhc1*

The distribution of nuclei was observed in 100 tip and 100 hyphal cells of the wildtype $\Delta ku80$ and the $\Delta dhc1$ strains 1, 2 and 5. Nuclei in wildtype cells are located directly in the center of the cell, with only very few deviations. In the $\Delta dhc1$ strains, the differences in nuclei distribution are obvious (Fig. 24).

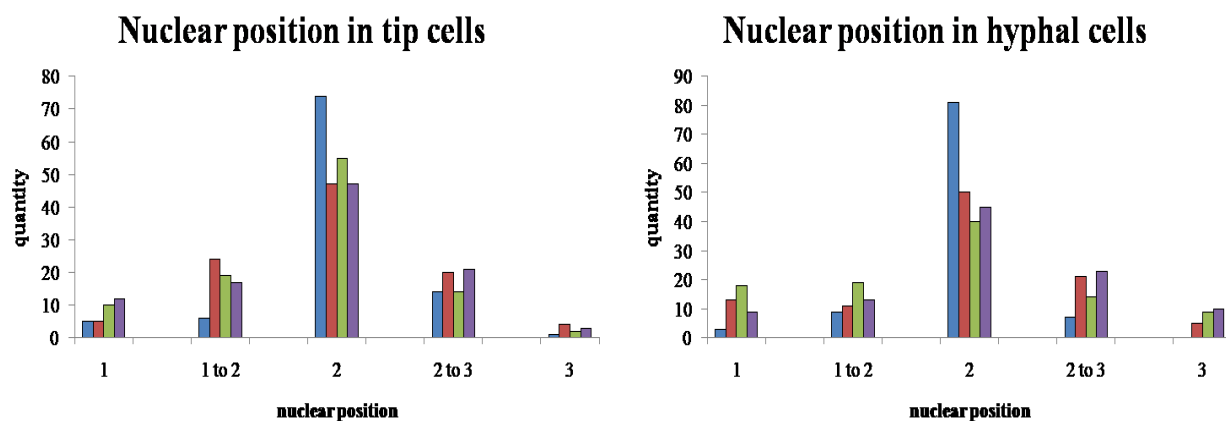


Figure 24: Diagram showing the nuclear position in the investigated strains. In tip cells, measurements were taken from the septa towards the tip, in hyphal cells from septa to septa. Position 1 shows the location of the nucleus close the old septa. Position 3 indicates a location at the tip, respectively at the new septa. (wildtype = blue, $\Delta dhc1_1$ = red, $\Delta dhc1_2$ = green, $\Delta dhc1_5$ = violet)

The distribution of nuclei was observed in 100 tip and 100 hyphal cells of the wildtype 12-43 and the $\Delta dhc1_59$. Nuclei in wildtype cells are located directly in the center of the cell with only very few meanderings. In $\Delta dhc1_59$ nuclei are distributed all over the cell, although the majority of cells contain the nucleus also in the center (Fig. 25).

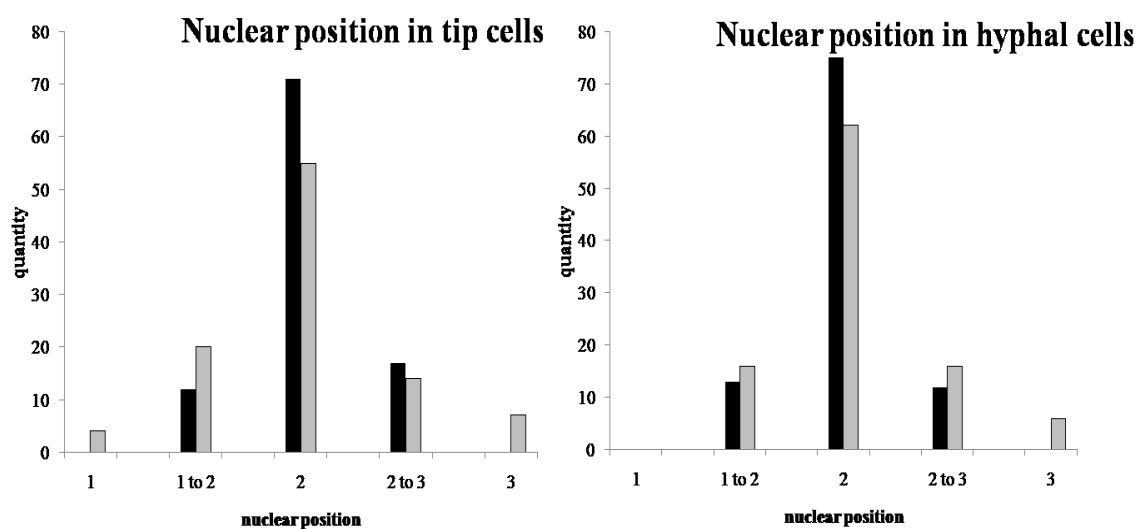


Figure 25: Diagram showing the nuclear position in the investigated strains. In tip cells, measurements were taken from the septa towards the tip, in hyphal cells from septa to septa. Position 1 shows the location of the nucleus close the old septa. Position 3 indicates a location at the tip, respectively at the new septa. (wildtype = black, $\Delta dhc1_59$ = grey).

3.4.3. Additional anomalies in the $\Delta dhc1$ strains

In microscopic investigations, several other characteristics were documented: a) $\Delta dhc1$ strains show a spherical, hyphal growth (Fig. 26); b) hyphae grow in coils in all investigated strains (Fig. 27); c) all strains show an increased branching rate (Fig. 28) and d) all investigated strains produce cells which contain more than one nucleus (Fig. 29).

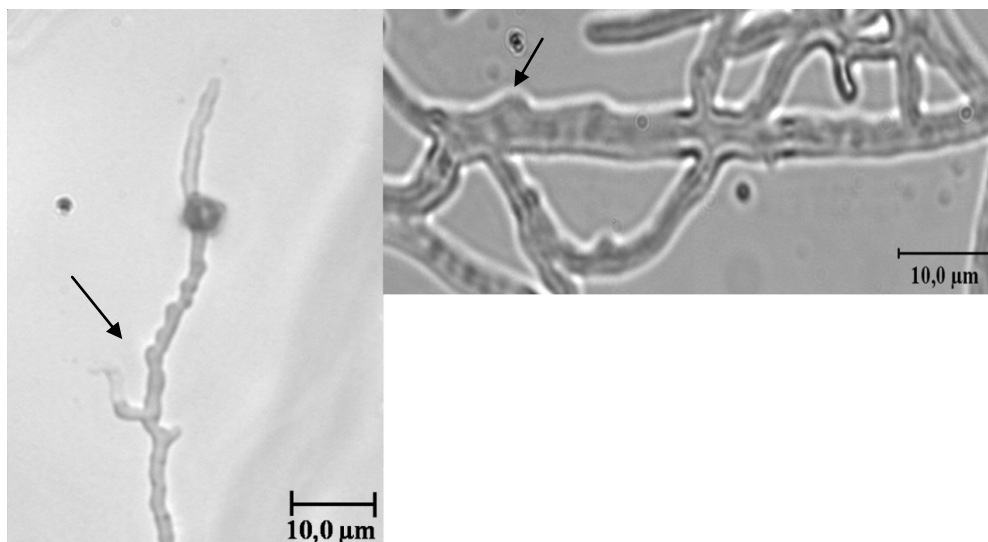


Figure 26: Protuberances at hyphae of $\Delta dhc1$ strains (arrow). A) strain $\Delta dhc1_{59}$ with a strong effect of spherical, hyphal growth. B) strain $\Delta dhc1_5$ showing less protuberances. For strain $\Delta dhc1_1$ see figure 29 A.

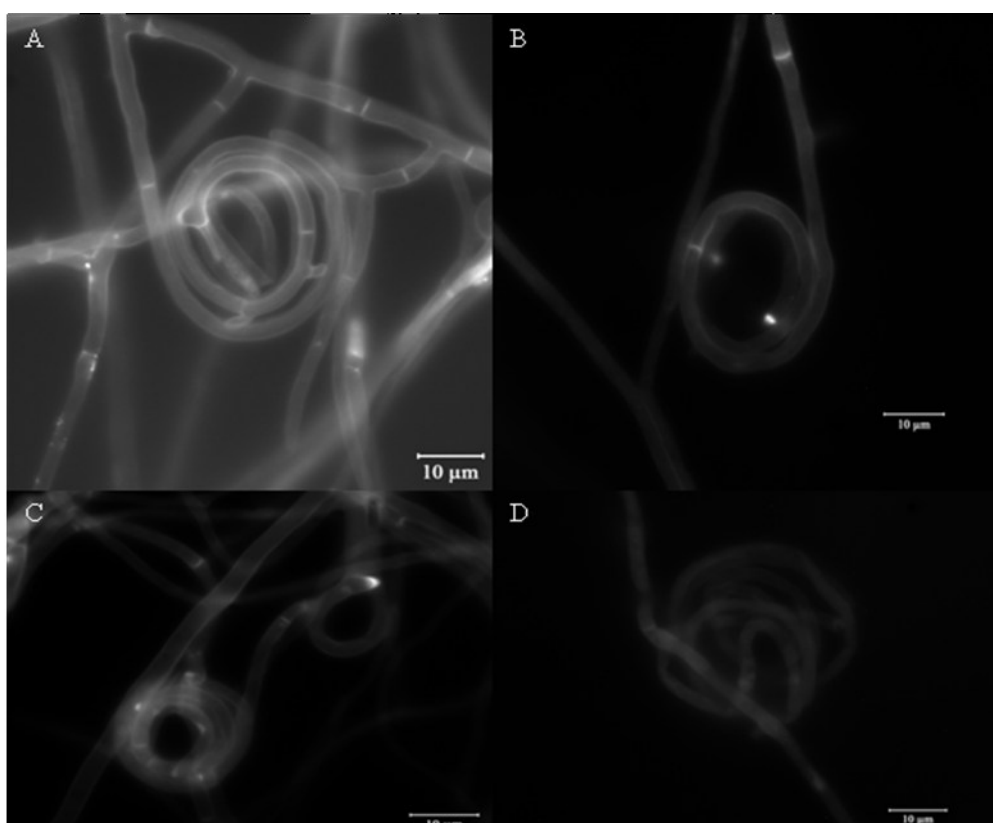


Figure 27: Coil formation in $\Delta dhc1$ strains. A) $\Delta dhc1_1$; B) $\Delta dhc1_2$; C) $\Delta dhc1_5$; D) $\Delta dhc1_{59}$.

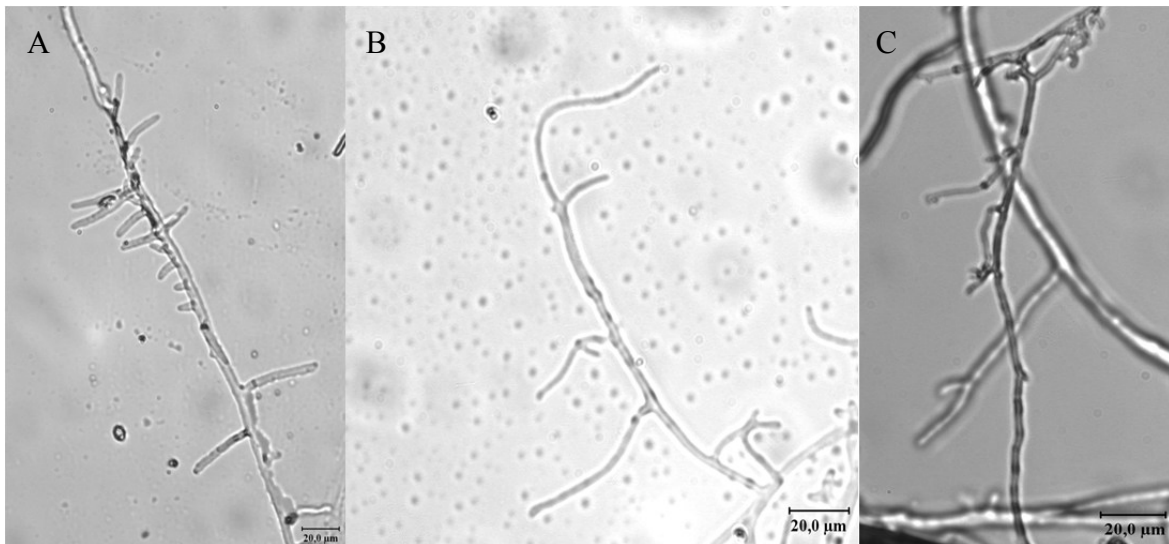


Figure 28: Hyper branching effects in $\Delta dhc1$ strains. A) $\Delta dhc1_1$; B) $\Delta dhc1_2$; C) $\Delta dhc1_{59}$.

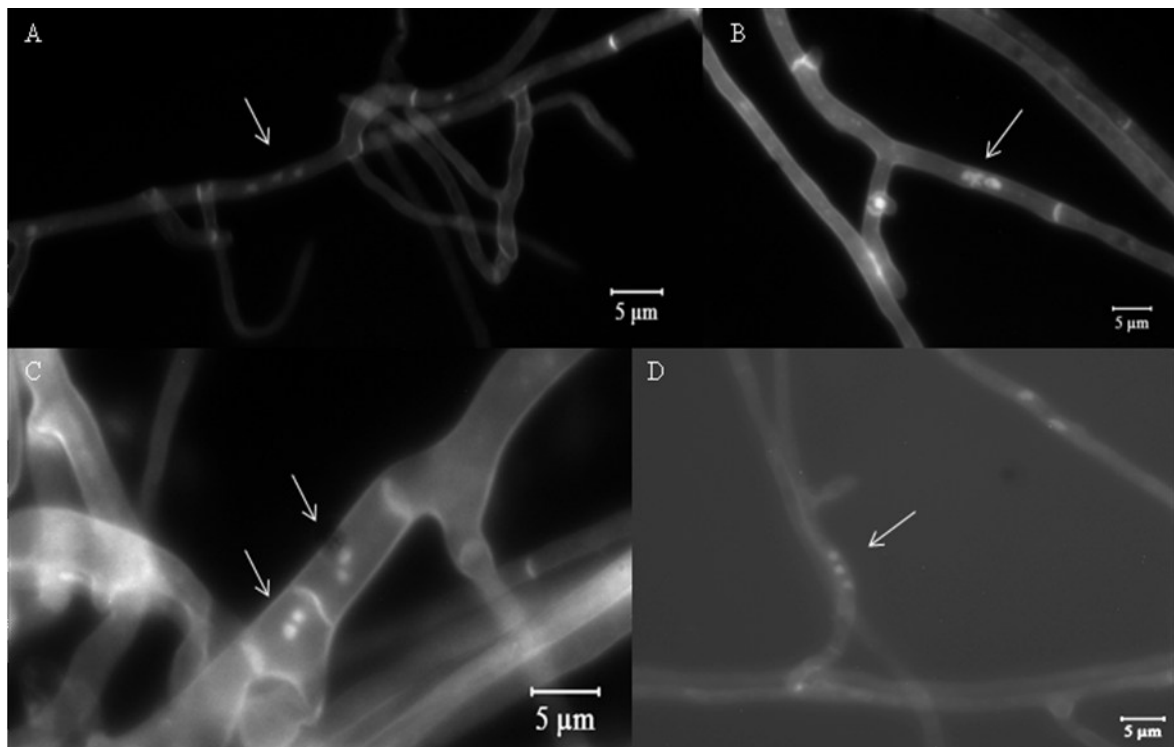


Figure 29: Bi – and Multinuclear cells in $\Delta dhc1$ strains. A) $\Delta dhc1_1$; B) $\Delta dhc1_2$; C) $\Delta dhc1_5$; D) $\Delta dhc1_{59}$.

3.4.4. Mating and sexual development

In a confrontation assay of a *dhc1* deletion strain with a compatible wildtype, strain T41, it was possible to observe fruiting bodies on both sides. The $\Delta dhc1$ strains are therefore able to accept and donate nuclei. On the wildtype side, typical *S. commune* fruiting bodies can be seen, which are unstiped and show a normal gill development. Fruiting bodies on the mutant side have a stem of approximately 1 cm length and lower gill formation (Fig. 30). Spores were produced from both fruiting body groups.

Strain $\Delta dhc1_{59}$ is also able to donate and accept nuclei. A stable dikaryon can be formed with a compatible mating partner. A higher amount of clamps was investigated in the mutant strain (Fig. 31 A). Under optimal conditions also fruiting bodies can be formed. These fruiting bodies are very small and not fully opened after 10 days after primordial appearance. No gills were seen in these fruiting bodies (Fig. 31 B).

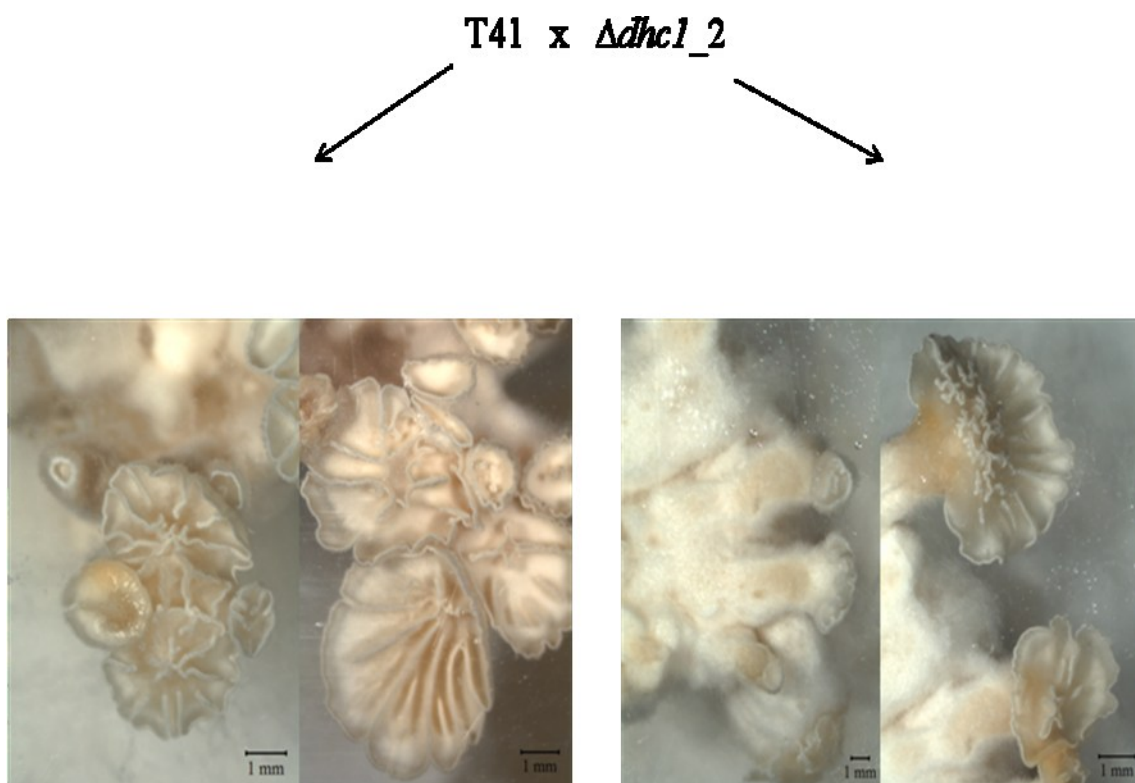
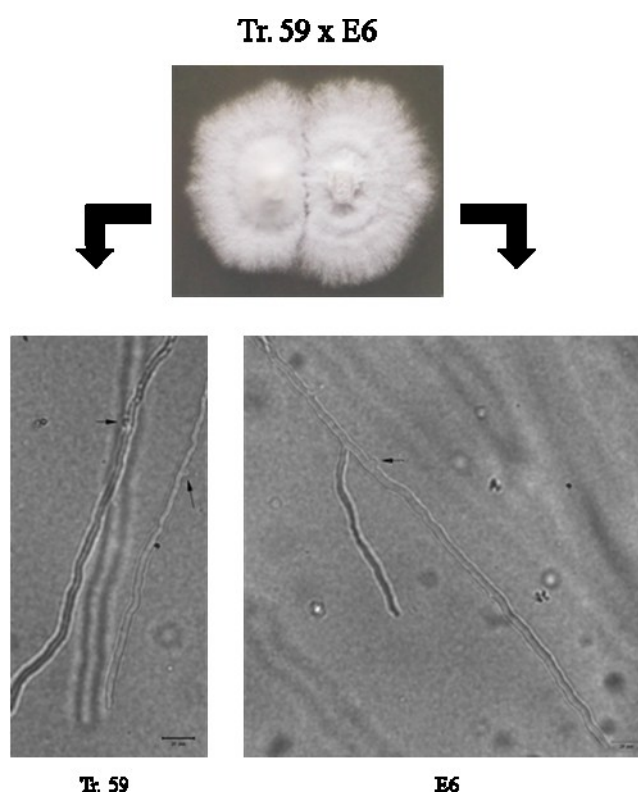


Figure 30: Fruiting body formation of the compatible mating interaction between wildtype T41 and $\Delta dhc1_2$.

A)



B)



Figure 31: Mating experiments between a compatible wildtype and $\Delta dhc1_{59}$. A) Formation of a dikaryon after 3 days of growth. Arrows are indicating clamp cell formation in both mating partners. After dikaryotization, strain $\Delta dhc1_{59}$ shows the phenotype of the wildtype B) Fruiting bodies in an early strage after 14 days of growth.

3.4.5. Comparison of $\Delta dhc1$ strains with $\Delta dhc2$

The phenotype of $\Delta dhc1$ strains can be compared to the already existing $\Delta dhc2$ strains. Similarities and differences are summarized in Table 8.

Table 8: Similarities and differences in dynein heavy chain deletion mutants

	$\Delta dhc1$ obtained from $\Delta ku80$	$\Delta dhc1$ obtained form 12-43	$\Delta dhc2$
strains viable?	yes	yes	yes
colony	- growth rate is not reduced - colony shape is varying between the single transformants	- 3 fold reduced growth rate - increase in aerial mycelium - fluffy colony structure	- 4 fold reduced growth rate - decrease in aerial mycelium - dense colony structure
hyphae	- curled hyphae with non polarized growth - blistered	- curled hyphae with non polarized growth - blistered	- curled hyphae with non polarized growth
cell length	- reduced compared to wild type	- reduced compared to wild type	- reduced compared to wild type
nucleus	- position varies in every cell	- position varies in every cell	- position varies in every cell
mating behaviour	- formation of a full dikaryon with a compatible mating partner	- formation of a full dikaryon with a compatible mating partner	- only donation of nuclei to mating partner
fruiting bodies	- fruiting bodies form a stem and less gills	- fruiting bodies are very small and not fully developed under given conditions	- normal fruiting body production on the mating partner side
spore production	- both mating partner produce spores	- no spore production observed under given conditions	- spore production only by mating partner

3.5. Transcriptome analysis *via* RNA-sequencing

For transcriptome studies, the two wildtype strains 12-43 and E6 and the deletion mutant $\Delta dhc2$ were used in RNA-sequencing experiments. For strain 12-43, a total mapping of 68.9 % was reached with a spliced mapping of 7.3 %. For strain E6, total mapping of 69 % and spliced mapping of 7.2 % were observed. In the mutant, total mapping reached 73.3 % and spliced mapping of 7.6 %.

The three investigated strains 12-43, E6 and $\Delta dhc2$ of *S. commune* were used to analyze differentially expressed genes. Approximately 14650 genes could be identified *via* RNA sequencing in every tested strain. Differential expression of genes in the different conditions compared (see table 9), was determined for approximately 13600 genes. A gene was accepted

as differentially expressed, if all four statistical tests (DeSeq, EdgeR, BaySeq, and Noiseq) confirm the fact. In a comparison of two wildtypes, 642 genes show differences in expression. 12-43 compared to $\Delta dhc2$ features 734 differentially expressed genes, while E6 vs. $\Delta dhc2$ shows 726 genes with an up- or down-regulated expression in the mutant (Tab. 9).

Table 9: Number of genes identified to be differentially expressed

	12-43 vs. E6	12-43 vs. $\Delta dhc2$	E6 vs. $\Delta dhc2$
differentially expressed genes identified in total	13596	13545	13580
4 statistical tests TRUE	642	734	726
3 statistical tests TRUE	1221	1267	1775
2 statistical tests TRUE	2377	2500	3839
1 statistical test TRUE	1419	1234	1244
no statistical test TRUE	7937	7810	5996

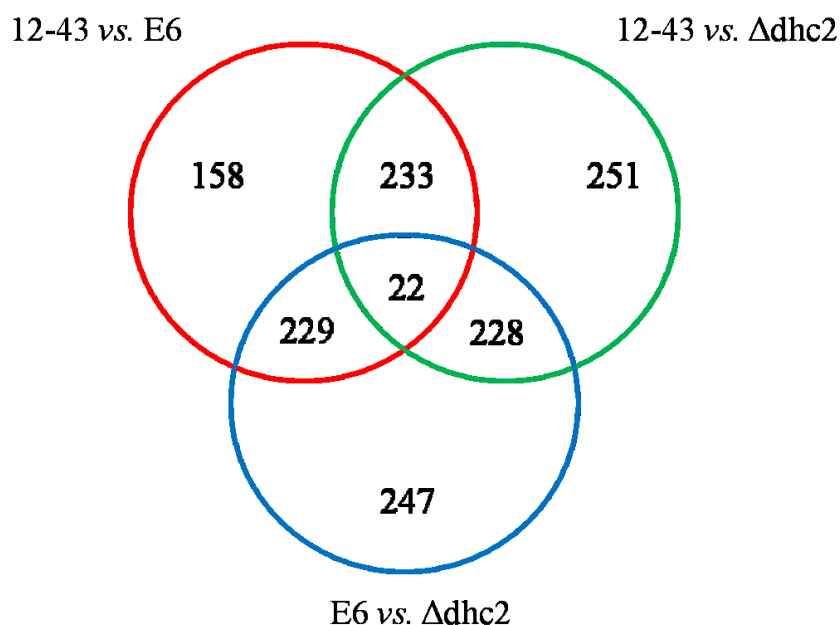


Figure 32: Venn diagram of RNA-Sequencing. Differentially regulated genes in the comparison 12-43 vs. E6 are in red, 12-43 vs. $\Delta dhc2$ are in green and E6 vs. $\Delta dhc2$ are marked in blue. The 22 genes in the center of the diagram indicate the genes which are differentially regulated in all comparisons, respectively in all 3 strains.

The Venn diagram (Fig. 32) shows 22 genes which are differentially regulated in all three investigated conditions, with nine of them not yet having been annotated in *S. commune*. For four genes, annotations in other basidiomycetes were found. The two identified WSC-domain-containing genes gave hits in several basidiomycetes, e.g. in *C. cinerea*, that one can emanate from the sameness in *S. commune*. The annotated genes are coding mainly for extracellular proteins or are involved in pathways of protein secretion or secretion of organic matter (Tab. 10).

Table 10: 22 differentially regulated genes in all three strains. Non-annotated genes are indicated with /. For details see discussion and table A2.

Accession number	Gene	NCBI blast
1037942	/	no result found in other fungi
1038458	Major facilitator superfamily MFS-1	
1039406	/	Proteophosphoglycan ppg4 (<i>R. glutinis</i>)
1081190	/	Actin-like ATPase domain-containing gene (<i>A. delicata</i>)
1082687	Cutinase	
1105422	Glycoside hydrolase, family 61	
1135605	/	no result found in other fungi
1151728	NmrA-like	
1187228	/	WSC-domain-containing gene, identified in several fungi
1188048	/	no result found in other fungi
1189960	/	no result found in other fungi
1191755	/	no result found in other fungi
1212538	Cytochrome P450	
1213381	Heat shock protein Hsp20	
1215940	Thaumatin, pathogenesis-related	
1340620	Glutathione S-transferase, C-terminal	
1359387	/	WSC-domain-containing gene, identified in several fungi
235431	Glycosyl hydrolase, family 13, catalytic region	
54466	Glycoside hydrolase, family 61	
56366	Glycoside hydrolase, family 16	

64748	Peptidase M14, carboxypeptidase A	
66483	Glycoside hydrolase, family 20, catalytic core	

3.5.1. Detailed investigation of $\Delta dhc2$

Protoplasts of strain 12-43 were transformed with the deletion plasmid p $\Delta dhc2$. To avoid possible lethality of that knock-out, a stable dikaryon was produced by adding macerated mycelium of the compatible strain E6 to the transfected protoplasts. The resulting dikaryon produced fruiting bodies and spores, which were plate on selective medium.

S. commune strains with a deletion in *dhc2* showed different phenotypes. The fluffy colony structure of wildtype colonies was altered to yield a very dense and granular structure with less aerial mycelium. The growth rate of the mutant strain is 4 fold reduced; hyphae spread sinuously and undirected on the media. Cells in $\Delta dhc2$ are truncated, and a defect in nuclear positioning was observed. Additionally, the acceptance of nuclei from a mating partner failed.

250 genes have a different expression in $\Delta dhc2$ (Fig. 33). Many genes are not annotated or do not have a classification on the *S. commune* homepage. Most differentially expressed genes with a clear function are localized in metabolic pathways.

From the 250 genes, 163 genes are annotated. 110 of these genes can be assigned to a pathway by KOG (Fig. 34), while 53 genes have no classification for KOG. A high amount of genes show a predicted function only. Also in metabolic pathways, a high amount of genes were differentially expressed.

However, the deletion of *dhc2* is not lethal, as has been described for other basidiomycetes. *Via* RNA-sequencing of 12-43, E6 and $\Delta dhc2$, an up-regulation of motor proteins kinesin-2 (4.6 fold upregulated in $\Delta dhc2$) and kinesin-14 (9.2 fold upregulated in $\Delta dhc2$) was detected in strain $\Delta dhc2$ compared to 12-43. Both kinesin genes are microtubule-associated motor proteins.

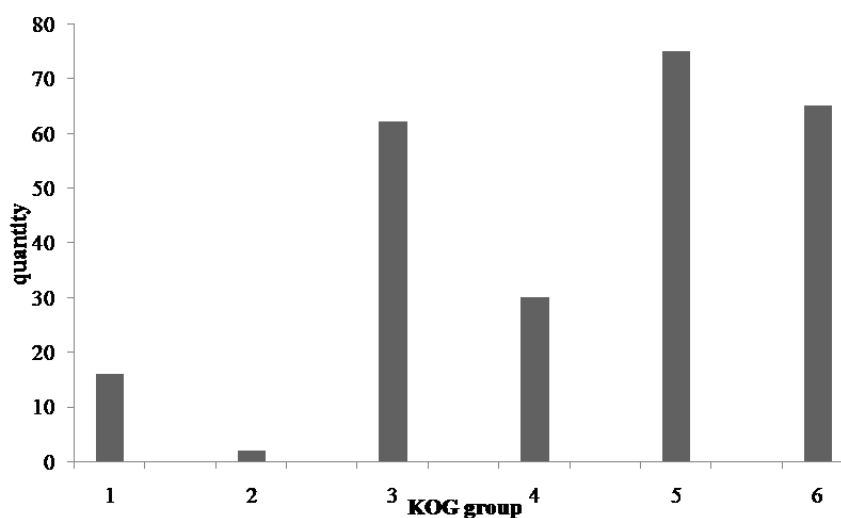


Figure 33: Distribution of 250 differentially regulated genes in $\Delta dhc2$ to the defined KOG groups adopted from <http://genome.jgi.doe.gov/cgi-bin/kogBrowser?db=Schco2>. 1 = Cellular processing and signaling; 2 = Information storage and processing; 3 = Metabolism; 4 = Poorly characterized; 5 = not annotated; 6 = no classification

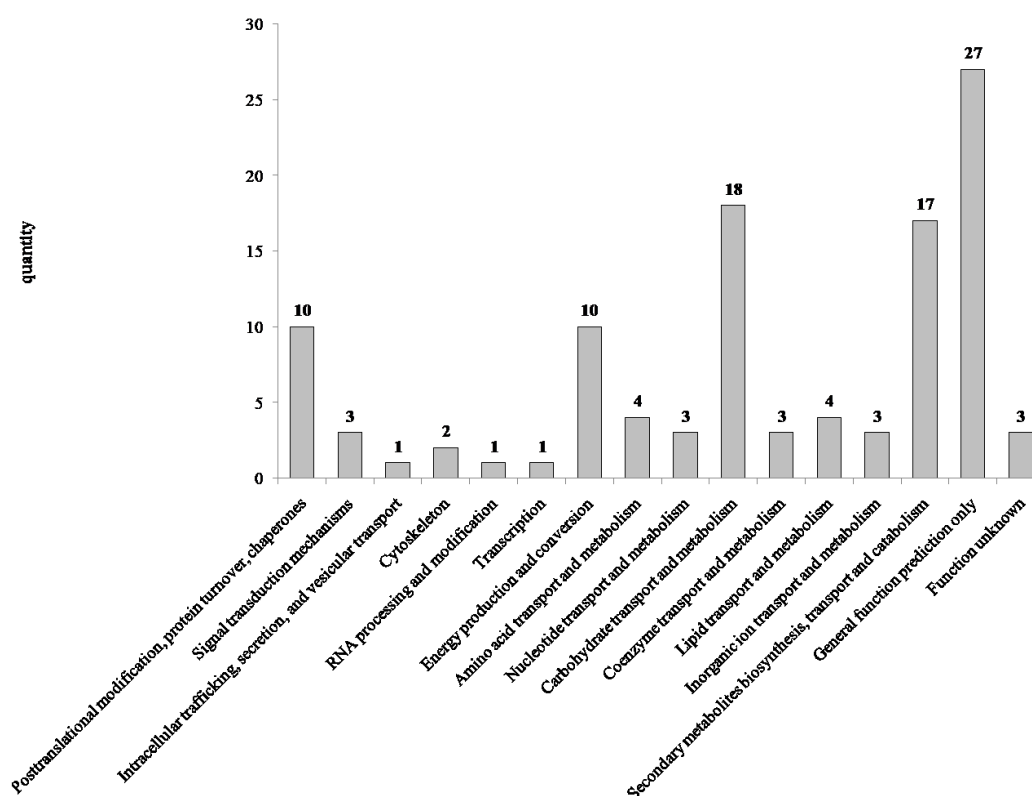


Figure 34: Distribution of 110 annotated, differentially regulated genes in $\Delta dhc2$ to the defined KOG groups adopted from <http://genome.jgi.doe.gov/cgi-bin/kogBrowser?db=Schco2>.

3.5.2. Transcriptome differences between the wildtypes 12-43 and E6

642 genes show a differential expression in strain E6 compared to 12-43. This is a difference of 4.7 % of the total transcriptome of both strains. A \log_2 (fold change) ± 2.0 was observed for 564 genes. A $\log_2(\text{fold change}) \pm 5.0$ was calculated for 93 genes (Fig. 35). The 10 lowest and the 10 highest expressed genes were used for illustration (Fig. 36).

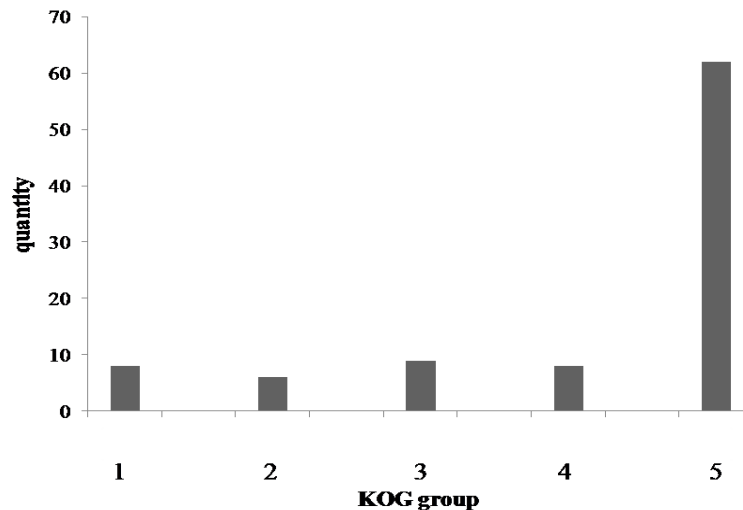


Figure 35: Distribution of 93 differentially regulated genes in 12-43 compared to E6 to the defined KOG groups adopted from <http://genome.jgi.doe.gov/cgi-bin/kogBrowser?db=Schco2>. 1 = Cellular processing and signaling; 2 = Information storage and processing; 3 = Metabolism; 4 = Poorly characterized; 5 = not annotated

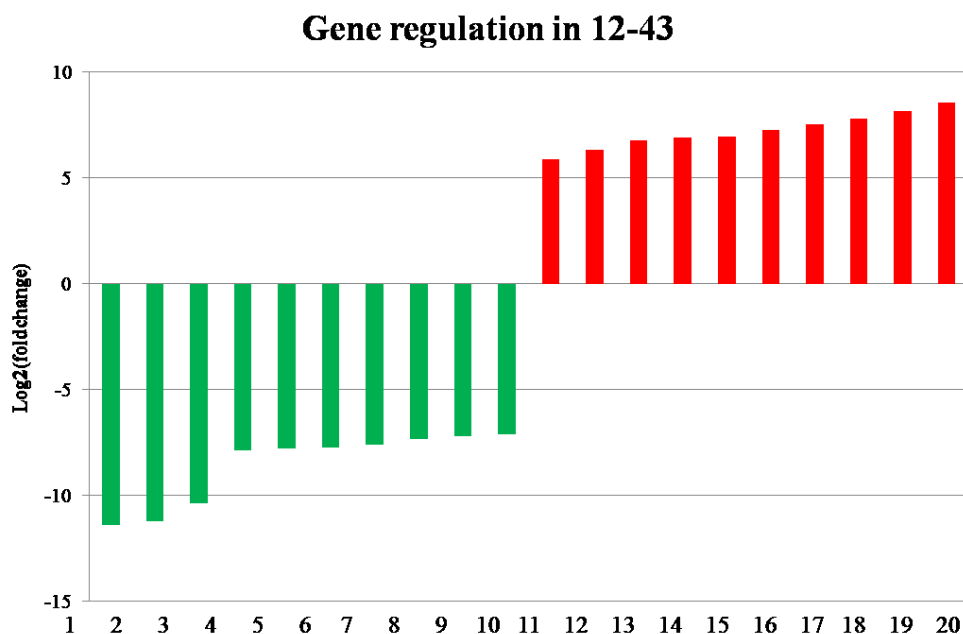


Figure 36: Gene regulation in 12-43 compared to E6. Illustrated are the 10 highest and lowest regulated, annotated genes from the comparison 12-43 vs. E6. 1 = Predicted E3 ubiquitin ligase; 2 = Splicing coactivator SRm160/300, subunit SRm300; 3 = Nuclear localization sequence binding protein; 4 = SAM-dependent methyltransferases; 5 = Large RNA-binding protein (RRM superfamily); 6 = von Willebrand factor and related coagulation proteins; 7 = Nucleolar GTPase/ATPase p130; 8 = Protein kinase PITSLRE and related kinases; 9 = Molecular chaperone (small heat-shock protein Hsp26/Hsp42); 10 = Cytochrome P450 CYP3/CYP5/CYP6/CYP9 subfamilies; 11 = mating pheromone activity; 12 = Putative transcriptional regulator DJ-1; 13 = L-kynurenine hydrolase; 14 = Molecular chaperone (DnaJ superfamily); 15 = O-methyltransferase; 16 = O-methyltransferase; 17 = MYND Zn-finger and ankyrin repeat protein; 18 = mating pheromone activity; 19 = Splicing coactivator SRm160/300, subunit SRm300; 20 = mating pheromone activity

3.6. The proteome of *S. commune*

To simplify the work on proteomic studies, a protein map of *S. commune* was established. The reference strain 12-43 was used to create the master-gel of cytosolic proteins for this fungus. A second monokaryotic strain, 4-39, was used to compare two monokaryotic strains. A dikaryon, 12-43 x W22, was used to compare different developmental stages.

The protein map of strain 12-43 cytosolic proteome of *S. commune* could differentiate 417 proteins with identification, with additional 14 spots not being identified. The Mascot Score of at least 54.0 was not reached by 95 analyzed spots (Fig. 37, 38).

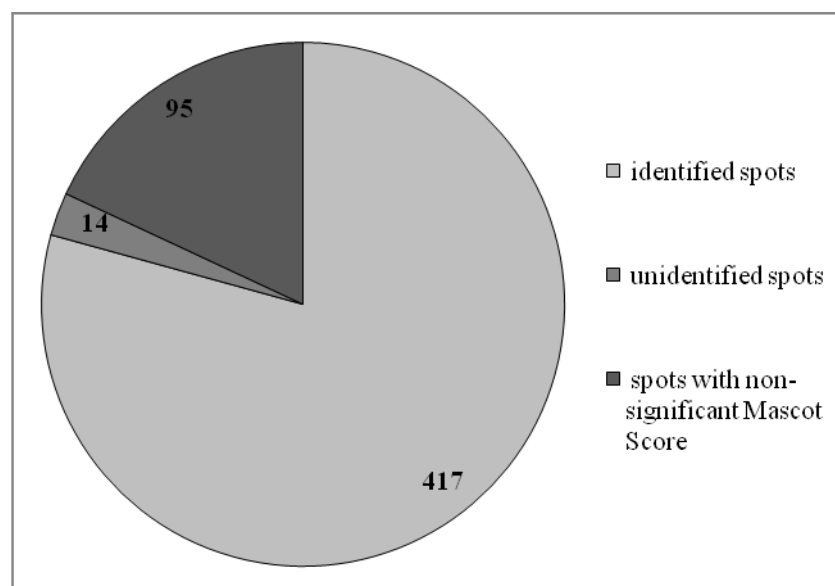


Figure 37: Distribution of analyzed proteins of the mastergel from strain 12-43.

For a comparison of two different monokaryotic strains, 4-39 was analyzed with 91 proteins showing a different abundance to 12-43. A higher abundance can be seen for 29 proteins, while 41 proteins had a lower abundance (Fig. 39, 40).

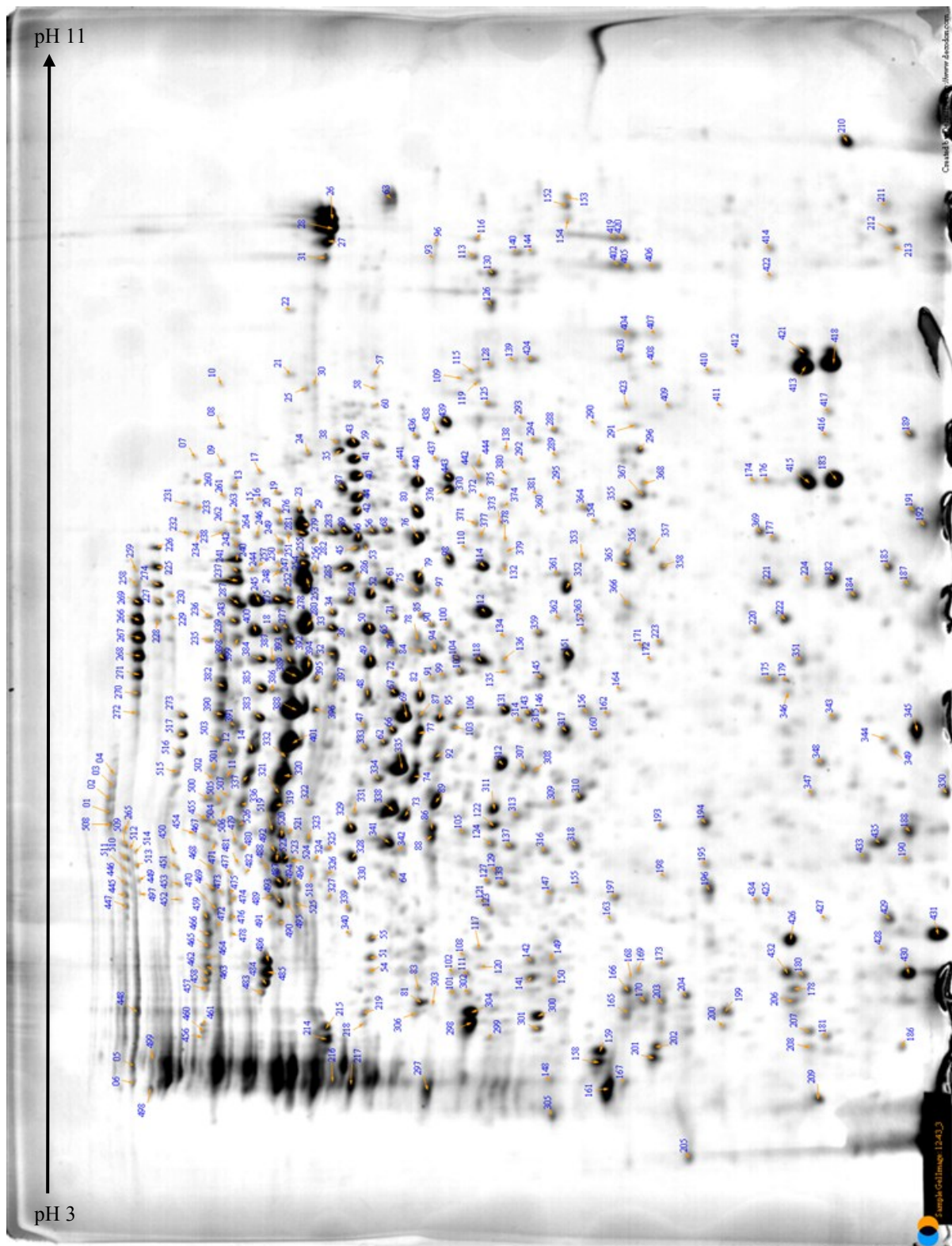


Figure 38: Protein map of cytosolic proteins of strain 12-43 of *S. commune*. All 527 selected spots are labeled.

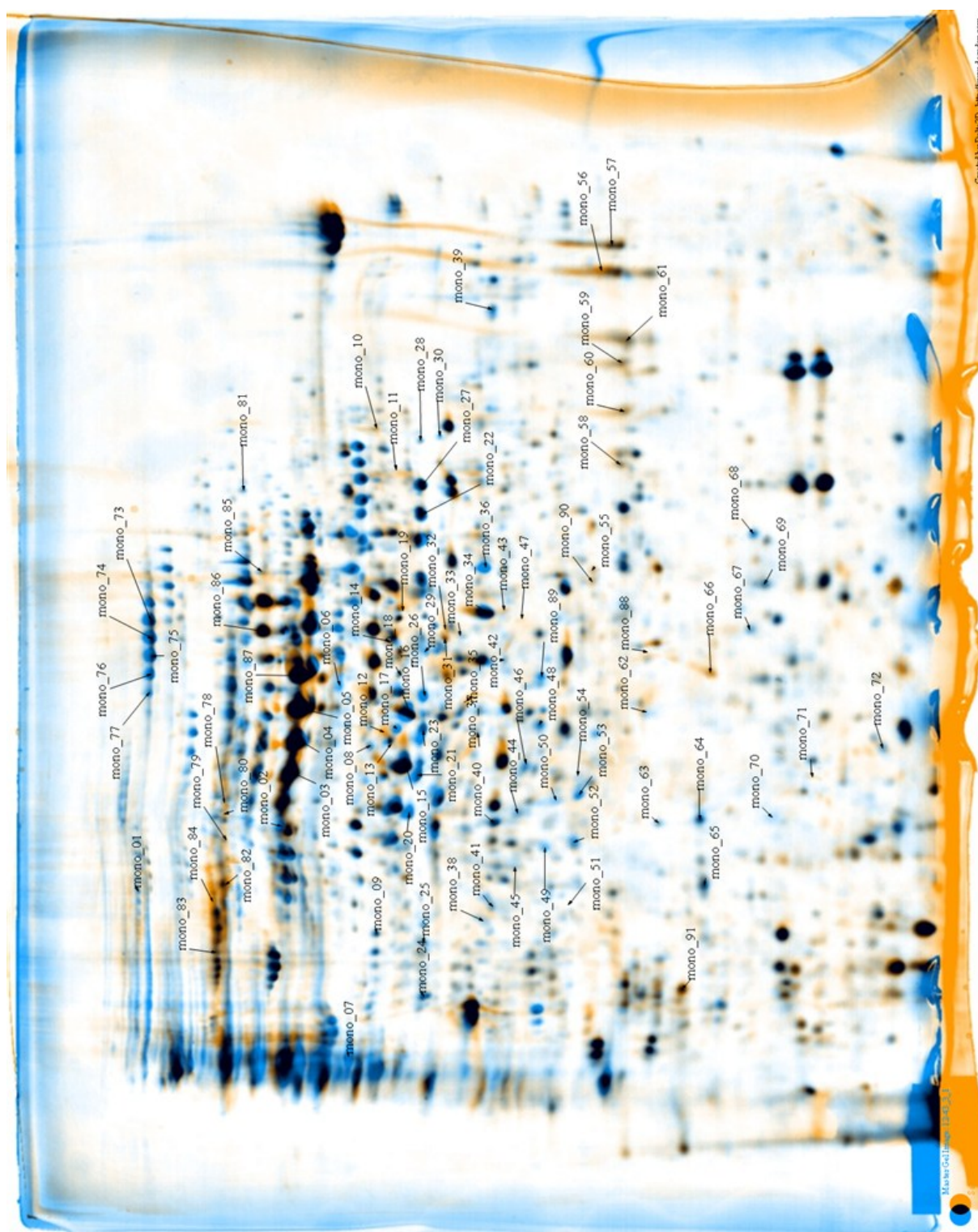


Figure 39: Differential expression between two monokaryotic strains. 12-43 image in blue, 4-39 image in orange. Black spots indicate equal amounts of protein in both strains. For pH range, see master gel (Fig. 38).

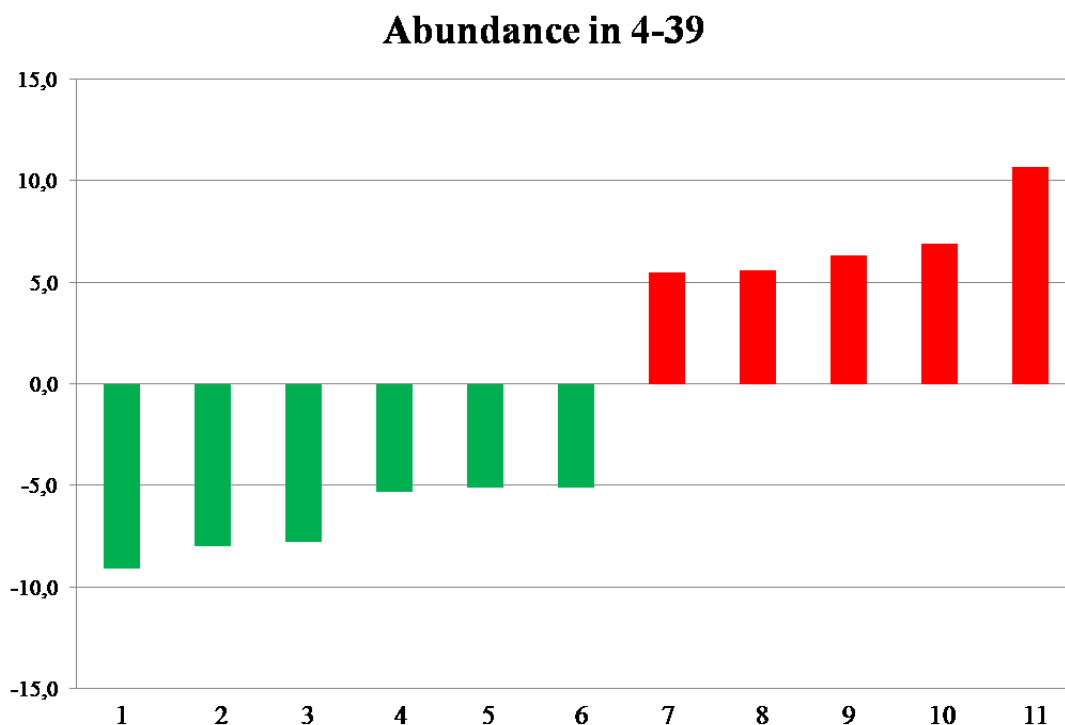


Figure 40: Diagram showing the different abundance of proteins in strain 4-39 compared to 12-43. 1 = ATPase, F1/V1/A1 complex, alpha/beta subunit, nucleotide-binding, 2 = Lactate/malate dehydrogenase, 3 = not annotated, 4 = Methyltransferase type 11, 5 = Lactate/malate dehydrogenase, 6 = Methyltransferase type 11, 7 = Alpha-D-phosphohexomutase, C-terminal, 8 = Alpha/beta hydrolase, 9 = Protein kinase, core, 10 = NADH dehydrogenase (ubiquinone), 30 kDa subunit*, 11 = RNA polymerase I associated factor, A49-like*, * indicates spots present only in strain 4-39

The dikaryon established after mating interaction is a developmental state with the capacity to form fruiting bodies. Thus, the two different mycelia of monokaryon and dikaryon were compared for their proteome profiles. A different abundance in the dikaryon can be seen for 121 proteins. An increase of abundance was observed for 51 proteins, a decrease for 37 spots (Fig. 41). Proteins with a 5-fold regulation are shown in Fig. 42.

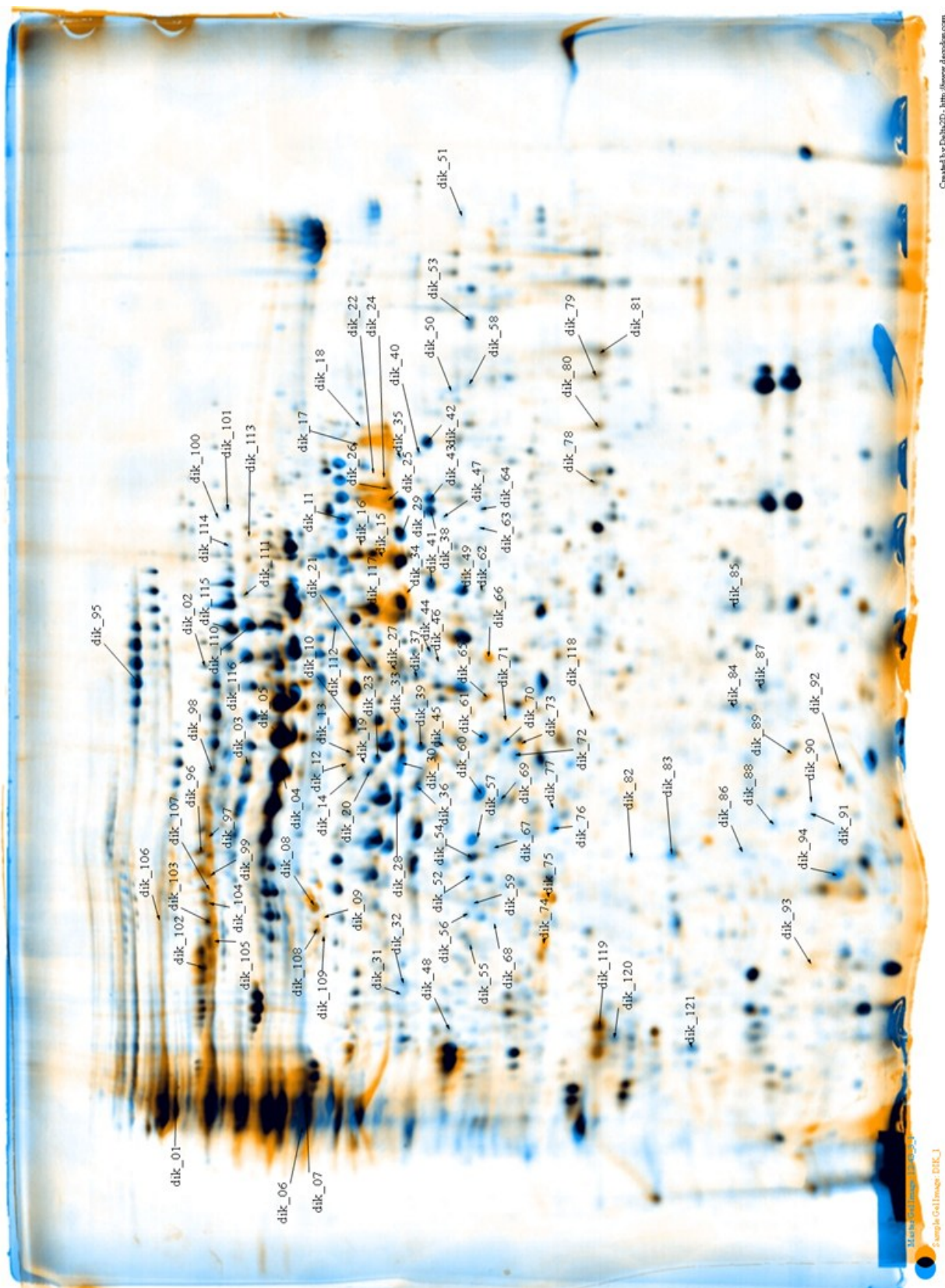


Figure 41: Comparison of cytosolic proteins of the mastergel with the dikaryon. 12-43 image in blue, dikaryon image in orange. Black spots indicate equal proteins in both gels. Orientation of pH range is equal to mastergel (Fig. 38).

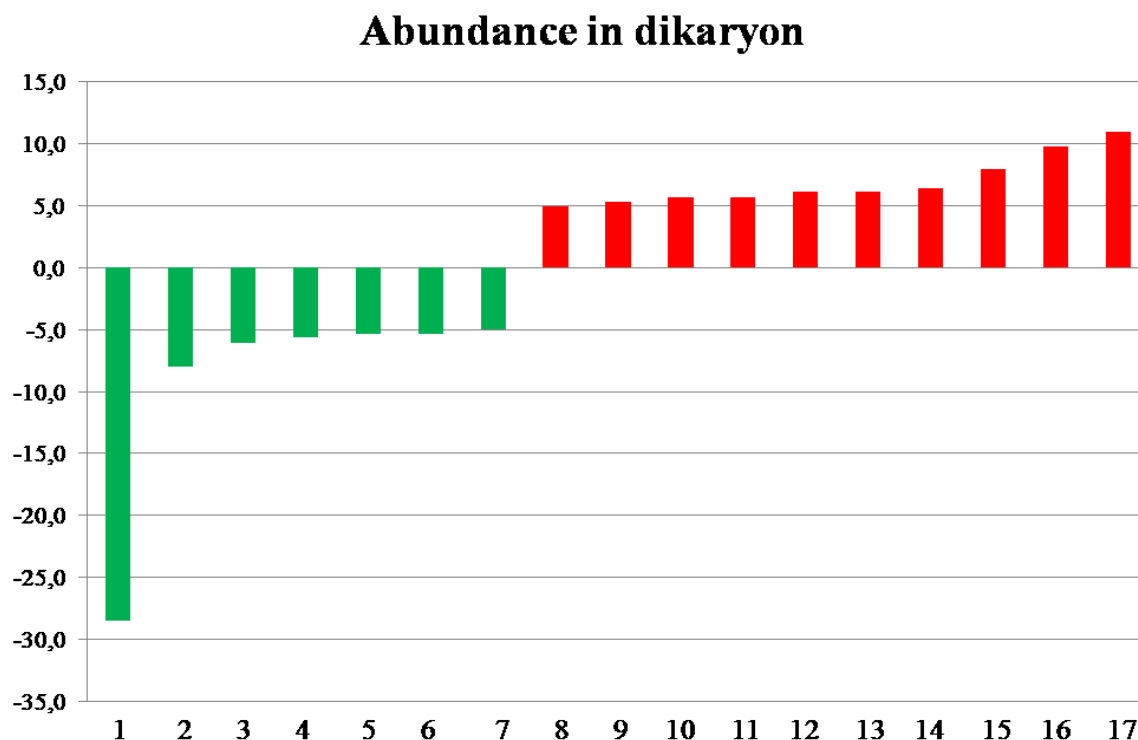


Figure 42: Diagram showing the different abundance of proteins in the dikaryon compared to 12-43. 1 = Protein kinase, core, 2 = BTB/POZ fold (SKP1 component, dimerisation), 3 = Haloacid dehalogenase-like hydrolase, 4 = D-isomer specific 2-hydroxyacid dehydrogenase, catalytic region, 5 = Translation elongation factor EF1B, gamma chain, conserved, 6 = Phosphoglycerate kinase*, 7 = Cyclin-like F-Box, 8 = Glyceraldehyde 3-phosphate dehydrogenase*, 9 = Protein synthesis factor, GTP-binding*, 10 = ATP-citrate lyase/succinyl-CoA ligase, 11 = not annotated, 12 = Alpha-D-phosphohexomutase, C-terminal, 13 = Glyceraldehyde 3-phosphate dehydrogenase, 14 = Peroxisome membrane protein, Pex16*, 15 = Glyceraldehyde 3-phosphate dehydrogenase*, 16 = Protein synthesis factor, GTP-binding, 17 = Glyceraldehyde 3-phosphate dehydrogenase* ; * indicates spots present only in dikaryon

4. Discussion

Sexual development and hyphal growth in *S. commune* is dependent on transport processes such as nuclear migration and vesicle transport, as well as on the precise distribution of nuclei after mitosis in the cell cycle. Thereby, the motor protein dynein plays an essential role. The dynein complex transports its cargo to the minus-end of microtubules. Energy for this movement is gained from the conversion of chemical to mechanical energy at the dynein heavy chain protein. In *S. commune*, the dynein heavy chain is encoded by two separate proteins. Dhc1 forms the N-terminal region of the heavy chain encoding the dimerization domain. The larger protein Dhc2 encodes the motor machinery and the microtubule binding domain.

4.1. Phylogeny of the dynein heavy chain

The phylogenetic tree based on the current phylogeny of fungi, shows dynein heavy chain gene structure in different phyla. An exception can be seen only with Saccharomycotina and Taphrinomycotina, which cluster, in contrast to the fungal phylogeny, as a monophyletic clade. This could be caused by a higher mutation rate within this groups resulting in long-branch effects in the phylogenetic tree (Matheny *et al.*, 2006; Hibbett *et al.*, 2007; Ebersberger *et al.*, 2012).

Phylogenetic studies have shown three independent splits of the dynein heavy chain in higher Basidiomycota. In the basal Pucciniomycota and Tremellomycetes, the dynein heavy chain is encoded by a single, full-length heavy chain of cytoplasmatic dynein. The organization and the type of split of the dynein heavy chain are highly conserved in every group.

The three splits of the dynein heavy chain within the Basidiomycota lead to the assumption of a unique function of the gene among higher Basidiomycetes, because in all other Eukaryotes the dynein heavy chain is unsplit. The dynein heavy chain is a very large protein (~ 4500 aa), which is responsible for spindle organization and elongation during mitosis in fungi (Steinberg, 2000). In Ascomycetes and Zygomycetes the nuclear envelope stays intact during mitosis, so that the nuclear pore complex is required for contact between the chromosomes and the cytoplasm. In this “closed mitosis”, all required proteins need to pass the nuclear envelope to fulfill their function inside the nucleus (Zickler, 1970; Butt and Humber, 1989; Theisen *et al.*, 2008). The protein, encoding the dynein heavy chain, responsible for the right process of mitosis, could be too large to pass the nuclear pore complex. Therefore, a split dynein heavy chain would be beneficial to avoid this problem. In other basidiomycetes, like *U.*

maydis, the nuclear envelope breaks down during mitosis. This process is called “open mitosis” (Straube *et al.*, 2005). In *S. commune*, a late “open mitosis“ takes place, which also leads to the break-down of the nuclear envelope. Therefore, the dynein heavy chain protein easily migrates into the nucleus, at least during anaphase. The hypothesis, that the size of the dynein heavy chain protein could be the reason for its split in higher basidiomycetes, thus, cannot be confirmed.

It could be shown that Dhc1 and Dhc2 are localized in the cytoplasm. Both proteins are distributed all over the cell, in dikaryotic strains both can be found also in the clamp cells. Co-localization was observed between both proteins, specifically close to nuclei, but also at other positions within the cell. In detailed fluorescence images, no gap between Dhc1 and Dhc2 exists. It is thus possible that both proteins form a complex. With cNLS Mapper (cut-off > 5), no signal sequence for the localization of Dhc1 in the nucleus was observed. In contrast, for Dhc2, two sequences were found at 1581-1610 aa and 3850-3879 aa, which indicate an uptake into the nucleus, at least during specific stages in the cell cycle. That leads to the suggestion that Dhc1 has to form a connection to Dhc2, or other protein(s) are needed for migration into the nucleus during mitosis (Kosugi *et al.*, 2009). This hypothesis is supported by the analysis with cello v. 2.5, where a localisation in the cytoplasm is predicted for Dhc1, while Dhc2 can occur in the cytoplasm and in the nucleus. By the fused sequences of both proteins, a localization of the complex in the cytoplasm and in the nucleus is predicted (Yu *et al.*, 2006). Additionally, the software WoLF PSORT puts out the same result for the localization of Dhc1 and Dhc2 (Horton *et al.*, 2007). Co-immunoprecipitation experiments for Dhc1 and Dhc2 failed so far and no complex formation could be observed. On one hand, it is possible that no complex formation is necessary for the full functionality of both proteins. On the other hand, a connection of ligands to either Dhc1, Dhc2, or both, is possible, which might lead to a conformation change.

The split point between Dhc1 and Dhc2 is conserved in all Agaricomycetes showing the same split pattern like *S. commune*. The last 8 aa of Dhc1 cannot be found in Agaricomycetes with an unsplit dynein heavy chain. Also the aa upstream of the NSSTAAAVTFITFVQ-motif in Dhc2 are missing in the unsplit protein. That leads to a reorganization which could result in the split of the dynein heavy chain. By analyzing the sequence of Dhc1 upstream of the split point, a possible dimerization domain to connect Dhc1 to Dhc2 was not found so far.

Taken together, a reason of the split of the dynein heavy chain remains unanswered.

4.2. The deletion of either *dhc1* or *dhc2* is viable

In the filamentous Ascomycetes *N. crassa* and *A. nidulans*, mutants with a deletion for the dynein heavy chain gene have been described. In *N. crassa*, colonies of dynein heavy chain deletion mutants show a reduced growth rate. Hyphae grow sinuously and show an irregular nuclear distribution of nuclei in cells (Bruno *et al.*, 1996). In *A. nidulans*, nuclei divide in conidia but they do not migrate into the germ tube. Colonies of *A. nidulans* mutants form small colonies (Xiang *et al.*, 1994). In summary, both dynein heavy chain mutants show a growth change and a defect in nuclear migration and distribution.

In *Candida albicans*, the deletion of the dynein heavy chain gene leads to an extended cell cycle time as well as defects in spindle assembly during mitosis. Cells of the fungus grow larger and show a reduced number of bi- or multinucleate cells. During the filamentous growth stage, hypha formation and hyphal growth show defects (Martin *et al.*, 2004).

In the corn-smut fungus *Ustilago maydis* (Basidiomycota – Ustilaginomycetes) the first dynein heavy chain mutants for basidiomycetes were described. In this dimorphic fungus, the dynein heavy chain is encoded by two genes, *dyn1* and *dyn2*. The knock-out of one of these genes in *U. maydis* is lethal, which was overcome by the generation of knock-down mutants. Cells in the mutant strains grow larger, and the cell shape was spherical. A defect in nuclear migration was also observed (Straube *et al.*, 2001). In contrast to *U. maydis*, the knock-out of either *dhc1* or *dhc2* is not lethal in *S. commune*.

4.2.1 Δ *dhc1* strains show a different phenotype

In strain Δ *dhc1*-59 a reduced growth rate was measured. Also a change in the colony morphology was observed, resulting in a higher amount of aerial mycelium. For the mutants obtained from Δ ku80, no reduction in growth rate or morphological changes in the colony shape were documented. Only Δ *dhc1*_5 shows a phenotype similar to the “flat” phenotype of semicompatible mating interactions of *S. commune*. A *thin* mutation, which can occur in context with transformation experiments in *S. commune*, where one characteristic is a reduced formation of aerial mycelium, can be excluded for this strain (Fowler and Mitton, 2000).

Cells in Δ *dhc1* strains are considerably shorter, which is different from the *U. maydis* mutants. A similarity in phenotypes was the spherical shape of the cells in Δ *dhc1* strains, which hints at a function in cell shape for Dhc1. Supporting this feature, cells in Δ *dhc1* strains with two

nuclei in a monokaryotic strain were documented. A possible defect in septae formation on the precise position of the mitotic spindle, or a defect in nuclear distribution is likely.

A defect in nuclear positioning was also observed. Nuclei usually are located at the cell center. In $\Delta dhc1$ strains, the nucleus can take any position in the cell, even close to a septum. Nuclei can be donated to a mating partner, and can be accepted. Thus, for $Dhc1$ a defect in nuclear migration could not be shown. In accordance with this, fruiting body formation and sporulation could take place. In contrast to $\Delta dhc1$ strains, $\Delta dhc2$ strains can donate nuclei to a mating partner, but fail to accept nuclei. Therefore, fruiting bodies can be formed only at the side of the mating partner. In contrast to $dhc1$, $dhc2$ functions in nuclear migration during the life cycle of *S. commune*. The deletion of $dhc1$ has no influence on the migration during dikaryon formation itself.

In $\Delta dhc2$ strains, a reduction in aerial mycelium formation and a 4 fold reduced growth rate of colonies were observed. Hyphae grow sinuously in every direction in contrast to directed growth of wildtype hyphae. The knock-out of $dhc2$ leads to truncated cells and to a defect in nuclear distribution and migration. The knock-out of $dhc1$ leads to phenotypic changes similar to the knock-out of $dhc2$. Both genes thus seem to cooperate with a common function in cell cycle with three major activities: (i) maintaining cell shape; (ii) distribution of nuclei and (iii) positioning of the nucleus in every cell (Bruns *et al.*, 2012).

The increased formation of aerial mycelium in $\Delta dhc1_{59}$ strain gives a hint, that hydrophobins could be affected to the deletion of $dhc1$. Hydrophobins are secreted proteins which coat the hyphal tip as a monolayer at hydrophobic-hydrophilic interfaces. Thus, hyphae are able to grow straight to the air to assure fruiting body formation and consequently spore production for distribution of the fungus (Bayry *et al.*, 2012). Especially the *Sc3* hydrophobin, which is active in mono- and dikaryons of *S. commune* could show a higher regulation in the mutant obtained from 12-43. In the mutants obtained from $\Delta ku80$ this effect is not as distinct as in the one from 12-43. Possibly, both wildtype strains have a different expression in *Sc3* (Schuurs *et al.*, 1997).

4.2.2. Phenotypes in $\Delta dhc1$ strains are dependent on the parental background

Genetical manipulation in *S. commune* was performed by transfecting protoplasts with a deletionplasmid. In these experiments an ectopic integration caused by nonhomologous end-joining (NHEJ) is much more probable than the designated replacement of the gene of interest with the deletion cassette. Latter is caused by homologous recombination. To increase the

homologous recombination rate, either one of the important genes, $\Delta ku70$ or $\Delta ku80$, which form a dimer in the first step of NHEJ, needs to be inactivated. The NHEJ-pathway is interrupted and so, DNA-repair takes place by homologous recombination (Choquer *et al.*, 2008; Wang *et al.*, 2011).

For *S. commune*, a $\Delta ku80$ strain exists. In this strain, the transformation rate was dramatically decreased, with only 15 transformants, but 7 (47 %) showing the desired deletion of *dhc1*. In the transformation experiment with the wildtype strain 12-43, only 1 % of 105 transformants contained the deletion cassette at the correct position in the genome. Although the transformation rate in $\Delta ku80$ is much lower than in other wildtypes of *S. commune*, the efficiency of homologous recombination is increased.

In the transformants obtained in this study, an influence of the genetic background on the phenotype was observed. In transformants of the wildtype strain 12-43, e.g. with $\Delta dhc1_{59}$, cell shape and nuclear positioning defects are stronger as compared to mutants derived from $\Delta ku80$. As *ku80* functions in DNA-repair during cell metabolism, mitosis and meiosis, these processes are affected by the deletion of *ku80* (Koike *et al.*, 1999). Phenotypical changes caused by the missing DNA-repair process as well as an influence of the deletion of *ku80* on further gene deletions in this strain, cannot be excluded.

4.2.3. Kinesin-5 and Kinesin-14 can substitute for the function of *dhc2*

RNA-sequencing was used to identify genes that can take over the function of *dhc2*. For fungi, a kinesin-14 is described, which is a minus-end directed kinesin (Steinberg, 2007). In our investigation, we found a 9-fold upregulation of kinesin-14 in the $\Delta dhc2$ strain compared to the wildtype 12-43. In the two investigated wildtypes used to generate the $\Delta dhc2$ strain, also a 9-fold upregulation of kinesin-14 was found in the wildtype strain E6 compared to 12-43. For strain 12-43, less reads for this gene were found in the transcriptome, while for E6 and $\Delta dhc2$ an equal amount of reads was found. This was the initial evidence that strain 12-43 lacks either the gene for kinesin-14 or has no sufficient sequence similarity in *kin14*. In Hanisch (2012), this phenomenon was proven with different PCR experiments. A general PCR with primers at the beginning and the end of the gene gave no result in 12-43. Different primer sets for qRT-PCR gave a result in strain E6, but again yielded no bands for 12-43. This leads to the hypothesis, that $\Delta dhc2$ strains are only viable, if the kinesin-14 of strain E6 is present in their genome. However, investigation of additional $\Delta dhc2$ strains on the presence of kinesin-14 in their genome is necessary.

Kinesin-5 also can provide minus-end directed transport along microtubules, when it interacts with dynactin (Kardon and Vale, 2009). An up-regulation of kinesin-2, the *S. commune* homolog to kinesin-5 of *A. nidulans*) was found in strain $\Delta dhc2$. Thus, this motor also can take over the function of *dhc2*.

In strain $\Delta dhc1_{59}$, which has also the genetical background of strain 12-43, kinesin-14 cannot have an influence on the viability of the strain, as the kinesin-14 copy is missing or not conserved in the genome of 12-43.

4.2.4. The transcriptome of $\Delta dhc2$ shows differences in 250 genes

The genetic background of $\Delta dhc2$ consists of two *S. commune* wildtypes. The regulation of a gene may not only depend on the deletion of *dhc2* in this strain, but also on the genomic composition in the $\Delta dhc2$ genome, depending from the parental origin of every specific gene. In the resulting *dhc2* deletion mutants, phenotypic differences cannot be seen. All seven $\Delta dhc2$ strains have an identical morphology, colony shape and cell shape.

In $\Delta dhc2$, 110 annotated genes with a proposed function show different regulation. More than the half of these genes is involved in metabolic pathways, including the transport of different substrates, organic compounds and metabolic products. Significant in this group are genes for transporters for several substrates. Twelve major facilitator superfamilies (MFS) are differentially regulated in the mutant strain: with only three exceptions, all the differentially expressed MFS genes are upregulated in the two wildtypes compared to $\Delta dhc2$. Several general substrate transporters and three ABC (ATP-binding cassette) transporter-like genes are upregulated in $\Delta dhc2$. The active and passive transport over membranes is realized by these genes, which contribute to multidrug resistance, e.g. in *S. cerevisiae*, where the genes are involved in cell protection and biogenesis of fatty acids (Kovalchuk and Driessen, 2010). Furthermore, three specialized transporters are upregulated in $\Delta dhc2$: two sulphate transporters and a malic acid transporter. Possibly, the $\Delta dhc2$ strain produces more metabolic products, which need to be secreted.

In addition, the high number of differentially expressed genes involved in metabolic pathways could be a hint for an increase of cell metabolism. Transporters need to work more efficiently to introduce substrates for the pathways, which could lead to an up-regulation of transporter genes in the mutant strain. This would coincide with increased cell stress, as seen with an up-regulation of two heat-shock proteins in $\Delta dhc2$. The expression of these genes increases with rising stress in the cell. This could be underlined by several Cytochrome P450 genes, which

show an up-regulation in $\Delta dhc2$. Up-regulation of these genes means high oxidative stress in the mutant which correlates with the up-regulation of heat-shock proteins (Lewis, 2002).

A high number of genes involved in secretion or in producing secreted proteins were identified. This correlates with the differentially expressed genes according to metabolism and cellular transport. A changed metabolism could lead to different secretion products in $\Delta dhc2$.

Fungal mating-type pheromones are also differentially regulated in $\Delta dhc2$. All four identified genes are up-regulated in the mutant. The mutant has the parental background of both wildtypes. It should have the mating specificity of either 12-43 or E6 or a mix of both. As the mating-type of every strain of *S. commune* is specific, also pheromones and pheromone-receptors are strain specific. Thus, genes according to mating-types are always identified as differentially expressed, because every strain has different transcripts for its mating-type genes.

The *dhc1* gene was never identified as a differentially expressed gene in $\Delta dhc2$. This leads to the hypothesis, that the knock-out of *dhc2* has no effect on the expression of *dhc1*. A down-regulation of *dhc1* would mean that this gene is dependent on *dhc2* in transcript regulation, which is not likely. An up-regulation, in contrast, would show a compensatory transcriptional response. Both situations can be excluded with RNA-sequencing data, which underlines the autonomy of the two genes encoding the dynein heavy chain in *S. commune*.

4.3. Transcriptome differences can be found in all three investigated strains

4.3.1. High genomic diversity between different strains of *S. commune* wildtypes

In the comparison of *S. commune* 12-43 to *S. commune* E6, 642 differentially regulated genes were identified. With an up- or down-regulation of more than 2^5 , still 93 genes were identified. In this study, the 10 lowest and the 10 highest expressed genes were used to show dramatic differences between two monokaryotic wildtypes of *S. commune*. It was shown that nearly 7 % nucleotide differences occur between two strains of *S. commune* in the housekeeping gene *ura1*. This underlines the divergence within the genus *S. commune* (Lengeler and Kothe, 1994). Also the high number of possible mating-types in nature results in constant genetic exchange during dikaryon formation and following spore distribution in *S. commune*.

The 10 down-regulated genes have postulated functions in cellular processes and metabolism. The lowest expressed gene in 12-43, with a down-regulation of 2700 fold, is a predicted E3

ubiquitin ligase. This gene is responsible for degradation of destroyed, misfolded or unnecessary proteins in the cell. Together with the E2 ubiquitin-conjugating enzyme, an attachment of ubiquitin to lysine residues in the targeted protein is realized. This ubiquitination is a well known posttranslational modification (PMS) targeting proteins to the proteasome. Another PMS causing gene did show a significant down-regulation of 147 fold in strain 12-43 – the molecular chaperone coding for the small heat-shock protein Hsp26/Hsp42. They play an important role in protein-protein-interactions, as well as in protein folding and unfolding. Additionally, they avoid protein aggregation.

With a downregulation between 1300 fold (nuclear localization sequence binding protein) and 2400 fold (splicing co-activator SRm160/300) two genes involved in transcription and RNA processing and modification were identified in 12-43. The SRm160/300 was also identified as nuclear matrix antigen (McCracken *et al.*, 2005). The different expression in two wildtypes could be due to the strain specific nuclear antigens. These antigens could play a role in nuclei-recognition during the mating process. An S-adenyl-L-methionine- dependent methyltransferase was seen with a downregulation of 240 fold in 12-43. This gene is responsible for protein trafficking and sorting. Additionally, it functions in biosynthesis and gene expression. Thus, considerable differences between two strains of *S. commune* in general cellular functions have been observed.

The 10 highest up-regulated genes in strain 12-43 compared to E6 belong mainly to mate recognition, with an up-regulation between 57 and 388 fold for pheromone response genes. Since Strains 12-43 and E6 are two fully compatible strains and would form a functional dikaryon. This is due to their different mating-type genes. A significant upregulation, respectively downregulation of these genes is expected in the comparison of two compatible strains. Strain 12-43 has different pheromone receptors to recognize compatible mating partners than strain E6.

Three metabolic genes were identified with a high up-regulation: a kynureninase and two O-methyltransferases. O-methyltransferases act as degraders of lignin and possibly are necessary for detoxification in white-rot fungi (Jeffers *et al.*, 1997). Kynureninases are involved in the catabolism of tryptophane. Strain 12-43 is able to degrade tryptophane out of the substrate by itself. Strain E6 in contrast needs an addition of tryptophane in the media for optimal growth and therefore has a defective tryptophane catabolism. This could explain the higher expression of a gene involved in tryptophane catabolism in strain 12-43 compared to E6 (Phillips, 2011).

While one molecular chaperone was downregulated in strain 12-43, another chaperone (encoding the small heat-shock protein Hsp40) was up-regulated. This could mean that not every heat-shock protein is either present or active in every monokaryotic strain of *S. commune*. Both phenomena could be due to possible divergence in the gene sequences. Additionally, as mentioned for *kin-14*, the composition of the genome is strain specific in *S. commune*.

The up-regulated splicing co-activator SRm130/300 in strain 12-43 could be the complementary gene to the up-regulated copy in E6. As mentioned before, this gene functions as a nuclear antigen. It is identified as differentially expressed in both strains because both strains should have a special nuclear antigen with different genomic sequence.

Two genes involved in transcription are upregulated in strain 12-43. A putative transcription regulator of the DJ-1 family was identified. A real function in transcription of DJ-1 is mostly reported in humans (Wilson, 2011). In plants this gene functions in several processes like protecting the organism against oxidative stress and assures cell survival (Lin *et al.*, 2011). A function in fungi is unclear but an overlapping function to the one in plants seems likely. The second gene identified was a MYND Zinc fingers containing the MYND domain which is necessary for protein-protein interaction of transcriptional co-repressor proteins (Wang *et al.*, 2010).

In summary, differentially expressed genes in a wildtype comparison fulfill a wide range of functions and are present in all pathways in *S. commune*. A network for strain specific characterizations cannot be confirmed. As a nucleotide difference of 7 – 9 % is common between monokaryotic strains in *S. commune*, differences in amount of reads per transcript of a gene can occur.

4.3.2. Between all three strains 22 genes show differential regulation

Only 22 of more than 14,000 genes are differentially regulated in all 3 investigated strains. 9 of them are still not annotated. The other genes are extracellular proteins itself or are involved in secretory processes in *S. commune*. Proteins of the glycosyl hydrolase family are already identified in secretome studies of *S. commune*. Members of this family extract cellulases and hemicellulases, as well as amylases (Ring, 2012). One major facilitator superfamily (MFS) was identified. This gene belongs to a uniporter-symporter-antiporter family. They transport only small molecules in response to chemiosmotic ion gradients (Pao *et al.*, 1998). This gene has the highest regulation in strain E6. This strain has no copy of tryptophane in its genome.

Tryptophane needs to be added to the growth media and needs to be taken up by the fungus. Possibly, the MFS is responsible for this uptake and therefore, this gene is higher expressed in E6. A cutinase is also differentially expressed in all strains. This gene is common in plant pathogenic fungi, which secrete the cutinase to degrade the cuticle of plants for easy penetration of their host (Dutta *et al.*, 2009). Differentially regulated glutathione-s-transferase is involved in detoxification. Glutathione is bound to organic matter and is secreted or degraded in vacuoles (Morel *et al.*, 2009). Other genes are expressed under stress conditions, like thaumatin and heat shock proteins. Thaumatin is used for plant transformation to increase the resistance of plants against fungal pathogens (Popowich *et al.*, 2007). The highest expression of the majority of identified genes in all three strains can be found in 12-43. This leads to the conclusion, that this strain has an increased pathogenicity compared to the other strains, as cutinase and thaumatin are highly expressed. The glycoside hydrolases are both regulated in the two wildtypes dependent from the saccharide they need or used as a carbon source.

4.3.3. Correlation between the transcriptome und proteome in monokaryons

As mentioned before, the composition of the genetic information varies from strain to strain in *S. commune*. Also on the proteomic level differentially abundant proteins were found. Again a few proteins stay unclear because of the missing annotation.

The identified proteins with a varying abundance higher or lower than 5 fold, are involved in different metabolic pathways. Again, the known strains of *S. commune* seem to have a different cell metabolism.

Conspicuous is the protein kinase found with a higher abundance in strain 4-39. Protein kinases are essential for signal transduction, metabolism, movement, etc. Two main groups of protein kinases are serine/threonine and tyrosine kinases are known. They regulate protein phosphorylation and dephosphorylation, which lead to PMS. Protein kinases influence a high number of cellular functions in metabolism. The higher abundance of this protein in 4-39 could also accompany the different abundances of metabolic proteins in this strain (Park *et al.*, 2011).

The transcriptome and proteome of *S. commune* monokaryons show differences in metabolic pathways. Identified genes and proteins do not correlate in detail. On the one hand it is not possible to synchronize transcripts and proteins. On the other hand the growth conditions of *S. commune* strains for both analyses differ in culture design and age of the cultures. For

proteome analysis, four days old liquid culture was used while for RNA-sequencing cultures grew on solid media for seven days. Differences between the biological replicates in both experiments were minimal. Thus, the number of replicates should not have an influence on the comparability of transcriptome and proteome of *S. commune*.

4.4. A protein map of *S. commune* will allow future analyses

The proteome of *S. commune* was analyzed on 2-dimensional protein gels. A wide pH-range was used to illustrate the cytosolic proteome. More than 900 protein spots were recognized on a gel of a monokaryotic strain of *S. commune*, but not all of them could be used for mass spectrometry because of their weak abundance in the gel. In total, 526 protein spots were analyzed, most of which were distributed at isoelectric point between 3 and 7. Alkaline proteins with their isoelectric point between 8 and 12 were rare.

A number of proteins with the same molecular weight, but differences in their isoelectric point, likely are caused by posttranslational modifications (PMS). Aside from glycosilation, acetylation and ubiquination, phosphorylation is the most common PMS (Glinski and Weckwerth, 2006). Phosphate groups are bound to serine or threonin residues (Leach and Brown, 2012). Indeed, mass spectrometry could show that these protein chains are formed by several copies of the same protein.

Not every selected protein was identified. Almost 1/5 of the analyzed proteins did not reach the threshold of 54.0. Nevertheless, the mascot score of these proteins was close to the threshold. Even after 4 repetitions of the mass spectrometry, there was no clear result for these spots. The reason rather is a bioinformatics problem related to the high sequence divergence between different strains discussed above. For creating the sequenced genome of *S. commune*, the monokaryotic strain H4-8 was used, which is also the basis for the database for identifying peptides (Ohm *et al.*, 2010). The strain used for the proteomic studies is 12-43.

Only 14 spots gave no result. This could be the case, if the analyzed protein had a low concentration. Also, the genomic variation between strain 12-43 and H4-8 could lead to no result for some spots.

4.5. Differences associated with the dikaryotic proteome

During the change from a monokaryotic life phase to a dikaryotic stage in *S. commune*, the MAPK pathway has to be passed through. By pheromone recognition of a compatible mating-partner, a signal cascade is activated. In this process, the pheromone receptor interacts with

the pheromone and the G-protein, linked to the receptor, dissociates into subunits $G\alpha$ and $G\beta\gamma$. Consecutively, the MAPK is induced, where several protein kinases are involved. The expression of the transcription factor Ste12 induces the mating response (Raudaskoski and Kothe, 2010). The protein kinase is upregulated until the dikaryon formation takes place. After dikaryotization, the expression of the protein kinase decreases. The protein kinase found on the 2D- gel of the dikaryotic strain is approximately 28 fold decreased. A detailed annotation which protein kinase is annotated with the protein ID 1029853 is not given in the genome sequence of *S. commune*. Additionally, a cyclin-like F-box is downregulated in the dikaryon. This protein could possibly be a part of the transcription factor needed for the initiation of the mating response.

Again, several proteins of metabolic pathways show different abundance in the dikaryon compared to strain 12-43. This may lead to the assumption that dikaryotic strains have a changed metabolism, especially in glycolysis. For four glyceraldehyde-3-phosphate dehydrogenases (GPD), a higher abundance in the dikaryon was observed (Harmsen *et al.*, 1992). Three spots were identified as GPDs which are located at the same molecular weight on the 2dimensional gel with only small switches of their position concerning their isoelectric point. PMS could cause these additional spots coding a GPD present in the dikaryotic proteom.

Possible hints on more differences on the genetic composition of a dikaryon could be delivered by transcriptome analysis. 2d-gel electrophoresis illustrates only a fraction of the genomic background of *S. commune* and is maybe not sensitive enough to capture all differences between two compared strains.

4.6. Outlook

With the present work, it was shown that the dynein heavy chain in the basidiomycete *S. commune* is encoded by two separate genes. The knock-out of either *dhc1* or *dhc2* is viable. For complementation of the investigations, a double knock-out mutant is necessary. Furthermore, other components of the cytoskeleton within the $\Delta dhc1$, $\Delta dhc2$ and $\Delta dhc1dhc2$ strains should be investigated in more detail with microscopical techniques concerning possible changes in their cellular organization, structure or position.

Additionally, the deletion of *kin-5* and/or *kin-14* in the dynein heavy chain mutants could be interesting to show that viability of the dynein strains is dependent from other microtubule-associated minus-end transporters.

The co-localization of both genes in the cell was proven via immunofluorescence of *dhc1* or *dhc2*. To show a possible interaction, co-immunoprecipitation or FRET experiments should be performed. Also, possible interactions with other proteins could be shown this way. By labeling each gene with either GFP or RFP, life images of the dynein molecule can be taken. Possible co-localization of Dhc1 and Dhc2 can potentially also be seen also with this method.

RNA-sequencing data for three different wildtype strains (12-43, E6, T26) of the fungus are available now, allowing for comparison of differential expression of genes in new mutant strains. At the same time, differences in gene structure, intron distribution or intron abundance in other wildtype strains will be possible, as well as an optimized gene annotation with the existing genome sequence. Detailed analysis of the RNA-sequencing results should be done to find other interesting or strain specific genes of *S. commune*. To date, expression studies in *S. commune* strains were performed using RNA microarrays. The available data could be compared to RNA-sequencing to find either overlapping expression of elected genes, or differences and limitations of both methods.

Strain specific differences were shown for *S. commune* wildtypes on the proteome level, as well as an initial investigation of developmental stages. Proteome studies should be completed by analyzing the proteome at different stages of fruiting body formation, like primordia and fully developed fruiting bodies. Additionally, investigation of the *S. commune* proteome under different growth conditions and substrates including wood, or a comparison to the proteome of new mutant strains has now become possible with the proteome map.

The transcriptome-analyzis gives hints that also the secretome of *S. commune* varies between monokaryotic strains. In addition to the first experiments on secretory proteins, more strains of *S. commune* should be included in the experimental design as well as growth of the strains on different media.

In general, the base for further analysis on the transcriptome and proteome of *S. commune* was established with the present work. This is helpful for new research approaches and the corresponding experimental designs within the work field of *S. commune*.

5.) Summary

The split gill fungus *Schizophyllum commune* (*Agaricomycetes*) is a model organism in microbiological research. It is characterized by a tetrapolar mating-system leading to intensive studies on fungal development. The mating system is formed by two independent loci, *A* and *B*, each of which is composed of different subloci. Thus, more than 23,000 different mating types occur in nature. Furthermore, an efficient transformation protocol was developed for *S. commune*, allowing the molecular manipulation of the genome.

During the formation of the characteristic, dikaryotic, clamped mycelium of Basidiomycetes, a fast nuclear transport and exchange is necessary. This is assured by the motor protein dynein. Dynein molecules transport their cargo along microtubules, a component of the cytoskeleton. Crucial for the full function of the molecule is the dynein heavy chain, which converts chemical to mechanical energy and therefore enables the movement of dynein along its microtubule tracks. In higher basidiomycetes, dynein heavy chain is encoded by two genes – one N-terminal and one C-terminal part of the generally unipartite proteins in other fungi or throughout the eukaryote domain. In phylogenetic analyses, it could be shown that within the group of Basidiomycetes, three independent splits of the dynein heavy chain took place. In each split, a structural rearrangement of both genes occurred. The third split appeared within the Agaricomycetes, where the gene structure is highly conserved in all investigated fungi. In *S. commune*, a member of the Agaricomycetes, both genes could be isolated and were named *dhc1* and *dhc2*. Knock-out strains for both genes were created. The knock-out of *dhc1* is viable and shows different phenotypes, like truncated, spherical cells and a defect in nuclear migration and positioning. A knock-out of *dhc2* in *S. commune* is also viable, and the mutant shows phenotypical changes with a clear function in nuclear migration and nuclei positioning, which is overlapping to the function of *dhc1*. The viability of $\Delta dhc2$ is ensured by a higher expression of kinesin-14, a minus-end directed kinesin in fungi, which was proven *via* RNA-sequencing. With this method, transcriptome differences between two wildtypes were shown which were verified by proteome studies. Also differences between monokaryotic strains and a dikaryon could be shown.

6.) Zusammenfassung

Der Gemeine Spaltblättling *Schizophyllum commune* (*Agaricomycetes*) zählt in der Wissenschaft als Modellorganismus. Er zeichnet sich insbesondere durch sein tetrapolares Mating-System aus, an dem intensive Entwicklungsstudien durchgeführt werden können. Das Mating-System wird durch zwei unabhängige Loci, *A* und *B*, charakterisiert, wobei zu jedem der beiden Gene verschiedene Subloci existieren. Dadurch kommen in der Natur mehr als 23000 verschiedene Kreuzungstypen vor. Desweiteren wurde für *S. commune* ein effizientes Transformationsprotokoll entworfen, sodass das Genom des Basidiomyceten gezielt manipuliert werden kann.

Während der Formation des charakteristischen, dikaryotischen Schnallenmyzels der Basidiomyceten ist ein schneller Zellkerntransport und -austausch nötig. Dieser wird durch das Motorprotein Dynein gewährleistet. Dyneinmoleküle transportieren gebundene Ladung entlang von Mikrotubuli, einem Grundbaustein des Zytoskeletts. Ausschlaggebend für die volle Funktionsfähigkeit dieses Vorgangs ist die schwere Kette des Dyneinmoleküls, welche chemische Energie in mechanische umwandelt und somit die Bewegung des Dyneinmoleküls ermöglicht. In höheren Basidiomyceten wird die schwere Kette von zwei Genen kodiert – einem N-terminalen und einem C-terminalen Teil. In phylogenetischen Untersuchungen konnte festgestellt werden, dass innerhalb der Basidiomyceten drei voneinander unabhängige Teilungen der schweren Kette des Dyneins stattfanden. Bei jeder Teilung fand eine Umorganisation der Strukturen der beiden Gene statt. Die dritte Teilung kam innerhalb der *Agaricomycetes* vor, bei der die Genstruktur in allen untersuchten Arten hochkonserviert ist. In *S. commune* konnten beide Gene isoliert werden und wurden mit *dhc1* und *dhc2* bezeichnet. Es ist gelungen, *dhc1* und *dhc2* in *S. commune* zu deletieren und phänotypische Veränderungen zu beobachten. Auf Grund dessen konnte beiden Genen eine überlappende, eindeutige Funktion in der Kernwanderung und -positionierung zugewiesen werden. Die Überlebensfähigkeit der $\Delta dhc2$ Stämme wird durch die höhere Expression von Kinesin-14, einem Minus-End-gerichteten Kinesin in Pilzen, gewährleistet. Diese Expressionsunterschiede wurde mittels RNA-Sequenzierung nachgewiesen. Mit dieser Methode konnten ebenfalls Unterschiede im Transkriptom zweier Wildtypstämme gezeigt werden. Auch Proteomuntersuchungen bestätigten Unterschiede zwischen Wildtypstämmen, sowie Unterschiede zwischen einem Monokaryon und einem dikaryotischen Stamm.

7.) References

- Asai, D. J., Koonce, M. F., 2001.** The dynein heavy chain: structure, mechanics and evolution. *Trends in Cell Biology*. 11, 196-202.
- Bartnicki-Garcia, S., Bracker, C. E., Gierz, G., López-Franco, R., Lu, H., 2000.** Mapping the growth of fungal hyphae: orthogonal cell wall expansion during tip growth and the role of turgor. *Biophysic J* 79, 2382-90.
- Bayry, J., Amanianda, V., Guijarro, J. I., Sunde, M., Latgé, J.-P., 2012.** Hydrophobins – unique fungal proteins. *PLoS Pathogens* 8. 1-4.
- Bordier, C., 1981.** Phase separation of integral membrane proteins in Triton X-114 solution. *J Biol Chem*, 256, 1604-07.
- Bradford, M. J., 1976.** A rapid and sensitive method for the quantitation of microgram quantities of protein utilizing the principle of protein-dye binding. *Anal Biochem* 72, 248-54.
- Bruno, K. S., Tinsley, J. H., Minke, P. F., Plamann, M., 1996.** Genetic interactions among cytoplasmic dynein, dynactin, and nuclear distribution mutants of *Neurospora crassa*. *Proc Natl Acad Sci U S A*. 93, 4775-80.
- Brunsch, M., Schubert, D., Gube, M., Linde, J., Ring, C., Krause, K. and Kothe, E. (2012).** Dynein heavy chain, encoded by two genes in agaricomycetes, is required for pheromone response in *Schizophyllum commune*. (Accepted for publication in *Fungal Genet and Biol* pending revision, Manuscript-ID FGB 12-90)

- Butt, T. M., Humber, R. A., 1989.** An immunofluorescence study of mitosis in a mite-pathogen, *Neozygites sp.* (Zygomycetes: Entomophthorales). *Protoplasma* 151, 115-23.
- Carter, A. P., Cho, C., Jin, L., Vale R. D., 2011.** Crystal structure of the dynein motor domain. *Science*. 331, 1159-65.
- Choquer, M., Robin, G., Le Pêcheur, P., Giraud, C., Levis, C., Viaud, M., 2008.** *Ku70* or *Ku80* deficiencies in the fungus *Botrytis cinerea* facilitate targeting of genes that are hard to knock out in a wild-type context. *FEMS Microbiol Lett* 289, 225-32.
- Cooke, W. B., 1961.** GENUS SCHIZOPHYLLUM. *Mycologia*. 53, 575-99.
- de Jong, J. F., Ohm, R. A., de Bekker, C., Wösten, H. A., Lugones, L.G., 2010.** Inactivation of *ku80* in the mushroom-forming fungus *Schizophyllum commune* increases the relative incidence of homologous recombination. *FEMS Microbiol Lett* 310, 91-95.
- Dutta, K., Sen, S., Veeranki, V. D., 2009.** Production, characterization and applications of microbial cutinases. *Proc. Biochem.* 44, 127-34.
- Ebersberger, I., de Matos Simoes, R., Kupczok, A., Gube, M., Kothe, E., Voigt, K., von Haeseler, A., 2012.** A Consistent Phylogenetic Backbone For the Fungi. *Mol Biol Evol.* 29, 1319-34.
- Fischer, R., Timberlake, W. E., 1995.** *Aspergillus nidulans* *apsA* (anucleate primary sterigmata) encodes a coiled-coil protein required for nuclear positioning and completion of asexual development. *J Cell Biol* 128, 485-98.

- Fischer, R., Zekert, N., Takeshita, N., 2008.** Polarized growth in fungi - interplay between the cytoskeleton, positional markers and membrane domains. *Mol Microbiol.* 68, 813-26.
- Foth, B. J., Goedecke, M. C., Soldati, D., 2006.** New insights into myosin evolution and classification. *Proc Natl Acad Sci U S A.* 103, 3681-6.
- Fowler, T. J., Mitton, M. F., 2000.** Scooter, a new active transposon in *Schizophyllum commune*, has disrupted two genes regulating signal transduction. *Genetics* 156, 1585-94.
- Girbardt, M., 1957.** Der Spitzenkörper von *Polystictus versicolor* (L.). *Planta* 50, 47-59.
- Glinski, M. and Weckwerth, W., 2006.** The role of mass spectrometry in plant systems biology. *Mass Spectrom Rev.* 25, 173-214.
- Hall, T., 1999.** BioEdit: a user-friendly biological sequence alignment editor and analysis program for Windows 95/98/NT. *Nucl. Acids. Symp. Ser.* 41: 95-98.
- Hanisch, L., 2012.** Analyse des Transkriptoms einer $\Delta dhc2$ Mutante des Basidiomyceten *Schizophyllum commune*. (Bachelorthesis).
- Harmsen, M. C., Schuren, F. H. J., Moukha, S. M., van Zuilen, C. M., Punt. P. J., Wessels, J. G. H., 1992.** Sequence analysis of the glyceraldehyde-3-phosphate dehydrogenase genes from the basidiomycetes *Schizophyllum commune*, *Phanerochaete chrysosporium* and *Agaricus bisporus*. *Curr Genet.* 22, 447-54.
- Hennessey, E. S., Drummond, D. R., Sparrow, J. C., 1993.** Molecular genetics of actin function. *Biochem J.* 291 (Pt 3), 657-71.
- Hibbett, D. S., 2006.** A phylogenetic overview of the Agaricomycotina. *Mycologia* 98, 917-25.

- Hibbett, D. S., Binder, M., Bischoff, J. F., Blackwell, M., Cannon, P. F., Eriksson, O. E., Huhndorf, S., James, T., Kirk, P. M., Lücking, R., Lumbsch, H.T., Lutzoni, F., Matheny, P. B., McLaughlin, D. J., Redhead, S., Schoch, C. L., Spatafora, J. W., Stalpers, J. A., Vilgalys, R., Aime, M. C., Aptroot, A., Bauer, R., Begerow, D., Benny, G. L., Castlebury, L. A., Crous, P. W., Dai, L. C., Gams, W., Geiser, D. M., Griffith, G. W., Gueidan, C., Hawksworth, D. L., Hestmark, G., Hosaka, K., Humber, R. A., Hyde, K. D., Ironside, J. E., Kõljalg, U., Kurtzmann, C. P., Larsson, K. H., Lichtwardt, R., Longcore, J., Miadlikowska, J., Miller, A., Moncalvo, J. M., Mozley-Standridge, S., Oberwinkler, F., Parmasto, E., Reeb, V., Rogers, J. D., Roux, C., Ryvarden, L., Sampaio, J. P., Schüssler, A., Sugiyama, J., Thorn, R. G., Tibell, L., Untereiner, W. A., Walker, C., Wang, Z., Weir, A., Weiss, M., White, M. M., Winka, K., Yao, Y. J., Zhang, N., 2007.** A higher-level phylogenetic classification of the Fungi. *Mycol Res.* 111, 509-47.
- Hirakawa, E., Higuchi, H., Toyoshima, Y. Y., 2000.** Processive movement of single 22S dynein molecules occurs only at low ATP concentrations. *Proc Natl Acad Sci U S A.* 97, 2533-7.
- Holzbaur, E. L., Vallee, R. B., 1994.** DYNEINS: molecular structure and cellular function. *Annu Rev Cell Biol.* 10, 339-72.
- Horton, P., Park, K.-J., Obayashi, T., Fujita, N., Harada, H., Adams-Collier, C.J., Nakai, K., 2007.** "WoLF PSORT: Protein Localization Predictor", *Nucleic Acids Research*, doi:10.1093/nar/gkm259,
- Hoyt, M. A., Hyman, A. A., Bähler, M., 1997.** Motor proteins of the eukaryotic cytoskeleton. *Proc Natl Acad Sci U S A.* 94, 12747-8.

- Huelsenbeck, J. P., Ronquist, F., 2001.** MRBAYES: Bayesian inference of phylogenetic trees. *Bioinformatics*. 17, 754-5.
- Jeffers, M. R., McRoberts, W. C., Harper, D. B., 1997.** Identification of a phenolic 3-O-methyltransferase in the lignin-degrading fungus *Phanerochaete chrysosporium*. *Microbiol* 143, 1975-81.
- Kardon, J. R., Vale, R. D., 2009.** Regulators of the cytoplasmic dynein motor. *Nat Rev Mol Cell Biol*. 10, 854-65.
- Karki, S., Holzbaur, E. L., 1999.** Cytoplasmic dynein and dynactin in cell division and intracellular transport. *Curr Opin Cell Biol*. 11, 45-53.
- Katoh, K., Toh, H., 2008.** Recent developments in the MAFFT multiple sequence alignment program. *Brief Bioinform*. 9, 286-98.
- King, S. J., Brown, C. L., Maier, K. C., Quintyne, N. J., Schroer, T. A., 2003.** Analysis of the dynein-dynactin interaction in vitro and in vivo. *Mol Biol Cell*. 14, 5089-97.
- Kniep, H., 1920.** Über morphologische und physiologische Geschlechtsdifferenzierung. (Untersuchungen an Basidiomyzeten) Verhandlungen der Physikalisch Medizinischen Gesellschaft in Würzburg 46, 1 – 18.
- Kniep, H., 1922.** Über Geschlechtsbestimmung und Reduktionsteilung. (Untersuchungen an Basidiomyzeten) Verhandlungen der Physikalisch Medizinischen Gesellschaft in Würzburg 47.
- Koike M., Awaji, T., Kataoka, M., Tsujimoto, G., Kartasova, T., Koike, A., Shiomi, T., 1999.** Differential subcellular localization of DNA-dependent protein kinase

- components Ku and DNA-Pkcs during mitosis. *J Cell Science* 112, 4031-39.
- Koltin, Y., Stamberg, J., Bawnik, N., Tamarkin, A., Werczberger, R., 1979.** Mutational analysis of natural alleles in and affecting the *B* incompatibility factor of *Schizophyllum*. *Genetics*. 93, 383-91.
- Korn, E. D., 2000.** Coevolution of head, neck, and tail domains of myosin heavy chains. *Proc Natl Acad Sci U S A*. 97, 12559-64.
- Kosugi S., Hasebe M., Tomita M., Yanagawa H. 2009.** Systematic identification of yeast cell cycle-dependent nucleocytoplasmic shuttling proteins by prediction of composite motifs. *Proc. Natl. Acad. Sci. USA* 106, 10171-76.
- Kothe, E., 1996.** Tetrapolar fungal mating types: sexes by the thousands. *FEMS Microbiol Rev.* 18, 65-87.
- Kothe, E., 1999.** Mating types and pheromone recognition in the Homobasidiomycete *Schizophyllum commune*. *Fungal Genet Biol.* 27, 146-52.
- Kovalchuk, A. and Driessen, A. J., 2010.** Phylogenetic analysis of fungal ABC transporters. *BMC Genomics* 11, 177.
- Kvam, V. M., Liu, P., Si, Y., 2012.** A comparison of statistical methods for detecting differentially expressed genes from RNA-seq data. *Am J Bot.* 99, 248-56.
- Lakämper, S., Kallipolitou, A., Woehlke, G., Schliwa, M., Meyhöfer, E., 2003.** Single fungal kinesin motor molecules move processively along microtubules. *Biophys J.* 84, 1833-43.
- Leach, M.D. and Brown, A. J., 2012.** Posttranslational modifications of proteins in the pathobiology of medically relevant fungi. *Eukaryot Cell.* 11, 98-108.

- Lengeler, K., Kothe, E., 1994.** Molecular characterization of *ural*, a mutant allele for orotidine-5'-monophosphate decarboxylase in *Schizophyllum commune*. FEMS Microbiol Lett 119, 243-48.
- Lewis, D. F. V., 2002.** Oxidative stress: the role of cytochromes P450 in oxygen activation. J Chem Tech and Biotech 77, 1095-100.
- Lin, J., Nazareus, T. J., Frey, J. L., Liang, X., Wilson, M. A., Stone, J. M., 2011.** A plant DJ-1 homolog is essential for *Arabidopsis thaliana* chloroplast development. PLoS One 6, 1-8.
- Mai, L., 2012.** Nachweis der erfolgreichen Deletion von *dhc1* im Agaricomyceten *Schizophyllum commune*. (Bachelorthesis).
- Markus, S. M., Plevock, K. M., St Germain, B. J., Punch, J. J., Meaden, C. W., Lee, W. L., 2011.** Quantitative analysis of Pac1/LIS1-mediated dynein targeting: Implications for regulation of dynein activity in budding yeast. Cytoskeleton (Hoboken). 68, 157-74.
- Martin, R., Walther, A., Wendland, J., 1994.** Deletion of the dynein heavy-chain gene DYN1 leads to aberrant nuclear positioning and defective hyphal development in *Candida albicans*. Eukaryot Cell, 3, 1574-88.
- Matheny, P. B., Gossmann, J. A., Zalar, P., Arun Kumar, T. K., Hibbett, D. S., 2006.** Resolving the phylogenetic position of the Wallemiomycetes: an enigmatic major lineage of Basidiomycota. Can J Bot. 84,1794-1805.
- McCracken, S., Longman, D., Marcon, E., Moens, P., Downey, M., Nickerson, J. F., Jessberger, R., Wilde, A., Caceres, J. F., Emili, A., Blencowe, B. J., 2005.** Proteomic analysis of SRm160-containing complexes reveals a conserved association with cohesin. J Biol Chem 280, 42227-36.

- Morel, M., Ngadin, A. A., Droux, M., Jaquot, J.-P., Gelhaye, E., 2009.** The fungal glutathione S-transferase system. Evidence of new classes in the wood-degrading basidiomycete *Phanerochaete chrysosporium*. *Cell. Mol. Life Sci.* 66, 3711-25.
- Niederpruem, D. J., Wessels, J. G., 1969.** Cytodifferentiation and morphogenesis in *Schizophyllum commune*. *Bacteriol Rev.* 33, 505-35.
- Ohm, R. A., de Jong, J. F., Lugones, L. G., Aerts, A., Kothe, E., Stajich, J. E., de Vries, R. P., Record, E., Levasseur, A., Baker, S. E., Bartholomew, K. A., Coutinho, P. M., Erdmann, S., Fowler, T. J., Gathman, A. C., Lombard, V., Henrissat, B., Knabe, N., Kües, U., Lilly, W. W., Lindquist, E., Lucas, S., Magnuson, J. K., Piumi, F., Raudaskoski, M., Salamov, A., Schmutz, J., Schwarze, F. W., vanKuyk P. A., Horton, J. S., Grigoriev, I. V., Wösten, H. A., 2010.** Genome sequence of the model mushroom *Schizophyllum commune*. *Nat Biotechnol.* 28, 957-63.
- Palmer, G. E., Horton, J. S., 2006.** Mushrooms by magic: making connections between signal transduction and fruiting body development in the basidiomycete fungus *Schizophyllum commune*. *FEMS Microbiol Lett.* 262, 1-8.
- Pao, S. S., Paulsen, I. T., Saier, Jr., M. H., 1998.** Major facilitator superfamily. *Microbiol. Mol. Biol. Rev.* 62, 1-34.
- Papazian, H. P., 1950.** The incompatibility factors and a related gene in *Schizophyllum commune*. *Genetics* 36, 441-59.
- Park, G., Servin, J. A., Turner, G. E., Altamirano, L., Colot, H. V., Collopy, P., Litvinkova, L., Li, L., Jones, C. A., Diala, F.-G., Dunlap, J. C., Borkovich, K. A.,**

- 2011.** Global Analysis of Serine-Threonine Protein Kinase Genes in *Neurospora crassa*. Eukaryot Cell 10, 1553-64.
- Pfister, K. K., Shah, P. R., Hummerich, H., Russ, A., Cotton, J., Annuar, A. A., King, S. M., Fisher, E. M., 2006.** Genetic analysis of the cytoplasmic dynein subunit families. PLoS Genet. 2, e1. doi:10.1371/journal.pgen.0020001.
- Phillips, R. S., 2011.** Structure, mechanism, and substrate specificity of kynureninase. Biochimica et Biophysica Acta 1814, 1481-88.
- Plamann, M., Minke, P. F., Tinsley, J. H., Bruno, K. S., 1994.** Cytoplasmic dynein and actin-related protein Arp1 are required for normal nuclear distribution in filamentous fungi. J Cell Biol. 127, 139-149.
- Popowich, E. A., Firsov, A. P., Mitiouchkina, T. Y., Filipenya, V. L., Dolgov, S. V., Reshetnikov, V. N., 2007.** *Agrobacterium*-mediated transformation of *Hyacinthus orientalis* with thaumatin II gene to control fungal diseases. Plant Cell Tiss Organ Cult. 90, 237-44.
- Raju, T.R., Dahl, D., 1982.** Immunofluorescence staining of cultured neurons: a comparative study using tetanus toxin and neurofilament antisera. Brain Research, 248, 196-200.
- Raper, J. R., Miles, P. G., 1958.** The Genetics of *Schizophyllum commune*. Genetics. 43, 530-46.
- Raudaskoski, M., Koltin, Y., 1973.** Ultrastructural aspects of a mutant of *Schizophyllum commune* with continuous nuclear migration. J Bacteriol. 116, 981-88.

- Raudaskoski, M., Kothe, E., 2010.** Basidiomycete mating type genes and pheromone signaling. *Eukaryot Cell*. 9, 847-59.
- Redecker, D., 2002.** Molecular identification and phylogeny of arbuscular mycorrhizal fungi. *Plant and Soil* 244, 67-73.
- Ring, C., 2012.** Analyse des Sekretoms des Basidiomyceten *Schizophyllum commune*. (Bachelorthesis).
- Schliwa, M., Woehlke, G., 2003.** Molecular motors. *Nature*. 422, 759-65.
- Schubert, D., Raudaskoski, M., Knabe, N., Kothe, E., 2006.** Ras GTPase-activating protein gap1 of the homobasidiomycete *Schizophyllum commune* regulates hyphal growth orientation and sexual development. *Eukaryot Cell*. 5, 683-95.
- Schuster, M., Sreedhar, K., Ashwin, P., Lin, C., Severs, N. J., Steinberg, G., 2011.** Controlled and stochastic retention concentrates dynein at microtubule ends to keep endosomes on track. *EMBO* 30, 652-64.
- Schuurs, T. A., Schaeffer, E. A. M., Wessels, J. G. H., 1997.** Homology-dependent silencing of the *Sc3* gene in *Schizophyllum commune*. *Genetics* 147, 589-96.
- Shevchenko, A., Wilm, M., Vorm, O., Mann, M., 1996.** Mass spectrometric sequencing of proteins silver-stained polyacrylamide gels. *Anal Chem*, 68, 850-58.
- Specht, A. C., Munoz-Rivas, A., Novotny, C. P., Ullrich, R. C., 1988.** Transformation of *Schizophyllum commune*: an analysis of parameters for improving transformation frequencies. *Experimental Mycol.* 12, 357-66.

- Stajich, J. E., Berbee, M. L., Blackwell, M., Hibbett, D. S., James, T. Y., Spatafora, J. W., Taylor, J. W., 2009.** The fungi. *Curr Biol* 19, 18, 840-45.
- Stamatakis, A., Hoover, P., Rougemont, J., 2008.** A rapid bootstrap algorithm for the RAxML Web servers. *Syst Biol.* 57, 758-71.
- Stankis, M. M., Specht, C. A., Giasson, L., 1990.** Sexual incompatibility in *Schizophyllum commune*: from classical genetics to a molecular view. *Seminars in Developmental Biol* 1, (Raper, C. A. & Johnson, D. I., eds), 195-206.
- Steinberg, G., 2000.** The cellular roles of molecular motors in fungi. *Trends in Microbiol* 162, 8, 4.
- Steinberg, G., 2007a.** Preparing the way: fungal motors in microtubule organization. *Trends Microbiol.* 15, 14-21.
- Steinberg, G., 2007b.** Hyphal growth: a tale of motors, lipids and the Spitzenkörper. *Eukaryot Cell* 6, 351-60.
- Straube, A., Enard, W., Berner, A., Wedlich-Soeldner, R., Kahmann, R., Steinberg, G., 2001.** A split motor domain in a cytoplasmic dynein. *EMBO Journal.* 20, 5091-100.
- Straube, A., Weber, I., Steinberg, G., 2005.** A novel mechanism of nuclear envelope breakdown in a fungus: nuclear migration strips off the envelope. *EMBO Journal* 24, 1674-85.
- Tarazona, S., García-Alcalde, F., Dopazo, J., Ferrer, A., Gonesá, A., 2011.** Differential expression in RNA-Seq: a matter of depth. *Genome Res.* 21 (12), 2213-23.

- Theisen, U., Straube, A., Steinberg, G., 2008.** Dynamic rearrangement of nucleoporins during fungal "open" mitosis. *Mol. Biol. of the Cell* 19, 1230-40.
- Torisawa, T., Nakayama, A., Furuta, K., Yamada, M. Hirotsune, S., Toyoshima, Y. Y., 2011.** Functional dissection of LIS1 and NDEL1 towards understanding the molecular mechanisms of cytoplasmic dynein regulation. *J Biol Chem.* 286, 1959-65.
- Wang, L., Yu, X., Yang, Y., Chen, J., Hu, D., Deng, C., Yang, X., Hu, X., Xu, J., 2010.** Molecular characterization and expression of the MYND-ZF gene from *Clonorchis sinensis*. *Parasitol Res* 107, 1249-55.
- Wang, N.-Y., Yang, S. L., Lin, C.-H., Chung, K.-R., 2011.** Gene inactivation in the citrus pathogenic fungus *Alternaria alternata* defect at the *ku70* locus associated with non-homologous end joining. *World J Microbiol Biotechnol* 27, 1817-26.
- Wessels, J. G. H., 1986.** Cell wall synthesis in apical hyphal growth. *Int. Rev. Cytol.* 104, 37-79.
- Wilson, M. A., 2011.** The role of cysteine oxidation in DJ-1 function and dysfunction. *Antioxidants & Redox Signaling* 15, 111-22.
- Xiang, X., Beckwith, S. M., Morris, N. R., 1994.** Cytoplasmic dynein is involved in nuclear migration in *Aspergillus nidulans*. *Proc Natl Acad Sci U S A.* 91, 2100-4.
- Xiang, X., 2003.** LIS1 at the microtubule plus end and its role in dynein-mediated nuclear migration. *J Cell Biol.* 160, 289-90.

- Xiang, X., Plamann, M., 2003.** Cytoskeleton and motor proteins in filamentous fungi. *Curr Opin Microbiol.* 6, 628-33.
- Xiang, X., Fischer, R., 2004.** Nuclear migration and positioning in filamentous fungi. *Fungal Genet. Biol.* 41, 411 - 19.
- Yamamoto, A., Hiraoka, Y., 2003.** Cytoplasmic dynein in fungi: insights from nuclear migration. *J Cell Sci.* 116, 4501-12.
- Yu C.S., Chen Y.C., Lu C.H., Hwang J.K., 2006.** Prediction of protein subcellular localization. *Proteins: Structure, Function and Bioinformatics*, 64, 643-51.
- Zickler, D., 1970.** Division spindle and centrosomal plaques during mitosis and meiosis in some Ascomycetes. *Chromosoma* 30, 287-304.

8.) Appendix

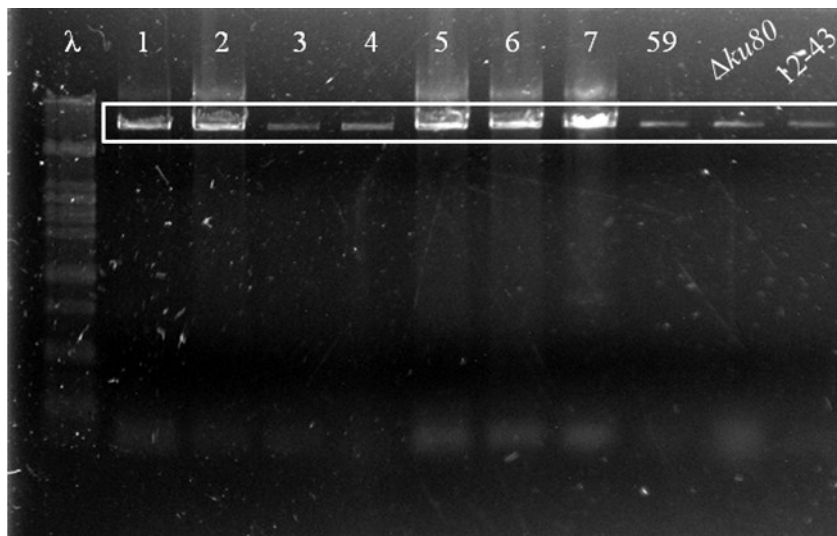
Table A1: Dataset of phylogenetic tree (representatives of Agaricomycotina are indicated as classes, for Wallemiomycetes no subphylum is assigned)

species	phylum	subphylum/class	database	accession number(s)
<i>Agaricus bisporus</i> <i>var bisporus</i> H97	<i>Basidiomycota</i>	<i>Agaricomycetes</i>	Joint Genome Institute	188324 214780
<i>Agaricus bisporus</i> <i>var burnetti</i> JB137- S8	<i>Basidiomycota</i>	<i>Agaricomycetes</i>	Joint Genome Institute	80770 50984
<i>Ashbya gossypii</i>	<i>Ascomycota</i>	<i>Saccharomycotina</i>	NCBI	NP983660
<i>Aspergillus</i> <i>fumigates</i>	<i>Ascomycota</i>	<i>Pezizomycotina</i>	NCBI	XP753470
<i>Aspergillus nidulans</i>	<i>Ascomycota</i>	<i>Pezizomycotina</i>	NCBI	XP657722
<i>Auriculara delicata</i> SS-5 v 1.0	<i>Basidiomycota</i>	<i>Agaricomycetes</i>	Joint Genome Institute	78165 179093
<i>Bjerkandera adusta</i> v 1.0	<i>Basidiomycota</i>	<i>Agaricomycetes</i>	Joint Genome Institute	164640 210459
<i>Candida albicans</i>	<i>Ascomycota</i>	<i>Saccharomycotina</i>	NCBI	XP723061
<i>Coniophora puteana</i> v 1.0	<i>Basidiomycota</i>	<i>Agaricomycetes</i>	Joint Genome Institute	114255 133816
<i>Coprinopsis cinereus</i> <i>Okoyama</i> 7#130	<i>Basidiomycota</i>	<i>Agaricomycetes</i>	Joint Genome Institute	11129 3276
<i>Cryptococcus</i> <i>bacillospor</i>	<i>Basidiomycota</i>	<i>Tremellomycetes</i>	Broad Institute	CNBF3870
<i>Cryptococcus gatti</i> WM276	<i>Basidiomycota</i>	<i>Tremellomycetes</i>	NCBI	XP003194894
<i>Cryptococcus</i> <i>neoformans</i> var <i>neoformans</i> JEC21	<i>Basidiomycota</i>	<i>Tremellomycetes</i>	NCBI	XP571532
<i>Dacryopinax</i> sp. DJM 731 SSP-1 v 1.0	<i>Basidiomycota</i>	<i>Dacryomycetes</i>	Joint Genome Institute	67652 116759
<i>Dichomitus squalens</i> v 1.0	<i>Basidiomycota</i>	<i>Agaricomycetes</i>	Joint Genome Institute	172670 182524
<i>Fomitiporia</i> <i>mediterranea</i> v 1.0	<i>Basidiomycota</i>	<i>Agaricomycetes</i>	Joint Genome Institute	106792 121816
<i>Fomitopsis pinicola</i> SS1 v 1.0	<i>Basidiomycota</i>	<i>Agaricomycetes</i>	Joint Genome Institute	140971 150781
<i>Ganoderma</i> sp 10597 SS1 v 1.0	<i>Basidiomycota</i>	<i>Agaricomycetes</i>	Joint Genome Institute	113078 140853
<i>Gloeophyllum</i> <i>trabeum</i> v 1.0	<i>Basidiomycota</i>	<i>Agaricomycetes</i>	Joint Genome Institute	69644 135602

<i>Heterobasidion annosum</i> v 2.0	Basidiomycota	Agaricomycetes	Joint Genome Institute	157884 167275
<i>Homo sapiens</i>	Mammalia	Hominidae	NCBI	NP001267
<i>Laccaria bicolor</i> v 2.0	Basidiomycota	Agaricomycetes	Joint Genome Institute	385191 300914
<i>Magnaporthe oryzae</i> 70 50	Ascomycota	Pezizomycotina	NCBI	EDK04833
<i>Malassezia globosa</i>	Basidiomycota	Ustilaginomycotina	Joint Genome Institute	1036 1033
<i>Melampsora laricis populina</i> v 1.0	Basidiomycota	Pucciniomycotina	Joint Genome Institute	46877
<i>Moniliophthora perniciosa</i>	Basidiomycota	Agaricomycetes		(personal communication)
<i>Mucor circinelloides</i>	“Zygomycota”	Mucoromycotina	Joint Genome Institute	90435
<i>Mus musculus</i>	Mammalia	Rodentia	NCBI	NP084514
<i>Nectria haematococca</i>	Ascomycota	Pezizomycotina	NCBI	EEU40393
<i>Neurospora crassa</i>	Ascomycota	Pezizomycotina	NCBI	XP962616
<i>Phanerochaete carnosa</i> HHB-10118-Sp v 1.0	Basidiomycota	Agaricomycetes	Joint Genome Institute	256688 168059
<i>Phanerochaete chrysosporium</i> v. 2.0	Basidiomycota	Agaricomycetes	Joint Genome Institute	7743 7621
<i>Phlebia brevispora</i> HHB-7030 SS6 v 1.0	Basidiomycota	Agaricomycetes	Joint Genome Institute	77449 138126
<i>Phlebiopsis gigantea</i> v 1.0	Basidiomycota	Agaricomycetes	Joint Genome Institute	34940 29508
<i>Pichia pastoris</i> GS115	Ascomycota	Saccharomycotina	NCBI	XP002491674
<i>Pleurotus ostreatus</i> PC9 v 1.0	Basidiomycota	Agaricomycetes	Joint Genome Institute	90323 85298
<i>Pleurotus ostreatus</i> PC15 v 2.0	Basidiomycota	Agaricomycetes	Joint Genome Institute	1074656 49217
<i>Puccinia graminis</i> f sp tritici CRL 75 36 700 3	Basidiomycota	Pucciniomycotina	NCBI	XP0033294
<i>Punctularia strigosozonata</i> v 1.0	Basidiomycota	Agaricomycetes	Joint Genome Institute	109520 139986
<i>Rhizopus oryzae</i> RA 99 880	“Zygomycota”	Mucoromycotina	Broad Institute	RO3G06230
<i>Rhodotorula glutinis</i>	Basidiomycota	Pucciniomycotina	NCBI	EGU12573
<i>Rhodotorula graminis</i> strain WP1	Basidiomycota	Pucciniomycotina	Joint Genome	34525

<i>v 1.0</i>			Institute	
<i>Saccharomyces cerevisiae</i>	<i>Ascomycota</i>	<i>Saccharomycotina</i>	NCBI	EDN59957
<i>Schizophyllum commune v 1.0</i>	<i>Basidiomycota</i>	<i>Agaricomycetes</i>	Joint Genome Institute	65157 65089
<i>Schizosaccharomyces pombe 972h</i>	<i>Ascomycota</i>	<i>Taphrinomycotina</i>	NCBI	XP001713108
<i>Serpula lacrymans S7 3 v 2.0</i>	<i>Basidiomycota</i>	<i>Agaricomycetes</i>	Joint Genome Institute	97057 158538
<i>Serpula lacrymans S7 9 v 1.0</i>	<i>Basidiomycota</i>	<i>Agaricomycetes</i>	Joint Genome Institute	358531 445906
<i>Sporisorium reilianum</i>	<i>Basidiomycota</i>	<i>Ustilaginomycotina</i>	Munich Information Center for Protein Sequences	sr13295 sr15257
<i>Sporobolomyces roseus v 1.0</i>	<i>Basidiomycota</i>	<i>Pucciniomycotina</i>	Joint Genome Institute	21679
<i>Stereum hirsutum FP- 91666 SS1 v 1.0</i>	<i>Basidiomycota</i>	<i>Agaricomycetes</i>	Joint Genome Institute	143406 151431
<i>Trametes versicolor v 1.0</i>	<i>Basidiomycota</i>	<i>Agaricomycetes</i>	Joint Genome Institute	111059
<i>Tremella mesenterica Fries v 1.0</i>	<i>Basidiomycota</i>	<i>Tremellomycetes</i>	Joint Genome Institute	62339
<i>Tuber melanosporum</i>	<i>Ascomycota</i>	<i>Pezizomycotina</i>	Institut national de la recherche agronomique	GSTUMT0000079400 1
<i>Ustilago maydis</i>	<i>Basidiomycota</i>	<i>Ustilaginomycotina</i>	Broad Institute	AAK91759 AAK91760
<i>Wallemia sebi v 1.0</i>	<i>Basidiomycota</i>	<i>Wallemiomycetes</i>	Joint Genome Institute	59093 67017
<i>Wolfiporia cocos MD-104 SS10 v 1.0</i>	<i>Basidiomycota</i>	<i>Agaricomycetes</i>	Joint Genome Institute	93003 159953

A



B

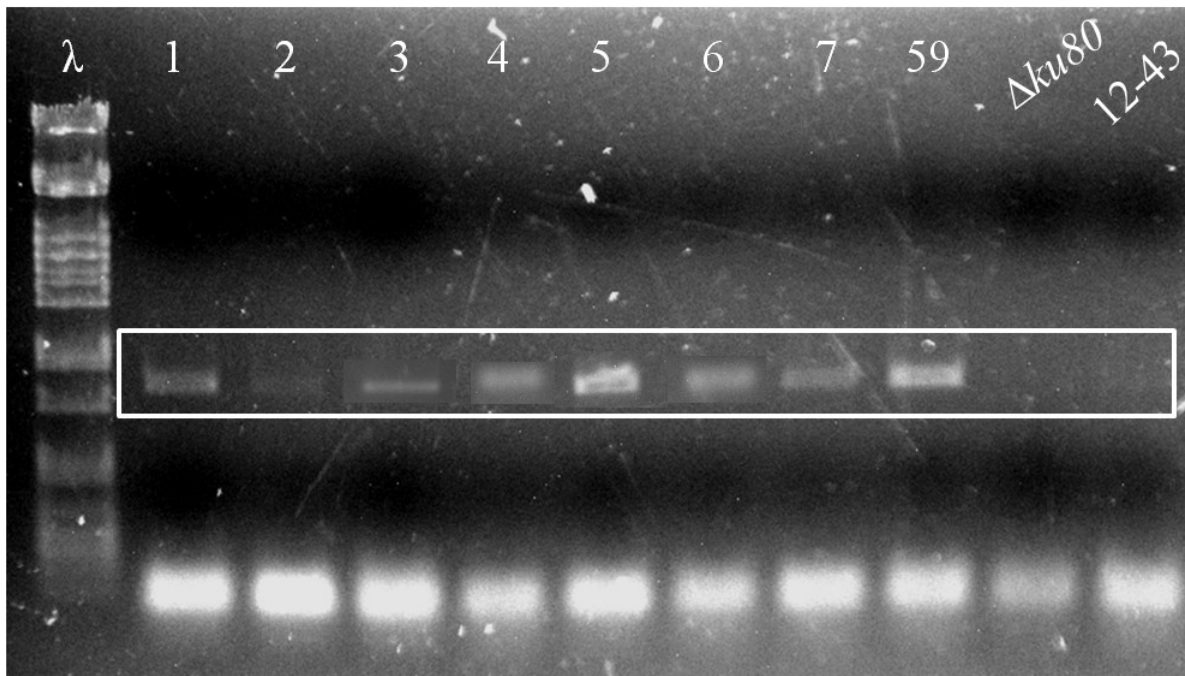


Figure A1: Proof of the successful deletion of *dhc1* via nested PCR A) first PCR with the amplified target DNA band at approximately 7 kb; B) second PCR with the amplified 905 bp fragment of the deletion cassette. PCR was run several times, to get results for every strain.

Table A2: Detailed list of 22 genes which are differentially regulated in all 3 investigated strains.

Protein ID	E6 vs $\Delta dhc2$	12-43 vs $\Delta dhc2$	12-43 vs E6	Gene	KOG-Group
1037942	4,756038377	7,134837956	2,38813215	/	not annotated
1038458	-2,8106233	2,301893606	5,12534357	Major facilitator superfamily MFS-1	Metabolism
1039406	4,37666862	2,479011453	-1,8853687	/	not annotated
1081190	-6,58651433	3,3506123	9,94776481	/	not annotated
1082687	2,563358063	-2,857426961	-5,4081719	Cutinase	no classification
1105422	-2,48649342	1,97353543	4,47240679	Glycoside hydrolase, family 61	no classification
1135605	-4,15359773	-1,986182636	2,17956538	/	not annotated
1151728	-2,96483547	-6,529363775	-3,5541785	NmrA-like	no classification
1187228	-2,44831603	-5,620075018	-3,1629499	/	not annotated
1188048	-1,82501541	-6,032979337	-4,1968045	/	not annotated
1189960	3,989492534	7,760293197	3,78362397	/	not annotated
1191755	6,445570164	4,695881738	-1,7382896	/	not annotated
1212538	-4,40448666	-2,030006509	2,38651578	Cytochrome P450	Metabolism
1213381	7,19398116	3,992076043	-3,1915584	Heat shock protein Hsp20	Cellular processes and signaling
1215940	-3,33030925	-7,338646539	-3,9985962	Thaumatococcus, pathogenesis-related	no classification
1340620	-2,7299548	-5,204703595	-2,4683577	Glutathione S-transferase, C-terminal	Cellular processes and signaling
1359387	-2,48183934	-5,648172754	-3,1573676	/	not annotated
235431	2,202807805	-2,875524048	-5,0686732	Glycosyl hydrolase, family 13, catalytic region	Metabolism
54466	-4,48708224	3,447893581	7,94770694	Glycoside hydrolase, family 61	no classification
56366	2,9450302	5,339721033	2,40555108	Glycoside hydrolase, family 16	no classification
64748	2,458022625	4,225666225	1,77989377	Peptidase M14, carboxypeptidase A	Poorly characterized
66483	5,84042826	2,83905026	-2,992082	Glycoside hydrolase, family 20, catalytic core	Metabolism

Table A3: 250 genes, differentially expressed in $\Delta dhc2$. Genes, which have a different expression in all 3 strains, are highlighted in grey.

Protein ID	E6 vs $\Delta dhc2$	12-43 vs $\Delta dhc2$	12-43 vs E6	Gene
1028812	-5,233937395	-6,145486934	-0,904505719	General substrate transporter
1029395	-2,361564788	-2,054796823	0,318629949	/
1029742	2,588970955	3,789296243	1,213478708	Major facilitator superfamily MFS-1
1030522	-6,770785519	-6,130318641	0,652352013	Pyridoxal phosphate-dependent transferase, major region
1030606	2,930187723	2,606926977	-0,312098741	/
1036814	-3,798366264	-4,526308203	-0,717836876	Orotidine 5'-phosphate decarboxylase, core
1037026	2,163169824	1,945923908	-0,206698987	/
1037295	2,217336847	3,147801555	0,94195259	Glutathione S-transferase, N-terminal
1037673	-4,528719656	-3,372573511	1,168390373	/
1037942	4,756038377	7,134837956	2,38813215	/
1038458	-2,810623297	2,301893606	5,125343566	Major facilitator superfamily MFS-1
1038719	2,925543306	3,413243566	0,499051883	/
1039162	2,39709372	2,265453573	-0,120504397	/
1039406	4,37666862	2,479011453	-1,88536871	/
1039504	2,356638996	2,721057778	0,378173235	General substrate transporter
1039542	3,520855801	4,351606785	0,845042911	/
1051032	-1,966546615	-1,959614101	0,018540661	Nucleoside diphosphate kinase, core
1051196	-4,810006623	-5,427520644	-0,599683427	Rare lipoprotein A
107357	2,54036482	3,834239327	1,304816859	Whey acidic protein, 4-disulphide core
1075347	-2,369999768	-2,98413102	-0,602066721	/
1081190	-6,58651433	3,3506123	9,947764811	/
1082687	2,563358063	-2,857426961	-5,408171923	Cutinase
1083807	5,893434828	6,69659658	0,811910739	/
1085853	-3,229775953	-2,943936687	0,297814975	Calcium-binding EF-hand
1088038	-3,87436375	-3,892026978	-0,007712376	NmrA-like

1088777	2,210471062	2,827690343	0,627476723	Epoxide hydrolase
1091573	-3,07336009	-2,483629852	0,600575649	C4-dicarboxylate transporter/malic acid transport protein
1091853	-4,254521919	-4,758009884	-0,49089782	/
1092711	-2,934949479	-3,030018151	-0,088737036	/
1093152	-5,971440214	-8,183793562	-2,199387433	/
1093619	2,836555649	2,030045785	-0,794103632	Major facilitator superfamily MFS-1
1094645	-3,155767319	-2,542019548	0,624882654	Aldo/keto reductase
1094937	-3,788446836	-4,150329003	-0,350287316	Short-chain dehydrogenase/reductase SDR
1096809	-2,780779156	-3,262011282	-0,468863919	Thaumatococcus, pathogenesis-related
1097314	2,461740701	3,312118694	0,861945514	/
1098598	-2,576721225	-3,380427171	-0,793581562	/
1099997	-2,214535351	-2,565928017	-0,340332781	Glucose-methanol-choline oxidoreductase, N-terminal
1100973	Inf	-Inf	0,565302987	Peptidase M35, deuterolysin
1103821	7,64650652	6,051737618	-1,586031257	/
1105422	-2,486493424	1,97353543	4,472406789	Glycoside hydrolase, family 61
1106207	-3,211902935	-2,310515205	0,914236143	/
1107476	1,953468863	2,215344239	0,272554103	Major facilitator superfamily MFS-1
1109087	-3,581615621	-2,26199611	1,332503098	/
1109355	2,935336737	2,525598082	-0,398770976	/
1111656	2,754298962	2,112541896	-0,630566524	Phosphoesterase
1111864	-1,851650375	-3,295593315	-1,433073593	Aldo/keto reductase
1113332	4,394579132	4,191639042	-0,19134657	/
1115881	2,614472197	1,91643395	-0,686805523	Major facilitator superfamily MFS-1
1118340	-2,471320642	-4,067425672	-1,582641239	NmrA-like
1118702	3,10809262	2,720646376	-0,375375738	/
1119592	3,507708987	2,978201569	-0,516277158	/
1120079	2,53156002	2,746521456	0,227262453	/
1122636	-3,643980133	-2,443613958	1,212038544	Cytochrome P450

1123577	-4,304578918	-2,486595097	1,830557943	Tetracycline resistance protein, TetB
1124058	-2,665791374	-2,200985887	0,477117168	Amino acid/polyamine transporter I
1124671	-6,946614174	-6,172072708	0,779600145	O-methyltransferase, family 3
1124856	-2,918579353	-4,475691493	-1,545482535	Aldo/keto reductase
1125392	-2,562132139	-3,030991624	-0,457417807	MFS general substrate transporter
1125617	4,112336974	3,19666479	-0,903599634	Major facilitator superfamily MFS-1
1126608	-5,121896744	-4,251247352	0,878725371	General substrate transporter
1126683	3,945339948	3,156807128	-0,778054834	Peptidase A1
1127677	-3,333083675	-1,783391017	1,560122202	Transketolase, N-terminal
1130317	-3,47303133	-3,82827313	-0,345906413	/
1132839	-3,144691752	-3,130283726	0,028471971	Aldehyde dehydrogenase
1134237	3,797929837	2,968795266	-0,830856963	CsbD-like
1134410	-4,455406372	-5,075278628	-0,609814938	Indoleamine 2,3-dioxygenase
1135605	-4,153597728	-1,986182636	2,179565384	/
113589	-4,553745123	-3,805089847	0,755848237	Barwin
1137498	-3,179767893	-3,368459752	-0,176032935	Monooxygenase, FAD-binding
1137798	-3,361886724	-2,679031353	0,693930554	Short-chain dehydrogenase/reductase SDR
1139130	-3,570652234	-4,226116159	-0,642915941	ABC transporter-like
1139537	4,205388237	4,456184967	0,26426866	/
1139544	-5,362076491	-5,794115302	-0,421606461	Thaumatococcus, pathogenesis-related
1141161	-3,461512886	-2,847171011	0,625174244	Aminotransferase, class V/Cysteine desulphurase
1141704	2,071117497	2,899178486	0,839536185	Cytochrome P450
1142239	-3,245822313	-5,479180785	-2,223963859	Short-chain dehydrogenase/reductase SDR
1145398	2,162427505	2,464431049	0,313571106	Major facilitator superfamily MFS-1
1147022	-2,342585167	-3,527738785	-1,173730467	Short-chain dehydrogenase/reductase SDR
1147271	2,229875626	3,281987504	1,059623309	Cytochrome P450
1147471	-3,252789728	-1,870522541	1,393753808	NAD(P)-binding
1147635	-3,959911043	-2,317492684	1,652346116	General substrate transporter

1147878	-4,766428876	-4,260750044	0,517524245	Alpha/beta hydrolase fold-1
1149020	-6,280503832	-5,345523224	0,942682554	ThiJ/PfpI
1149369	4,108490073	2,592789419	-1,511907121	RTA1 like protein
1149633	-3,855077577	-5,51233104	-1,649318871	FAD-binding, type 2
1149871	-3,686705742	-4,995896444	-1,29418741	/
1150903	-2,230806903	-2,513354398	-0,271386255	/
1151205	3,69966445	2,356103599	-1,338272574	Acyl-CoA N-acyltransferase
1151728	-2,96483547	-6,529363775	-3,554178506	NmrA-like
1151738	-2,555996543	-2,632230402	-0,064831649	Cupredoxin
1153190	-4,636782532	-5,027579276	-0,377144215	/
1153282	6,987778979	4,956822875	-2,026650667	Longevity-assurance protein (LAG1)
1153419	-3,177946498	-3,066359163	0,121623221	/
1153547	-4,8180565	-4,619714285	0,208201833	Aldo/keto reductase
1154143	-2,691131524	-3,722965528	-1,018404113	Ribonucleotide reductase
1154427	-3,146466502	-3,143885267	0,015521235	/
1155574	-3,76360115	-3,739960029	0,032511191	Isocitrate lyase and phosphorylmutase, core
1155753	-4,745420703	-3,274381309	1,482270794	/
1156712	-4,442014823	-4,564930823	-0,117988978	Alkyl hydroperoxide reductase/ Thiol specific antioxidant/ Mal allergen
1157013	-2,587570256	-2,205616743	0,393040104	Alcohol dehydrogenase, zinc-binding
1158244	-2,852693851	-2,372693172	0,490794993	/
1158444	-2,819439328	-2,974339208	-0,141641114	Glycoside hydrolase, catalytic core
1160870	-4,205179041	-6,511975721	-2,300141375	/
1161134	-9,812890179	-3,236075223	6,585288743	/
1161353	-7,097822803	-6,416733941	0,691124398	/
1161546	-2,508726083	-3,034811005	-0,518769207	Major facilitator superfamily MFS-1
1163017	-3,55852713	-3,97113793	-0,401034863	ABC transporter-like
1163462	-3,981812049	-3,301852466	0,690051464	Lipase, class 3
1165721	-2,299667964	-2,241838449	0,068708198	Aldose 1-epimerase

1166734	2,074760223	2,221064004	0,158275216	/
1166950	2,45085579	2,295856481	-0,143982319	Cytochrome P450
1171133	-3,89065428	-5,660531043	-1,758733085	NmrA-like
1171639	-3,209418431	-4,424795082	-1,204611326	Heat shock protein 9/12
1173577	5,279603731	3,728544688	-1,543339984	Peptidase M35, deuterolysin
1173683	2,178278698	2,457594175	0,289933176	Dienelactone hydrolase
1174098	-2,949595792	-3,001968929	-0,043161445	C4-dicarboxylate transporter/malic acid transport protein
1174659	7,879931993	5,65540728	-2,211067014	Methyltransferase type 11
1174660	-2,2250844	-5,372283	-3,139225865	tRNA-binding arm
1175533	-4,522684022	-3,499868134	1,031720275	Monooxygenase, FAD-binding
1177262	2,855926631	3,969626525	1,125854842	/
1177886	-2,47379666	-3,540209482	-1,057050191	FAD linked oxidase, N-terminal
1179498	4,599947946	5,926930478	1,335436473	Cytochrome P450
1181189	-2,3922495	-2,114176125	0,289880359	Sulphate transporter
1182337	-2,989790147	-2,859449656	0,142860299	Intradiol ring-cleavage dioxygenase, C-terminal
1183421	-2,850281698	-2,652120297	0,209925279	ATPase, F0/V0 complex, subunit C
1184739	3,986745074	3,786146948	-0,188212176	Cerato-platanin
1184854	-2,374696977	-2,158427476	0,228740116	High mobility group box, HMG1/HMG2
1184966	-2,676877522	-4,163885602	-1,478736891	Aldo/keto reductase
1185158	-3,414320498	-1,99443178	1,431753464	Zinc finger, C2H2-type
1186132	-4,226815569	-5,638446284	-1,400845082	Monooxygenase, FAD-binding
1186802	-2,982995021	-2,272652439	0,722170704	General substrate transporter
1186965	3,160125939	4,28619258	1,138798452	/
1187063	-3,257319762	-3,616961108	-0,347251598	Sulphate transporter
1187174	4,698666096	3,994331687	-0,692416533	/
1187228	-2,44831603	-5,620075018	-3,162949903	/
1187255	-2,202681429	-3,269143622	-1,059232084	/
1187303	1,959058561	3,061790019	1,11461988	2-oxo acid dehydrogenase, lipoyl-binding site

1187749	-3,166386968	-2,33290014	0,84272324	/
1188007	-3,478287564	-4,06129092	-0,572245539	/
1188048	-1,825015409	-6,032979337	-4,196804533	/
1188937	-4,840236604	-2,262731019	2,589753769	Cytochrome P450
1189135	-4,089865341	-3,842961472	0,254357181	/
1189554	-2,519510101	-2,93656401	-0,405839249	Peptidase M35, deuterolysin
1189910	2,455404113	2,22316972	-0,219933967	Cyclin-like F-box
1189960	3,989492534	7,760293197	3,783623974	/
1190496	-3,377623925	-2,351266157	1,037545194	Dak kinase
1191568	-3,307765869	-3,938315051	-0,624826055	/
1191755	6,445570164	4,695881738	-1,738289618	/
1191912	-3,408280722	-3,618864136	-0,198167675	Tyrosinase
1192157	-2,648071347	-2,438261025	0,221131442	Major facilitator superfamily MFS-1
1192730	-2,624751841	-3,762429241	-1,124690746	Sulphatase
1195144	-2,176713881	-2,395997747	-0,208237819	Glutathione-dependent formaldehyde-activating, GFA
1197868	-4,127341953	-3,813875146	0,316966533	Heat shock protein 9/12
1198083	-2,521692178	-2,708257047	-0,173328294	NAD-dependent epimerase/dehydratase
1198851	-2,966594236	-4,377915271	-1,398555262	General substrate transporter
1199179	2,630356156	3,432982392	0,813505879	/
1200136	-3,228062061	-4,528916131	-1,282607043	/
1200812	-3,796535004	-2,392519941	1,415274607	UbiA prenyltransferase
1204593	3,279025198	2,024985829	-1,242553104	Short-chain dehydrogenase/reductase SDR
1205547	-7,258371076	-6,057565409	1,203665686	O-methyltransferase, family 3
1205998	2,377112331	3,279467947	0,914666296	/
1208561	-3,661629471	-3,072492998	0,602756613	/
1210658	-3,461210916	-2,056221719	1,417429705	BTB/POZ fold
1210749	-4,250492662	-2,489385501	1,773709923	/
1211021	-2,097462445	-2,720412433	-0,612240487	SET

1212538	-4,404486662	-2,030065092	2,386515776	Cytochrome P450
1212602	-2,094064898	-2,168376592	-0,063288975	/
1213341	-3,619685245	-3,762320633	-0,133493309	Heat shock protein Hsp20
1213381	7,19398116	3,992076043	-3,191558369	Heat shock protein Hsp20
1213708	2,244990098	2,729933392	0,497169235	/
1214509	2,742767841	2,276525314	-0,454828931	/
1215519	3,202523792	2,990603234	-0,201924226	Glutathione S-transferase, C-terminal
1215531	2,512133567	3,019451329	0,518538742	Guanine-specific ribonuclease N1 and T1
1215940	-3,330309251	-7,338646539	-3,998596196	Thaumatococcus, pathogenesis-related
1216025	1,905765778	2,387669085	0,493449109	/
1216223	-2,016040302	-2,645337331	-0,616637023	Monoxygenase, FAD-binding
1217248	4,854685471	3,690040828	-1,153298452	/
1223568	-2,825834238	-2,326627392	0,512014258	/
1228183	5,094144745	3,901943273	-1,180763852	/
1228643	3,336170612	3,526342084	0,202672291	/
1245882	3,203221799	3,587066952	0,396012943	/
1268138	-2,828935891	-2,127607884	0,712489571	/
1307978	2,524757837	3,178764308	0,662827426	Peptidase aspartic, active site
1323626	3,060057726	2,562653948	-0,486579208	/
1323997	-3,063268172	-2,124117828	0,951174797	/
1325976	6,5089883	6,69676836	0,198678844	/
1335053	2,839004417	3,16063166	-0,309519827	Aldo/keto reductase
1335591	-5,129843211	-4,107502496	1,033269583	NAD(P)-binding
1338753	-2,26886637	-4,364609714	-2,083427022	/
1340620	-2,729954801	-5,204703595	-2,468357743	Glutathione S-transferase, C-terminal
1343927	-3,892800462	-5,704553285	-1,799331132	Short-chain dehydrogenase/reductase SDR
1345374	-4,522708326	-3,566854728	0,971130234	Heat shock protein Hsp20
1347654	-4,067568108	-2,572447583	1,506049635	Fungal transcriptional regulatory protein, N-terminal

1351204	-3,194711374	-2,903823032	0,303520564	/
1353568	3,997660441	4,86945765	0,859050553	Major facilitator superfamily MFS-1
1356507	7,084706768	5,969272461	-1,111304676	Cytochrome P450
1359387	-2,481839336	-5,648172754	-3,157367613	/
1359734	-3,236588686	-3,845192181	-0,597806537	/
15661	-2,480253212	-3,018158022	-0,524969996	Glycoside hydrolase, family 43
17250	-5,85543118	-2,956548434	2,909873859	Fungal mating-type pheromone
232248	-2,525915791	-3,172358136	-0,632924645	/
233281	-2,255074098	-2,787544659	-0,521720095	Glucose-methanol-choline oxidoreductase, N-terminal
233410	-4,134686144	-2,333933645	1,812795302	Glycoside hydrolase, catalytic core
235431	2,202807805	-2,875524048	-5,068673176	Glycosyl hydrolase, family 13, catalytic region
238362	-3,034370189	-2,604428302	0,440805768	Glycoside hydrolase, family 18, N-terminal
238478	-4,077630017	-4,693075804	-0,601034626	Pectate lyase, catalytic
251504	-8,584570624	-2,692477818	5,900450006	Fungal mating-type pheromone
256167	2,477993682	2,593795414	0,127886517	Major facilitator superfamily MFS-1
258476	-3,094163226	-2,265975471	0,838696318	Multicopper oxidase, type 1
258542	3,069949663	2,132464947	-0,925516075	Glycoside hydrolase, family 47
258787	-4,571995621	-4,558475492	0,025467372	Glycoside hydrolase, family 18, N-terminal
31674	-3,981327776	-3,961583143	0,032507541	Glycoside hydrolase, family 61
32888	3,268696339	1,861085014	-1,395529411	Glycoside hydrolase, catalytic core
47036	-3,566629846	-4,376121536	-0,798651834	Pectate lyase/Amb allergen
48473	3,43664288	2,806049948	-0,618969086	NAD-dependent epimerase/dehydratase
48614	-2,259809829	-1,85671941	0,415422073	Amino acid/polyamine transporter I
48635	2,651365146	3,20352762	0,562919368	Major facilitator superfamily MFS-1
50445	-2,312890493	-3,558293412	-1,233145263	Glycoside hydrolase family 2, immunoglobulin-like beta-sandwich
52512	-2,71624421	-3,829516664	-1,102272151	ABC transporter-like
53768	-2,487237887	-2,559604042	-0,060230662	Peptidase M20
54466	-4,487082236	3,447893581	7,947706941	Glycoside hydrolase, family 61

56366	2,9450302	5,339721033	2,405551077	Glycoside hydrolase, family 16
56644	-3,392641534	-3,544243773	-0,136286699	Manganese and iron superoxide dismutase
56968	-4,228118769	-4,102913564	0,136943351	Methyltransferase type 11
60079	-4,335077037	-4,189499723	0,156912125	Glycoside hydrolase, family 61
60520	-3,113761184	-2,311873082	0,815091355	Fungal mating-type pheromone
60526	-7,777467936	-2,926914759	4,85862465	Fungal mating-type pheromone
61626	-4,128809338	-4,267514972	-0,125083796	Glycoside hydrolase, family 71
61757	-3,566596358	-3,479495123	0,10098139	Glycoside hydrolase, family 71
61868	2,172623029	2,374636925	0,213367328	FAD dependent oxidoreductase
62798	-2,238864388	-3,07510274	-0,829679362	Beta-lactamase
62845	3,477255542	3,987753647	0,521609979	Cerato-platanin
62973	2,581251219	1,9293117	-0,642110618	Glycoside hydrolase, family 3, N-terminal
63828	2,111222777	3,268231078	1,167855528	Esterase, PHB depolymerase
64002	-4,094658312	-2,026644651	2,081286851	Glycosyl hydrolase 92
64227	2,449305434	2,136458816	-0,300516487	Beta-glucan synthesis-associated, SKN1
64748	2,458022625	4,225666225	1,779893766	Peptidase M14, carboxypeptidase A
65089	2,373976838	3,002633396	0,641403125	Dynein heavy chain dhc2
66397	-4,27065384	-3,966440366	0,315595945	Pectinesterase, catalytic
66483	5,84042826	2,83905026	-2,992082041	Glycoside hydrolase, family 20, catalytic core
67028	4,330260929	3,905159412	-0,41563144	Major facilitator superfamily MFS-1
72113	2,958783962	2,157168627	-0,789054773	Peptidase S28
75108	-2,410274237	-2,246553931	0,176639586	Glycoside hydrolase, family 37
76079	-4,244296436	-2,906167153	1,352764427	General substrate transporter
77687	4,06110824	3,71266316	-0,336539613	Peptidase S10, serine carboxypeptidase
80323	3,793246766	3,462313237	-0,319240979	Peptidase S53, propeptide
82440	3,320655564	5,203171665	1,89587493	Fungal hydrophobin
82827	3,573946413	4,166057306	0,599399909	2OG-Fe(II) oxygenase
82849	-2,41416994	-2,002360206	0,423839222	Glycoside hydrolase family 2, immunoglobulin-like beta-sandwich

86001

3,619568963

1,841253058

-1,765607096

/

Table A4: 93 differentially regulated genes in 12-43 compared to E6. Listed are all genes with a log₂(fold change) <math>< 5</math>.

Protein ID	log₂FC	kogdefline	kogClass
1181214	-11,39865075	Predicted E3 ubiquitin ligase	Posttranslational modification, protein turnover, chaperones
1190086	-11,23838989	Splicing coactivator SRm160/300, subunit SRm300	RNA processing and modification
1192801	-10,35556493	Nuclear localization sequence binding protein	Transcription
258439	-10,0479865		
1160763	-9,191965808		
1213416	-8,530665584		
1153773	-8,2817083		
1116666	-8,089350122		
1133333	-7,973003099		
1060048	-7,922405983		
1174659	-7,879931993	SAM-dependent methyltransferases	Lipid transport and metabolism
231556	-7,780168657	Large RNA-binding protein (RRM superfamily)	General function prediction only
1039338	-7,733668878	von Willebrand factor and related coagulation proteins	Extracellular structures
1103821	-7,64650652		
1192766	-7,588580736	Nucleolar GTPase/ATPase p130	Nuclear structure
1098328	-7,358194766	Protein kinase PITSLRE and related kinases	General function prediction only
1213381	-7,19398116	Molecular chaperone (small heat-shock protein Hsp26/Hsp42)	Posttranslational modification, protein turnover, chaperones
1356507	-7,084706768	Cytochrome P450 CYP3/CYP5/CYP6/CYP9 subfamilies	Secondary metabolites biosynthesis, transport and catabolism
1153282	-6,987778979	Protein transporter of the TRAM (translocating chain-associating membrane) superfamily	Intracellular trafficking, secretion, and vesicular transport
1201547	-6,664530944	beta-1,6-N-acetylglucosaminyltransferase, contains WSC domain	Carbohydrate transport and metabolism
1325976	-6,5089883		
1166513	-6,498029161		
1191755	-6,445570164		
269862	-6,440617764	Transcription factor MEIS1 and related HOX domain proteins	Transcription
1160643	-6,335616228		
1216302	-6,278454098		
1201650	-6,122174228		

1278106	-5,96465217		
1083807	-5,893434828		
1039395	-5,890519087		
1103294	-5,849290982		
66483	-5,84042826	Beta-N-acetylhexosaminidase	Carbohydrate transport and metabolism
1160354	-5,803856034		
78927	-5,545731468		
1105850	-5,440917754		
1085836	-5,435824731		
1160054	-5,411895477		
1154533	-5,406824788		
1172060	-5,396186168	von Willebrand factor and related coagulation proteins	Extracellular structures
1173577	-5,279603731		
1241207	-5,238430889		
28617	-5,211667297	Methylase	General function prediction only
1175085	-5,153403699	Myosin phosphatase, regulatory subunit	Posttranslational modification, protein turnover, chaperones
231154	-5,097609648		
1228183	-5,094144745		
1039931	-5,031058892		
1133387	-5,014661391		
1179524	5,08670485		
1126608	5,121896744	Predicted transporter (major facilitator superfamily)	General function prediction only
1335591	5,129843211		
1183987	5,142892226	Transcription factor of the Forkhead/HNF3 family	Transcription
1193195	5,145268557	O-methyltransferase	Secondary metabolites biosynthesis, transport and catabolism
1134903	5,228918477		
1028812	5,233937395	Predicted transporter (major facilitator superfamily)	General function prediction only
1176824	5,288633765	Multidrug resistance-associated protein/mitoxantrone resistance protein, ABC superfamily	Secondary metabolites biosynthesis, transport and catabolism
1139544	5,362076491		
1136373	5,418391662	Nucleolar GTPase	General function prediction only

1247302	5,687646979		
17250	5,85543118	Mating pheromone activity	
1105778	5,917275334		
1093152	5,971440214		
1149020	6,280503832	Putative transcriptional regulator DJ-1	General function prediction only
1210979	6,552858907		
1081190	6,58651433		
1030522	6,770785519	L-kynurenine hydrolase	Amino acid transport and metabolism
49803	6,941659415	Molecular chaperone (DnaJ superfamily)	Posttranslational modification, protein turnover, chaperones
1124671	6,946614174	O-methyltransferase	Secondary metabolites biosynthesis, transport and catabolism
1193121	7,052414769		
1161353	7,097822803		
1205547	7,258371076	O-methyltransferase	Secondary metabolites biosynthesis, transport and catabolism
1161129	7,354812577		
1314520	7,414224981		
1163888	7,429931009		
238931	7,478065869		
1164524	7,512903021	MYND Zn-finger and ankyrin repeat protein	General function prediction only
1257055	7,555379202		
1194165	7,610052785		
1108741	7,675688765		
1163891	7,723253728	Splicing coactivator SRm160/300, subunit SRm300	RNA processing and modification
60526	7,777467936	Mating pheromone activity	
1340215	7,789446875		
83333	8,131854928		
1238578	8,154026417	Splicing coactivator SRm160/300, subunit SRm300	RNA processing and modification
1176386	8,360473041		
1098759	8,366547511		
1136981	8,415377001		
1260454	8,553534897		

1313697	8,566279419
251504	8,584570624
1163885	8,763951546
1193176	9,181895452
1206596	9,293932585
1161134	9,812890179

Mating pheromone activity

Table A5: List of proteins identified on the mastergel of strain 12-43. Spots number 58, 60, 97, 169, 181, 258, 363, 377, 425, 441, 471, 479, 481, 505 were not identified.

Spot	Accession number	protein	KOG group
1	1075372	Peptidase M1, membrane alanine aminopeptidase, N-terminal	
2	1064886	Peptidase M1, membrane alanine aminopeptidase, N-terminal	
3	1075372	Peptidase M1, membrane alanine aminopeptidase, N-terminal	
4	1038421	/	not annotated
5	1028665	Methionine synthase, vitamin-B12 independent	metabolism
6	1067283	Prohibitin	Cellular processes and signaling
8	1061655	Pyridine nucleotide-disulphide oxidoreductase, NAD-binding region	metabolism
9	1061655	Pyridine nucleotide-disulphide oxidoreductase, NAD-binding region	metabolism
11	1029545	UTP--glucose-1-phosphate uridylyltransferase	
12	1040795	Alpha-D-phosphohexomutase	
13	1066394	Aldehyde dehydrogenase	metabolism
14	1049964	Argininosuccinate synthase	metabolism
15	1058212	Fumarate reductase/succinate dehydrogenase flavoprotein, N-terminal	metabolism
17	1063997	Fumarate reductase/succinate dehydrogenase flavoprotein, N-terminal	metabolism
18	1058187	Histidine acid phosphatase	
20	1029740	Fumarate lyase	
21	1050893	Eukaryotic translation initiation factor 2A, central region	Information storage and processing
23	1030367	Phosphoglycerate kinase	metabolism
25	1067292	/	not annotated
26	1037126	Translation elongation factor EF1A, eukaryotic and archaeal	Information storage and processing
27	1037126	Translation elongation factor EF1A, eukaryotic and archaeal	Information storage and processing
28	1230656	Translation elongation factor EFTu/EF1A, C-terminal	Information storage and processing
29	1043008	GroES-related	
30	1036383	Nrap protein	
31	1170259	/	not annotated
32	1057935	Alpha/beta hydrolase fold-1, Epoxide hydrolase, N-terminal	

33	1060779	Alpha/beta hydrolase fold-1, Epoxide hydrolase, N-terminal	
34	1033067	NAD(P)-binding	
35	1029475	Aminotransferase, class I and II	
36	1034798	Zinc finger, CCCH-type	
37	1053097	Aminotransferase, class I and II	
38	1061621	GroES-related	
39	1029475	Aminotransferase, class I and II	
40	1320176	D-isomer specific 2-hydroxyacid dehydrogenase, catalytic region	
41	1042547	D-isomer specific 2-hydroxyacid dehydrogenase, catalytic region	
42	1320176	D-isomer specific 2-hydroxyacid dehydrogenase, catalytic region	
43	1033906	D-isomer specific 2-hydroxyacid dehydrogenase, catalytic region	
44	1182045	D-isomer specific 2-hydroxyacid dehydrogenase, catalytic region	
45	1033906	D-isomer specific 2-hydroxyacid dehydrogenase, catalytic region	
46	1033906	D-isomer specific 2-hydroxyacid dehydrogenase, catalytic region	
47	1090946	Ketose-bisphosphate aldolase, class-II	
48	1090946	Ketose-bisphosphate aldolase, class-II	
49	1090946	Ketose-bisphosphate aldolase, class-II	
50	1090946	Ketose-bisphosphate aldolase, class-II	
51	1030706	/	not annotated
52	1090946	Ketose-bisphosphate aldolase, class-II	
53	1074666	NAD(P)-binding	
55	1073602	Transketolase, central region	metabolism
56	1034625	NAD(P)-binding	
59	1036393	Aldo/keto reductase	Poorly characterized
61	1034625	NAD(P)-binding	
62	1192436	Thiamine pyrophosphate enzyme, central region	metabolism
63	1037126	Protein synthesis factor, GTP-binding	
65	1033509	Aldo/keto reductase	Poorly characterized

66	1126931	Aldo/keto reductase	Poorly characterized
67	1126931	Aldo/keto reductase	Poorly characterized
68	1182696	Alcohol dehydrogenase, zinc-binding	metabolism
69	1151657	Transaldolase	metabolism
70	1155249	Aldo/keto reductase	Poorly characterized
71	1155249	Aldo/keto reductase	Poorly characterized
72	1117449	Ureohydrolase	
73	1193040	Aldo/keto reductase	Poorly characterized
74	55787	Methyltransferase type 11	
75	1137875	Lactate/malate dehydrogenase	metabolism
76	1137875	Lactate/malate dehydrogenase	metabolism
77	1035451	Aldo/keto reductase	Poorly characterized
78	1176919	Lactate/malate dehydrogenase	metabolism
79	1039379	Lactate/malate dehydrogenase	metabolism
80	1137875	Lactate/malate dehydrogenase	metabolism
81	76460	Serine/threonine-specific protein phosphatase and bis(5-nucleosyl)-tetrphosphatase	Cellular processes and signaling
82	55787	Methyltransferase type 11	
83	76460	Serine/threonine-specific protein phosphatase and bis(5-nucleosyl)-tetrphosphatase	Cellular processes and signaling
84	1047830	Lactate/malate dehydrogenase	metabolism
85	255629	Carbohydrate Esterase Family 1 protein	
86	1037222	Inorganic pyrophosphatase	
87	1065479	/	not annotated
88	1037222	Inorganic pyrophosphatase	
89	1037222	Inorganic pyrophosphatase	
90	1073136	Alpha/beta hydrolase	
91	79439	Alpha/beta hydrolase fold-1	
92	233273	Short-chain dehydrogenase/reductase SDR	
95	233273	Short-chain dehydrogenase/reductase SDR	

96	1165373	MaoC-like dehydratase	
98	1029483	Peptidase M24, methionine aminopeptidase	
99	1077969	Dienelactone hydrolase	
101	1067558	/	not annotated
102	1227116	/	not annotated
103	1037141	Aldose 1-epimerase	
104	1029007	Purine phosphorylase, family 2	metabolism
105	1043137	/	not annotated
106	1061833	Short-chain dehydrogenase/reductase SDR	
107	1038271	Peptidase S9, prolyl oligopeptidase active site region	
108	1039066	Iron hydrogenase, large subunit, C-terminal	
110	1304086	RasGAP protein, C-terminal	
111	52674	Peptidase S9, prolyl oligopeptidase active site region	
112	1032747	Alpha/beta hydrolase fold-1	
113	1033356	DNA/RNA helicase, DEAD/DEAH box type, N-terminal	Information storage and processing
114	1032747	Alpha/beta hydrolase fold-1	
116	1053915	Porin, eukaryotic type	
118	1063481	Protein kinase, core	Cellular processes and signaling
121	1100595	Haloacid dehalogenase-like hydrolase	
122	1070300	Glutathione S-transferase, C-terminal-like	Cellular processes and signaling
123	1216719	Haloacid dehalogenase-like hydrolase	
124	1037295	Glutathione S-transferase, N-terminal	Cellular processes and signaling
125	1217138	Band 7 protein, Prohibitin	
126	1206168	Oxidoreductase FAD/NAD(P)-binding	
127	1035553	Haloacid dehalogenase-like hydrolase	
129	1093915	Dienelactone hydrolase	
130	1253000	Oxidoreductase FAD/NAD(P)-binding	
131	1070300	Glutathione S-transferase, C-terminal-like	Cellular processes and signaling

132	1203915	Glutathione S-transferase, N-terminal	
133	80259	Glutamine synthetase, catalytic region	metabolism
137	80259	Glutamine synthetase, catalytic region	metabolism
139	1206555	Protein kinase, core	
140	1189183	Ferredoxin	metabolism
141	49745	20S proteasome, A and B subunits	Cellular processes and signaling
142	1047604	14-3-3 protein	
143	1037883	Eukaryotic phosphomannomutase	
144	1054143	/	not annotated
145	1039848	Glutathione S-transferase, C-terminal-like	Cellular processes and signaling
146	1036460	Glutathione S-transferase, C-terminal-like	Cellular processes and signaling
149	1146126	Heat shock protein 70	Information storage and processing
150	1071278	Heat shock protein 70	
151	1039885	Triosephosphate isomerase	
152	1050048	Adenylate/cytidine kinase, N-terminal	
153	1030829	Adenylate/cytidine kinase, N-terminal	
154	1055855	Protein of unknown function DUF423	
156	1042761	Glycolipid transfer protein, GLTP	
157	1042761	Glycolipid transfer protein, GLTP	
158	1028714	Translationally controlled tumour-associated TCTP	
159	1050440	Translationally controlled tumour-associated TCTP	
160	1200944	RNA recognition motif, RNP-1	
161	1146700	Manganese and iron superoxide dismutase	metabolism
162	1308548	/	not annotated
165	1033258	Alkyl hydroperoxide reductase/ Thiol specific antioxidant/ Mal allergen	
166	1044657	Alkyl hydroperoxide reductase/ Thiol specific antioxidant/ Mal allergen	
167	1333364	Cytochrome P450	
168	1033258	Alkyl hydroperoxide reductase/ Thiol specific antioxidant/ Mal allergen	

170	1056827	Protein of unknown function DUF1000	
172	1173997	Peptidyl-prolyl cis-trans isomerase, cyclophilin-type	
173	1206555	Protein kinase, core	
175	1169523	Glycoside hydrolase, family 5	
176	1269693	Nucleoside diphosphate kinase, core	
177	1030755	/	not annotated
178	1123729	UspA	
180	1058798	Actin-binding, cofilin/tropomyosin type	
182	1033356	DNA/RNA helicase, DEAD/DEAH box type, N-terminal	Information storage and processing
183	78835	Peptidyl-prolyl cis-trans isomerase, cyclophilin-type	Cellular processes and signaling
184	1119410	/	not annotated
186	1028769	Cytochrome b5	metabolism
187	1068141	Cerato-platanin	
188	1031460	Cerato-platanin	
189	1033542	Peptidase S8 and S53, subtilisin, kexin, sedolisin	
190	1031109	Chromo domain	
192	1052962	DNA/RNA helicase, C-terminal	Information storage and processing
193	1029853	Protein kinase, core	Cellular processes and signaling
194	1213348	Redoxin	
195	1029853	Protein kinase, core	Cellular processes and signaling
196	1213348	Redoxin	
198	1029853	Protein kinase, core	Cellular processes and signaling
199	1033356	DNA/RNA helicase, DEAD/DEAH box type, N-terminal	Information storage and processing
201	1030607	mRNA capping enzyme (SKP1 component, dimerisation)	Information storage and processing
202	1119320	SKP1 component, dimerisation	
203	1033258	Alkyl hydroperoxide reductase/ Thiol specific antioxidant/ Mal allergen	
204	1043096	STAT transcription factor, coiled coil	Information storage and processing
205	1035114	Eukaryotic initiation factor 5A hypusine (eIF-5A)	

206	1064975	CS	
208	1063968	/	not annotated
209	1049189	Calcium-binding EF-hand	Cellular processes and signaling
210	1058336	Forkhead-associated	Information storage and processing
213	1031763	EB1, C-terminal	
214	1054530	Peptidase A1	
215	1028723	Peptidase A1	
216	1033356	DNA/RNA helicase, DEAD/DEAH box type, N-terminal	Information storage and processing
217	1029723	Isocitrate/isopropylmalate dehydrogenase	metabolism
218	1183126	BNR repeat	
219	1065769	Leucine-rich repeat	poorly characterized
220	1031733	Peptidyl-prolyl cis-trans isomerase, cyclophilin-type (BTB/POZ-like)	Cellular processes and signaling
222	1036025	Ubiquitin-conjugating enzyme, E2	Cellular processes and signaling
223	1050871	/	not annotated
224	1043438	Nucleoside diphosphate kinase, core	
225	1056543	/	not annotated
226	1030408	Transketolase, N-terminal	metabolism
227	1030408	Transketolase, N-terminal	metabolism
228	1030408	Transketolase, N-terminal	metabolism
231	1122277	/	not annotated
232	1043448	Pyridine nucleotide-disulphide oxidoreductase, NAD-binding region	
234	1033356	DNA/RNA helicase, C-terminal	Information storage and processing
235	1029180	Carbohydrate kinase, FGGY	
236	1065296	Carbohydrate kinase, FGGY	
237	1053772	Phosphoglucose isomerase (PGI)	
239	1031441	Alpha-D-phosphohexomutase, C-terminal	
241	1066394	Aldehyde dehydrogenase	metabolism
242	1065239	Glucose-6-phosphate dehydrogenase	

243	1062456	Phosphotransferase KptA/Tpt1	
244	1058187	Histidine acid phosphatase	
245	1058187	Histidine acid phosphatase	
247	1033356	DNA/RNA helicase, DEAD/DEAH box type, N-terminal	Information storage and processing
248	1063762	Methionine synthase, vitamin-B12 independent	metabolism
249	1080776	Fumarate lyase	
250	1029740	Fumarate lyase	
251	1061217	Citrate synthase-like	
252	1035869	6-phosphogluconate dehydrogenase	metabolism
253	1030367	Phosphoglycerate kinase	metabolism
254	1061217	Citrate synthase-like	
255	1032595	Citrate synthase, eukaryotic	
256	1031440	GroES-related	
259	1063762	Methionine synthase, vitamin-B12 independent	metabolism
260	1033356	DNA/RNA helicase, DEAD/DEAH box type, N-terminal	Information storage and processing
261	1030607	BTB/POZ fold (SKP1 component, dimerisation)	
262	1285518	Cytochrome P450	metabolism
265	1226901	Ubiquitin-activating enzyme, E1	Cellular processes and signaling
266	1255969	Aconitase/3-isopropylmalate dehydratase large subunit, alpha/beta/alpha	metabolism
267	1255969	Aconitase/3-isopropylmalate dehydratase large subunit, alpha/beta/alpha	metabolism
268	1255969	Aconitase/3-isopropylmalate dehydratase large subunit, alpha/beta/alpha	metabolism
269	1056633	Aconitase/3-isopropylmalate dehydratase large subunit, alpha/beta/alpha	metabolism
270	1136792	Aconitase/3-isopropylmalate dehydratase large subunit, alpha/beta/alpha	metabolism
271	1036152	Aconitase/3-isopropylmalate dehydratase large subunit, alpha/beta/alpha	metabolism
272	1036152	Aconitase/3-isopropylmalate dehydratase large subunit, alpha/beta/alpha	metabolism
273	1032669	Transketolase, C-terminal	metabolism
274	1030408	Transketolase, N-terminal	metabolism
275	1035780	Histidine acid phosphatase	

276	1029740	Fumarate lyase	
277	1047832	6-phosphogluconate dehydrogenase, C-terminal	metabolism
278	1066990	6-phosphogluconate dehydrogenase, C-terminal	metabolism
279	1063749	Phosphoglycerate kinase	metabolism
280	1051770	Phosphoglycerate kinase	metabolism
281	1061217	Citrate synthase-like	
282	1031440	GroES-related	
283	1255969	Aconitase/3-isopropylmalate dehydratase large subunit, alpha/beta/alpha	metabolism
284	1064705	Alcohol dehydrogenase, zinc-binding	metabolism
285	1064705	Alcohol dehydrogenase, zinc-binding	metabolism
286	1202878	D-isomer specific 2-hydroxyacid dehydrogenase, catalytic region	
287	1171073	Flavoprotein	
288	1039873	20S proteasome, A and B subunits	Cellular processes and signaling
289	1028599	/	not annotated
293	1060868	Cytochrome P450	metabolism
294	1051694	20S proteasome, A and B subunits	Cellular processes and signaling
296	1033162	Manganese and iron superoxide dismutase	metabolism
297	1070326	Inorganic pyrophosphatase	
298	63281	14-3-3 protein	
300	1143157	GCN5-related N-acetyltransferase	
301	1029296	GCN5-related N-acetyltransferase	
302	1072315	/	not annotated
303	82165	F-actin capping protein, beta subunit	
304	63281	14-3-3 protein	
305	1068022	Ran Binding Protein 1	Cellular processes and signaling
306	1304374	Serine/threonine-specific protein phosphatase and bis(5-nucleosyl)-tetraphosphatase	Cellular processes and signaling
307	1037883	Eukaryotic phosphomannomutase	
308	1040471	Eukaryotic phosphomannomutase	

310	1037101	/	not annotated
311	1037295	Glutathione S-transferase, N-terminal	Cellular processes and signaling
312	1037295	Glutathione S-transferase, N-terminal	Cellular processes and signaling
313	1037883	Eukaryotic phosphomannomutase	
314	1038847	20S proteasome, A and B subunits	Cellular processes and signaling
315	1039848	Glutathione S-transferase, C-terminal-like	Cellular processes and signaling
316	1092886	ATPase, F1/V1/A1 complex, alpha/beta subunit, nucleotide-binding	metabolism
317	1039885	Triosephosphate isomerase	
318	1056841	Protein synthesis factor, GTP-binding	
319	1035990	Enolase	
320	1035990	Enolase	metabolism
322	1177705	Isocitrate/isopropylmalate dehydrogenase	metabolism
323	1047924	Isocitrate/isopropylmalate dehydrogenase	metabolism
324	1261217	Actin/actin-like	
325	1040077	Mandelate racemase/muconate lactonizing enzyme, C-terminal	
327	1035814	ATP-citrate lyase/succinyl-CoA ligase	
328	1035986	Carbohydrate/purine kinase	
329	1043690	Carbohydrate/purine kinase	
330	1059894	Carbohydrate/purine kinase	
331	1183126	BNR repeat	
332	1035990	Enolase	metabolism
333	76328	Polyprenyl synthetase	metabolism
334	1192436	Thiamine pyrophosphate enzyme, central region	metabolism
335	1296643	Transaldolase	metabolism
336	1075294	DNA/RNA helicase, DEAD/DEAH box type, N-terminal	Information storage and processing
337	1049964	Argininosuccinate synthase	metabolism
338	1151657	Transaldolase	metabolism
339	1310806	Inositol monophosphatase	metabolism

341	1151657	Transaldolase	metabolism
342	1031159	Transketolase, C-terminal/Pyruvate-ferredoxin oxidoreductase, domain II	metabolism
343	1226362	/	not annotated
344	1174938	RNA polymerase Rpb2	
345	1031460	/	not annotated
346	1137869	/	not annotated
348	1038277	Ubiquitin-conjugating enzyme, E2	Cellular processes and signaling
350	1033754	/	not annotated
351	1200940	Mago nashi protein	
352	1039885	Triosephosphate isomerase	
353	1037677	20S proteasome, A and B subunits	Cellular processes and signaling
354	1037677	20S proteasome, A and B subunits	Cellular processes and signaling
355	1306137	/	
356	1064100	Manganese and iron superoxide dismutase	metabolism
357	1064216	/	not annotated
358	1034463	Carbohydrate-binding family V/XII	
359	1039848	/	not annotated
360	1122926	Ubiquitin-conjugating enzyme, E2	Cellular processes and signaling
361	1252590	NAD(P)-binding	
362	1039009	Glycolipid transfer protein, GLTP	
364	1030611	20S proteasome, A and B subunits	Cellular processes and signaling
365	1146700	Manganese and iron superoxide dismutase	metabolism
366	1121676	/	not annotated
367	1057324	Manganese and iron superoxide dismutase	metabolism
369	1093429	Peptidyl-prolyl cis-trans isomerase, cyclophilin-type	Cellular processes and signaling
370	1059126	Translation elongation factor EF1B, gamma chain, conserved	
373	1208590	NAD-dependent epimerase/dehydratase	
376	1185887	Protein synthesis factor, GTP-binding	

379	1040700	Glutathione S-transferase, omega-class	
382	1040795	Alpha-D-phosphohexomutase, C-terminal	
383	1136974	Pyridine nucleotide-disulphide oxidoreductase, NAD-binding region	metabolism
384	1136974	Pyridine nucleotide-disulphide oxidoreductase, NAD-binding region	metabolism
385	1036209	Pyridine nucleotide-disulphide oxidoreductase, NAD-binding region	metabolism
387	1058187	Histidine acid phosphatase	
388	1035990	Enolase	metabolism
389	1053810	Enolase	metabolism
390	1040795	Alpha-D-phosphohexomutase, C-terminal	
391	1203899	ATP-citrate lyase/succinyl-CoA ligase	
392	1066990	6-phosphogluconate dehydrogenase, C-terminal	metabolism
393	1251648	6-phosphogluconate dehydrogenase, C-terminal	metabolism
394	1068109	Isocitrate/isopropylmalate dehydrogenase	metabolism
395	1132439	S-adenosyl-L-homocysteine hydrolase	metabolism
396	1332703	Isocitrate/isopropylmalate dehydrogenase	metabolism
397	1264918	/	not annotated
398	1031441	Alpha-D-phosphohexomutase, C-terminal	
399	1061860	Aldehyde dehydrogenase	metabolism
400	1035780	Histidine acid phosphatase	
401	135990	Enolase	
404	1033957	ATPase, F1 complex, OSCP/delta subunit	
405	1054000	/	not annotated
408	1054000	/	not annotated
410	1203418	ARP23 complex 20 kDa subunit	
412	1040867	Protein-tyrosine phosphatase, low molecular weight	
413	1043438	Nucleoside diphosphate kinase, core	metabolism
415	1043438	Nucleoside diphosphate kinase, core	metabolism
416	1075846	Primosome PriB/single-strand DNA-binding	

417	1056618	Ubiquitin-conjugating enzyme, E2	Cellular processes and signaling
418	1034536	Peptidyl-prolyl cis-trans isomerase, cyclophilin-type	Cellular processes and signaling
419	1036002	/	not annotated
420	1239981	Glyceraldehyde 3-phosphate dehydrogenase	metabolism
421	1030402	Nucleoside diphosphate kinase, core	
424	232365	20S proteasome, A and B subunits	Cellular processes and signaling
426	1043853	/	not annotated
430	1028572	/	not annotated
431	1028572	/	not annotated
432	1058798	Actin-binding, cofilin/tropomyosin type	
433	1040825	CS	
434	1043240	Zinc finger, MYND-type	
435	1032111	Cyclin-like F-box	
436	1175015	Lactate/malate dehydrogenase	
438	1133744	Translation elongation factor EF1B, beta and delta chains, guanine nucleotide exchange	
439	1111154	/	not annotated
440	1137875	Lactate/malate dehydrogenase	metabolism
443	1185887	Protein synthesis factor, GTP-binding	
444	1055855	Protein of unknown function DUF423	
445	1178496	Methyltransferase type 11	metabolism
446	1226901	UBA/THIF-type NAD/FAD binding fold	Cellular processes and signaling
448	1028665	Methionine synthase, vitamin-B12 independent	metabolism
449	1032208	Peptidase S9, prolyl oligopeptidase active site region	
451	1058803	/	not annotated
452	1049556	Peptidase M24, catalytic core	
453	1049556	Peptidase M24, catalytic core	
455	1033356	DNA/RNA helicase, DEAD/DEAH box type, N-terminal	Information storage and processing
457	1222197	Thioredoxin domain	Cellular processes and signaling

458	1222197	Thioredoxin domain	Cellular processes and signaling
460	1222197	Thioredoxin domain	Cellular processes and signaling
461	1059220	Thioredoxin domain	Cellular processes and signaling
462	1058899	Thioredoxin domain	Cellular processes and signaling
463	1058899	Thioredoxin domain	Cellular processes and signaling
464	1052174	Heat shock protein 70	Information storage and processing
465	1052653	Chaperonin Cpn60/TCP-1	
466	1308241	Chaperonin Cpn60/TCP-1	
468	1205862	/	not annotated
469	1052174	Heat shock protein 70	Information storage and processing
470		/	not annotated
472	1170547	Alpha/beta hydrolase fold-3	
474	1058376	Aldehyde dehydrogenase	metabolism
475	1055515	ATPase, F1/V1/A1 complex, alpha/beta subunit, nucleotide-binding	metabolism
476	1307240	Peptidase M20	Poorly characterized
477	1040351	Peptidase M20	Poorly characterized
478	1307240	Peptidase M20	Poorly characterized
482	1033356	DNA/RNA helicase, DEAD/DEAH box type, N-terminal	Information storage and processing
483	1030136	ATPase, F1/V1/A1 complex, alpha/beta subunit, nucleotide-binding	metabolism
484	1051758	ATPase, F1/V1/A1 complex, alpha/beta subunit, nucleotide-binding	metabolism
485	1051758	ATPase, F1/V1/A1 complex, alpha/beta subunit, nucleotide-binding	metabolism
486	1051758	ATPase, F1/V1/A1 complex, alpha/beta subunit, nucleotide-binding	metabolism
487	1051869	Rab GTPase activator	
489	1076025	Protein kinase-like	Cellular processes and signaling
490	1051869	Rab GTPase activator	
492	1051869	Rab GTPase activator	
493	1033356	DNA/RNA helicase, DEAD/DEAH box type, N-terminal	Information storage and processing
494	1052507	Peptidase M16, N-terminal	

496	1166677	DNA/RNA helicase, DEAD/DEAH box type, N-terminal	Information storage and processing
497	1068491	Peptidase S9, prolyl oligopeptidase active site region	
498	1038186	Heat shock protein 70	Information storage and processing
499	1203234	ArgE/DapE/ACY1/CPG2/YscS, conserved site	
500	1042976	Thiamine pyrophosphate enzyme, C-terminal TPP-binding	metabolism
501	1120561	Zinc finger, MYND-type	
502	1046844	DNA/RNA helicase, ATP-dependent, DEAH-box type, conserved site	Information storage and processing
504	1040795	Alpha-D-phosphohexomutase, C-terminal	
506	1055515	ATPase, F1/V1/A1 complex, alpha/beta subunit, nucleotide-binding	metabolism
507	1143045	/	not annotated
508	1084035	Peptidase M, neutral zinc metallopeptidases, zinc-binding site	
509	1029068	UBA/THIF-type NAD/FAD binding fold	Cellular processes and signaling
511	1029068	UBA/THIF-type NAD/FAD binding fold	Cellular processes and signaling
512	1200371	Peptidase S9, prolyl oligopeptidase active site region	
513	1068491	Peptidase S9, prolyl oligopeptidase active site region	
514	1032208	Peptidase S9, prolyl oligopeptidase active site region	
515	1053171	Transketolase, N-terminal	metabolism
516	1062345	Transketolase, N-terminal	metabolism
517	1032669	Transketolase, N-terminal	metabolism
518	1036452	Actin/actin-like	
519	1178236	Peptidase M3A and M3B, thimet/oligopeptidase F	
520	1031877	Peptidase M16	
522	1052507	Peptidase M16	
523	1038421	/	not annotated
524	1115288	UBA/THIF-type NAD/FAD binding fold	Cellular processes and signaling
525	1052174	Heat shock protein 70	Information storage and processing
526	1049964	Argininosuccinate synthase	metabolism

Table A6: Spots with a mascot score lower as the defined threshold 54.0.

Spot	Accession number	Mascot Score	Protein
7	1075294	48.2	DNA/RNA helicase, DEAD/DEAH box type, N-terminal
10	1049508	47.7	Arf GTPase activating protein
16	1170547	39.0	Alpha/beta hydrolase fold-3
19	1070890	31,7	RNA-directed DNA polymerase (reverse transcriptase)
22	1117649	42.1	Major facilitator superfamily MFS-1
24	1067292	30,8	/
54	1198167	36.9	/
57	1199211	32.9	/
64	1067292	33.8	/
93	1170547	41.0	Alpha/beta hydrolase fold-3
94	1043176	35.4	Alcohol dehydrogenase, zinc-binding
100	1129649	47.9	Thioredoxin-like fold
109	1179264	46.4	Vesicle transport v-SNARE
115	1033356	46.7	DNA/RNA helicase, DEAD/DEAH box type, N-terminal
117	1051454	53.3	Glucose-methanol-choline oxidoreductase, N-terminal
119	1033356	49.2	DNA/RNA helicase, DEAD/DEAH box type, N-terminal
120	1051454	43.8	Glucose-methanol-choline oxidoreductase, N-terminal
128	1068325	46.0	Cyclin-like F-box
134	1112852	46.1	/
135	1066671	43.4	Glucose-methanol-choline oxidoreductase, N-terminal
136	1170547	41.1	Alpha/beta hydrolase fold-3
138	1033356	46.7	DNA/RNA helicase, DEAD/DEAH box type, N-terminal
147	1047443	41.2	O-methyltransferase, family 3
148	1043240	38.7	Zinc finger, MYND-type
155	1170547	41.0	Alpha/beta hydrolase fold-3

163	1059836	41.0	Haem peroxidase, animal
164	1127919	41.1	Cyclin-like F-box
171	1043176	46.6	Alcohol dehydrogenase, zinc-binding
174	1066671	45.3	Glucose-methanol-choline oxidoreductase, N-terminal
179	1072559	50.8	Zinc finger, MYND-type
185	1033356	51.2	DNA/RNA helicase, DEAD/DEAH box type, N-terminal
191	1037460	43.7	MFS general substrate transporter
197	1333111	38.7	Endonuclease/exonuclease/phosphatase
200	1202917	39.7	WD40 repeat
207	1068325	48.1	Cyclin-like F-box
211	1068325	50.6	Cyclin-like F-box
212	1033356	51.0	DNA/RNA helicase, DEAD/DEAH box type, N-terminal
221	1093742	37.2	Cyanate lyase, C-terminal
229	1046849	37.9	Conserved hypothetical protein CHP02464
230	1067292	36.9	/
233	1070633	42.7	Alcohol dehydrogenase, zinc-binding
238	1067292	36.9	/
240	1207436	44.7	/
246	1036161	51.1	Spc97/Spc98
257	1170547	39.0	Alpha/beta hydrolase fold-3
263	1337368	49.8	ABC transporter-like
264	1206039	41.8	Zinc finger, MYND-type
290	1299690	34.4	/
291	1170547	35.9	Alpha/beta hydrolase fold-3
292	1068325	47.9	Cyclin-like F-box
295	1204758	45.8	Integrase, catalytic core
299	1068325	46.0	Cyclin-like F-box
309	1129649	38.8	Thioredoxin-like fold

321	1061012	53.5	Uracil-DNA glycosylase
326	1088055	37.8	UBX
340	1223419	37.2	Vesicle transport v-SNARE
347	1041271	32.8	Prefoldin
349	1325728	49.9	/
368	1109258	47.7	Proteasome component region PCI
371	1048338	34.2	Heat shock protein Hsp20
372	1181912	33.9	/
374	1226362	43.6	/
375	1296669	41.7	/
378	1074854	48.1	Tetratricopeptide TPR-1
380	1203993	47.3	Methyltransferase type 11
381	1051694	51.0	20S proteasome, A and B subunits
386	1067422	47.1	Histidine acid phosphatase
402	1037174	51.0	Radical SAM
403	1050651	41.1	/
406	1037325	39.3	/
407	1133744	42.3	Translation elongation factor EF1B, beta and delta chains, guanine nucleotide exchange
409	1124521	31.0	/
411	1133744	43.7	Translation elongation factor EF1B, beta and delta chains, guanine nucleotide exchange
414	1080860	37.8	Mitochondrial substrate carrier
422	1033356	46.7	DNA/RNA helicase, DEAD/DEAH box type, N-terminal
423	1170547	43.4	Alpha/beta hydrolase fold-3
427	1072224	40.8	Aldo/keto reductase
428	1057544	43.4	WD40 repeat
429	1061002	52.6	/
437	1164667	34.5	AMP-dependent synthetase and ligase

442	1269418	37.8	Myosin head, motor region
447	1239245	51.6	ABC transporter-like
450	1066004	39.3	Cytochrome P450
454	1068095	39.6	Methyltransferase type 11
456	1129267	46.5	/
459	1033356	52.5	DNA/RNA helicase, DEAD/DEAH box type, N-terminal
467	1039694	36.9	Pinin/SDK/memA protein
473	1170547	46.3	Alpha/beta hydrolase fold-3
480	1043240	49.9	Zinc finger, MYND-type
488	1037302	36.8	/
491	1091079	48.8	Alpha/beta hydrolase fold-3
495	1349959	43.4	Methyltransferase type 11
503	1037460	45.5	MFS general substrate transporter
510	1102984	37.1	Cytochrome P450
521	1073605	41.8	Ribonuclease HII/HIII

Table A7: Different abundance of protein spots in the compared gels of strain 12-43 and 4-39. Green labeled spots have a lower abundance in strain 4-39, red labeled spots have a higher abundance compared to 12-43. If a protein has no spotnumber, they do not appear on the mastergel.

Ratio of mean normalized volume '4-39' / mean normalized volume '12-43'	Label	Spot	Protein
-15,25975	mono_70	/	
-9,0929	mono_50	316	ATPase, F1/V1/A1 complex, alpha/beta subunit, nucleotide-binding
-7,97793	mono_28	436	Lactate/malate dehydrogenase
-7,80051	mono_53	310	not annotated
-5,50982	mono_81	/	
-5,28556	mono_21	74	Methyltransferase type 11
-5,10888	mono_29	78	Lactate/malate dehydrogenase
-5,05096	mono_26	82	Methyltransferase type 11
-4,94444	mono_89	?	
-4,74509	mono_54	/	not annotated
-4,72008	mono_72	349	/
-4,62659	mono_20	73	Aldo/keto reductase
-4,41871	mono_01	511	UBA/THIF-type NAD/FAD binding fold
-4,33311	mono_48	315	Glutathione S-transferase, C-terminal-like
-3,71096	mono_36	114	Alpha/beta hydrolase fold-1
-3,6834	mono_33	100	/
-3,12321	mono_06	397	not annotated
-2,86501	mono_23	77	Aldo/keto reductase
-2,78299	mono_63	193	Protein kinase, core
-2,69625	mono_49	147	/
-2,68527	mono_52	310	not annotated
-2,68465	mono_17	66	Aldo/keto reductase
-2,62605	mono_38	121	Haloacid dehalogenase-like hydrolase

-2,56247	mono_76	271	Aconitase/3-isopropylmalate dehydratase large subunit, alpha/beta/alpha
-2,52299	mono_07	/	6-phosphogluconate dehydrogenase, C-terminal
-2,44323	mono_75	268	Aconitase/3-isopropylmalate dehydratase large subunit, alpha/beta/alpha
-2,28484	mono_74	267	Aconitase/3-isopropylmalate dehydratase large subunit, alpha/beta/alpha
-2,28107	mono_46	307	Eukaryotic phosphomannomutase
-2,27605	mono_24	81	Serine/threonine-specific protein phosphatase and bis(5-nucleosyl)-tetraphosphatase
-2,26112	mono_13	62	Thiamine pyrophosphate enzyme, central region
-2,26049	mono_45	/	
-2,24477	mono_30	438	Translation elongation factor EF1B, beta and delta chains, guanine nucleotide exchange
-2,23296	mono_37	/	HEAT
-2,19515	mono_68	369	Peptidyl-prolyl cis-trans isomerase, cyclophilin-type
-2,16926	mono_64	194	Redoxin
-2,10239	mono_77	270	Aconitase/3-isopropylmalate dehydratase large subunit, alpha/beta/alpha
-2,102	mono_62	/	not annotated
-2,08937	mono_73	266	Aconitase/3-isopropylmalate dehydratase large subunit, alpha/beta/alpha
-2,03042	mono_42	136	/
-2,02954	mono_67	220	Peptidyl-prolyl cis-trans isomerase, cyclophilin-type (BTB/POZ-like)
-2,00125	mono_41	/	
-1,99943	mono_34	112	Alpha/beta hydrolase fold-1
-1,97389	mono_44	313	Eukaryotic phosphomannomutase
-1,94418	mono_15	335	Transaldolase
-1,91928	mono_22	80	Lactate/malate dehydrogenase
-1,91711	mono_18	72	Ureohydrolase
-1,89326	mono_02	519	Peptidase M3A and M3B, thimet/oligopeptidase F
-1,87316	mono_09	55	Transketolase, central region
-1,85605	mono_39	126	Oxidoreductase FAD/NAD(P)-binding
-1,85011	mono_40	122	Glutathione S-transferase, C-terminal-like
-1,7849	mono_69	221	/

-1,75204	mono_08	333	Polyprenyl synthetase
-1,69213	mono_16	69	Transaldolase
-1,69091	mono_27	440	Lactate/malate dehydrogenase
-1,64844	mono_65	196	Redoxin
-1,63246	mono_25	/	
-1,55265	mono_51	/	
1,66305	mono_86	400	Histidine acid phosphatase
1,68778	mono_87	389	Enolase
1,77021	mono_05	388	Enolase
1,80665	mono_03	320	Enolase
1,9472	mono_57	419	not annotated
2,01419	mono_79	471	/
2,07677	mono_04	401	Enolase
2,20617	mono_58	/	
2,2254	mono_55	353	20S proteasome, A and B subunits
2,34161	mono_12	/	Thiamine pyrophosphate enzyme, central region
2,34882	mono_83	464	Heat shock protein 70
2,35253	mono_90	/	Carbohydrate-binding family V/XII
2,37083	mono_43	/	20S proteasome, A and B subunits
2,47114	mono_91	204	STAT transcription factor, coiled coil
2,53728	mono_85	244	Histidine acid phosphatase
2,69873	mono_10	/	
2,70988	mono_61	404	ATPase, F1 complex, OSCP/delta subunit
2,75291	mono_31	/	Dienelactone hydrolase
2,75956	mono_59	403	/
2,82405	mono_11	/	Alcohol dehydrogenase, zinc-binding
3,22397	mono_82	469	Heat shock protein 70
3,26771	mono_60	423	/

3,35506	mono_78	505	/
3,39952	mono_14	65	Aldo/keto reductase
3,70617	mono_56	402	/
3,72171	mono_19	/	Aldo/keto reductase
4,37752	mono_66	/	Myosin head, motor region
4,9874	mono_88	172	Peptidyl-prolyl cis-trans isomerase, cyclophilin-type
5,45443	mono_80	504	Alpha-D-phosphohexomutase, C-terminal
5,61715	mono_32	90	Alpha/beta hydrolase
5,71681	mono_71	/	
6,35365	mono_35	118	Protein kinase, core
6,90582	mono_47	/	NADH dehydrogenase (ubiquinone), 30 kDa subunit
10,64738	mono_84	/	RNA polymerase I associated factor, A49-like

Table A8: Different abundance of protein spots in the compared gels of strain 12-43 and the dikaryon. Green spots have a lower abundance in dikaryon, red spots have a higher abundance compared to 12-43. If a protein has no spotnumber, they do not appear on the mastergel.

Ratio of mean normalized volume 'Dikaryon' / mean normalized volume '12-43'	Label	Spot	Protein
-28,49976	dik_82	193	Protein kinase, core
-25,68726	dik_90	/	
-18,12844	dik_91	/	
-8,26992	dik_77	/	
-7,93872	dik_100	261	BTB/POZ fold (SKP1 component, dimerisation)
-7,30944	dik_88	347	/
-6,08090	dik_68	123	Haloacid dehalogenase-like hydrolase
-6,07972	dik_76	309	/
-5,57789	dik_11	44	D-isomer specific 2-hydroxyacid dehydrogenase, catalytic region
-5,32125	dik_47	370	Translation elongation factor EF1B, gamma chain, conserved
-5,30727	dik_07	/	Phosphoglycerate kinase
-5,03813	dik_94	435	Cyclin-like F-Box
-4,85439	dik_56	/	
-4,73116	dik_63	360	Ubiquitin-conjugating enzyme, E2
-4,60805	dik_86	/	
-4,33260	dik_30	74	Methyltransferase type 11
-4,29920	dik_57	311	Glutathione S-transferase, N-terminal
-4,23556	dik_50	109	/
-4,09937	dik_52	124	Glutathione S-transferase, N-terminal
-3,88657	dik_51	/	Glyceraldehyde 3-phosphate dehydrogenase
-3,83118	dik_06	/	Tetratricopeptide TPR-1
-3,83010	dik_32	/	

-3,66839	dik_35	436	Lactate/Malate dehydrogenase
-3,63733	dik_101	13	Aldehyde dehydrogenase
-3,50090	dik_61	131	Glutathione S-transferase, C-terminal-like
-3,47861	dik_121	199	DNA/RNA helicase, DEAD/DEAH box type, N-terminal
-3,31363	dik_31	/	DNA/RNA helicase, DEAD/DEAH box type, N-terminal
-3,03549	dik_64	381	/
-2,87909	dik_59	129	Dienelactone hydrolase
-2,77780	dik_60	312	Glutathione S-transferase, N-terminal
-2,72321	dik_39	95	Short-chain dehydrogenase/reductase SDR
-2,55619	dik_01	/	Heat shock protein 70
-2,51746	dik_120	170	Protein of unknown function DUF1000
-2,48496	dik_69	307	Eukaryotic phosphomannomutase
-2,48024	dik_45	106	Short-chain dehydrogenase/reductase SDR
-2,34638	dik_42	439	not annotated
-2,30672	dik_49	114	Alpha/beta hydrolase fold-1
-2,30127	dik_112	284	Alcohol dehydrogenase, zinc-binding
-2,29113	dik_114	262	Cytochrome P450
-2,27574	dik_38	376	Protein synthesis factor, GTP-binding
-2,27376	dik_43	443	Protein synthesis factor, GTP-binding
-2,23674	dik_85	221	/
-2,23647	dik_40	438	Translation elongation factor EF1B, beta and delta chains, guanine nucleotide exchange
-2,17144	dik_46	100	/
-2,17090	dik_58	128	/
-2,14388	dik_53	126	Oxidoreductase FAD/NAD(P)-binding
-2,12688	dik_67	313	Eukaryotic phosphomannomutase
-2,07850	dik_55	117	/
-2,06792	dik_116	400	Histidine acid phosphatase
-2,06420	dik_20	62	Thiamine pyrophosphate enzyme, central region

-2,02671	dik_70	143	Eukaryotic phosphomannomutase
-1,99039	dik_44	97	/
-1,91235	dik_83	194	Redoxin
-1,88971	dik_110	245	Histidine acid phosphatase
-1,87822	dik_28	74	Methyltransferase type 11
-1,87429	dik_62	132	Glutathione S-transferase, N-terminal
-1,86473	dik_54	122	Glutathione S-transferase, C-terminal-like
-1,83602	dik_37	84	Lactate/malate dehydrogenase
-1,82832	dik_41	376	Protein synthesis factor, GTP-binding
-1,81642	dik_84	175	Glycoside hydrolase, family 5
-1,72482	dik_33	82	Methyltransferase type 11
-1,70359	dik_02	235	Carbohydrate kinase, FGGY
-1,70028	dik_19	/	Glyceraldehyde 3-phosphate dehydrogenase
-1,65946	dik_87	351	Mago nashi protein
-1,65905	dik_72	315	Glutathione S-transferase, C-terminal-like
-1,63305	dik_23	66	Aldo/keto reductase
-1,62063	dik_48	302	not annotaed
-1,61635	dik_03	14	Argininosuccinate synthase
-1,58326	dik_36	92	Short-chain dehydrogenase/reductase SDR
-1,53141	dik_95	268	Aconitase/3-isopropylmalate dehydratase large subunit, alpha/beta/alpha
-1,52934	dik_14	333	Polyprenyl synthetase
-1,52641	dik_115	287	Flavoprotein
-1,50745	dik_29	80	Lactate/malate dehydrogenase
1,52959	dik_05	388	Enolase
1,55113	dik_119	166	Alkyl hydroperoxide reductase/ Thiol specific antioxidant/ Mal allergen
1,56814	dik_12	/	
1,62619	dik_10	48	Ketose-bisphosphate aldolase, class-II
1,70263	dik_04	401	Enolase

1,72319	dik_79	403	/
1,82209	dik_111	244	Histidine acid phosphatase
1,85755	dik_78	/	
1,88308	dik_81	404	ATPase, F1 complex, OSCP/delta subunit
1,92169	dik_16	56	NAD(P)-binding
1,99166	dik_98	503	/
2,0095	dik_73	146	Glutathione S-transferase, C-terminal-like
2,0576	dik_118	164	/
2,24216	dik_117	61	NAD(P)-binding
2,25756	dik_13	47	Ketose-bisphosphate aldolase, class-II
2,32374	dik_71	/	
2,36451	dik_80	423	/
2,41012	dik_27	78	Lactate/malate dehydrogenase
2,41669	dik_92	344	RNA polymerase Rpb2
2,5738	dik_18	60	/
2,6101	dik_103	469	Heat shock protein 70
2,7047	dik_17	/	Alcohol dehydrogenase, zinc-binding
2,75169	dik_102	466	Chaperonin Cpn60/TCP-1
2,84371	dik_96	455	DNA/RNA helicase, DEAD/DEAH box type, N-terminal
2,85745	dik_106	/	
2,88093	dik_97	507	not annotated
2,92846	dik_89	343	not annotated
3,09967	dik_104	477	Peptidase M20
3,23494	dik_65	135	/
3,25617	dik_66	134	/
3,48039	dik_08	325	Mandelate racemase/muconate lactonizing enzyme, C-terminal
3,86253	dik_22	/	
4,20559	dik_113	/	Prefoldin

4,25109	dik_21	65	Aldo/keto reductase
4,55114	dik_15	/	Glyceraldehyde 3-phosphate dehydrogenase
5,01743	dik_93	/	Glyceraldehyde 3-phosphate dehydrogenase
5,30427	dik_34	/	Protein synthesis factor, GTP-binding
5,69488	dik_108	327	ATP-citrate lyase/succinyl-CoA ligase
5,73834	dik_105	470	not annotated
6,09518	dik_99	504	Alpha-D-phosphohexomutase, C-terminal
6,14663	dik_24	/	Glyceraldehyde 3-phosphate dehydrogenase
6,37665	dik_107	471	/
6,4326	dik_109	/	Peroxisome membrane protein, Pex16
6,49062	dik_74	155	/
8,02187	dik_25	/	Glyceraldehyde 3-phosphate dehydrogenase
8,04216	dik_09	326	/
9,7595	dik_75	318	Protein synthesis factor, GTP-binding
10,8852	dik_26	/	Glyceraldehyde 3-phosphate dehydrogenase

9.) Acknowledgement

My particular thanks go to Prof. Dr. Erika Kothe, who gave me the possibility to conduct my dissertation successfully. With her help I was able to collect teaching experiences as well as experiences in the organization of the daily routine in laboratories. Additionally, she gave me the possibility to participate in national and international conferences and to spend a beautiful time during a research stay in the USA.

Furthermore, I want to thank Prof. Dr. Axel Brakhage as my second supervisor for the suggestions and discussion points according to this work as well as for the allocation of laboratory equipment at the Hans-Knöll-Institute, Jena.

I would like to thank Kirk A. Bartholomew, Ph.D for the very nice, helpful and finally successful research stay in his lab in 2011.

Thanks go to Katja Tuppatsch and Maria Pötsch (both Hans-Knöll-Institute, Jena) who introduced me the protein equipment at the Hans-Knöll Institute. Furthermore, I would like to thank Dr. Jörg Linde (Hans-Knöll-Institute, Jena), who converted the RNA-Seq raw data into understandable data.

I would like to thank all my colleagues at Microbial Communication for the support in the lab, for the numerous suggestions and criticism during our seminar as well as for the private conversations.

Selbständigkeitserklärung

Die vorliegende Dissertation habe ich selbständig verfasst und keine anderen als die von mir angegebenen Quellen, persönliche Mitteilungen und Hilfsmittel benutzt.

Ich habe die Dissertation noch nicht als Prüfungsarbeit für eine staatliche oder andere wissenschaftliche Prüfung eingereicht. Ferner habe ich nicht versucht, diese Arbeit oder eine in wesentlichen Teilen ähnliche oder eine andere Abhandlung bei einer anderen Hochschule als Dissertation einzureichen.

.....
Melanie Brunsch

Jena, den 09.10.2012